Chapter 6
Tethered and Implantable Optical Sensors

A. J. Thompson and Guang-Zhong Yang

List of Acronyms

AFI	Autofluorescence imaging
AMD	Age-related macular degeneration
Arch	Archaerhodopsin
ASIC	Application-specific integrated circuit
BE	Barrett's Esophagus
CCD	Charge-coupled device
ChR2	Channelrhodopsin-2
CW	Continuous wave
ECG	Electrocardiogram
GI	Gastro-intestinal
IBD	Inflammatory bowel disease
IOL	Intraocular lens
IR	Infrared
LDA	Linear discriminant analysis
LED	Light-emitting diode
LSI	Laser speckle imaging
LSR	Laser speckle rheology
NpHR	Halorhodopsin
OCT	Optical coherence tomography
OFDI	Optical frequency domain imaging
PCA	Principal components analysis
PPG	Photoplethysmography
PpIX	Protoporphyrin IX
PTT	Pulse transit time
PWV	Pulse wave velocity
RF	Radio-frequency
RGC	Retinal ganglion cell

A. J. Thompson (✉) · G.-Z. Yang
The Hamlyn Centre, Imperial College London, London, UK
e-mail: alex.thompson08@imperial.ac.uk

© Springer International Publishing AG 2018

G.-Z. Yang (ed.), *Implantable Sensors and Systems*
https://doi.org/10.1007/978-3-319-69748-2_6

RP	Retinitis pigmentosa
SECM	Spectrally encoded confocal microscopy
SEM	Scanning electron microscopy
SERS	Surface-enhanced Raman spectroscopy
SLM	Spatial light modulator
SNR	Signal-to-noise ratio
SO_2	Oxygen saturation
SSI	Surgical site infection
TCE	Tethered capsule endomicroscopy
UTI	Urinary tract infection
VEP	Visual-evoked potential
VPU	Visual processing unit
1D	1-dimensional
2D	2-dimensional
3D	3-dimensional
5-ALA	5-aminolevulinic acid
μLED	Micro-scale light-emitting diode

6.1 Introduction

Optical imaging and sensing modalities have been used in medical diagnosis for many years. An obvious example is endoscopy, which allows remote wide-field imaging of internal tissues using optical fibers and/or miniature charge-coupled device (CCD) cameras. While techniques such as endoscopy provide useful tools for clinicians, they do not typically allow a complete diagnosis to be made. Instead, physical biopsies may be required to confirm or refute the presence of disease. Furthermore, endoscopic procedures are both invasive and time-consuming. As such, much research is currently directed toward the development of devices that can provide a complete in vivo diagnosis without the requirement for a physical biopsy. Ideally, such devices should also be minimally or non-invasive, and they should provide immediate identification of disease at the point of care. Additionally, there is significant interest in the development of implantable diagnostic devices that can be left within patients' bodies for extended periods of time (for several days or longer). Such systems could be used for automated disease diagnosis, and example applications include the detection of post-surgical infections as well as monitoring of the health status of patients undergoing chemotherapy. This chapter focuses on the development of optical instruments that can provide in situ diagnosis at the point of care, with an emphasis on progress towards miniature devices that may function as implants in the future.

Most current optical techniques used clinically have tethered formats and use optical fibers for light delivery and collection. Some smaller, untethered

biophotonic devices have been reported for research purposes (including early clinical trials) and these may open the door to truly implantable optical sensors. Both tethered and fully implantable systems will have significant clinical utility, and the aim of this chapter is to provide an overview of optical technologies with clinical applications that are currently in use or under development. In keeping with the theme of the book, the scope is limited to addressing only those approaches that are aimed at minimally invasive tethered devices or fully implantable systems. In the following sections a collection of relevant topics are reviewed, and in each case the current state of development is summarized and potential future research directions are discussed.

6.2 Principles of Optical Sensing

Optical sensing for medical diagnostics first involves the illumination of a region of interest—typically a small volume of tissue in vivo or a clinical sample of some kind (e.g. urine or blood) ex vivo—with either broadband (i.e. spanning a wide wavelength range) or narrowband light. A chosen signal is then detected in response to the illumination and, in almost all cases, this is also optical in nature (a notable exception to this is the field of photo-acoustics, where ultrasonic pressure waves are detected in response to pulsed optical excitation). The measured signal can be the light that is reflected, transmitted, or scattered by the sample. Alternatively, it can consist of the fluorescence or phosphorescence that is emitted some time after absorption of the illumination. Generally, the detected light is quantified in some way, and in the simplest case this entails measurement of the light intensity. The detected signal can be also quantified in terms of its wavelength (i.e. spectroscopy), its polarization, or its lifetime (in the case of fluorescence or phosphorescence measurements) among other factors. Importantly, the quantification of different parameters provides different opportunities for contrast (for example, between healthy and diseased tissue).

The observed signals can be based on either endogenous components (i.e. scattering, absorbing, or fluorescent molecules within the sample itself) or on exogenous contrast agents, such as fluorescent dyes. The former provides a direct measurement of the behavior of the sample, while the latter is dependent on the interaction of the sample with the contrast agent; both are useful clinically. Endogenous measurements have the advantage of being label-free and, hence, intrinsically less invasive, while exogenous contrast agents tend to offer higher signal-to-noise ratios and can be tailored to give specific readouts. For example, fluorescent dyes can be designed to be bright in the presence of a chosen biomarker and dim in its absence. Additionally, environment-sensitive dyes are available that change color—i.e. they exhibit changes in their absorbance, reflectance and/or fluorescence profiles—in response to, for example, changes in the pH or oxygen

concentration in their immediate vicinity. Optical sensing has multiple prospective clinical applications and many devices have been and are being developed to exploit these opportunities.

Of course, for diagnostic applications it is often desirable to obtain images, and optical sensing techniques can be readily extended to imaging formats. This is typically achieved through the use of scanning mechanisms (e.g. galvanometric scanning mirrors) or pixelated detectors (e.g. CCD cameras) and acts to provide spatial resolution to the measurement, allowing the collection of morphological information. Such an approach is clearly useful in medicine where it is necessary to visualize lesions and to differentiate healthy from diseased tissue, often with tight constraints on the margins between the two. When developing implantable systems, however, it is also important to consider power consumption, as untethered devices will need to operate for a set period of time using either a battery or an external wireless powering technology. Imaging devices will naturally draw more power than systems employing single point detection. This represents an important tradeoff in the fabrication of optical implants. Nonetheless, both approaches can provide useful clinical information.

Indeed, numerous optical sensing and imaging techniques have been deployed clinically, and obvious examples include endoscopes and pulse oximeters. In addition, there has been significant progress in recent years towards the development of implantable devices that could be used, for example, to monitor for signs of infection after surgery. In particular, a number of miniature pulse and blood oxygen sensors have been developed (e.g. [1]) that are based on measurement of the diffuse reflectance (see Sect. 6.4.2). Devices of this sort can also be extended to provide blood pressure monitoring through the addition of electrodes that make electrocardiogram (ECG) measurements [2, 3]. The above are chip-based systems that can be made fully implantable (i.e. untethered) using ASIC (application-specific integrated circuit) technology, and many further examples of optical systems like this can be found in the field of optogenetics (discussed in Sect. 6.6), where a number of miniaturized, implantable devices have been developed for use in freely moving rodents. Tethered implants are also under development for medical applications, and these will still permit minimally invasive measurements to be made. Examples include optical fiber-based glucose and pH sensors (as well as other ionic sensors) that rely on the immobilization of a sensing layer on the tip of the optical fiber (e.g. [4]). The most common method of immobilization is the sol-gel approach, and sensors of this type are discussed in Sect. 6.4.5. Finally, the development of miniature imaging devices is also under way, and this includes the production of imaging capsules (e.g. wireless capsule endoscopy [5] and tethered capsule optical coherence tomography (OCT) [6]), as well as probes designed for insertion through catheters or needles (such as the combined OCT/fluorescence probe reported in [7]). All of the above sensors, along with a variety of other devices, are described in more detail in the following sections.

6.3 Optical Imaging Techniques

6.3.1 Endoscopy

Medical endoscopy involves the remote imaging of internal tissues, such as the gastro-intestinal (GI) tract, the lungs, or the bladder. Traditionally, an incoherent (i.e. non-imaging) optical fiber bundle is used to deliver white light illumination to the tissue of interest, and a second coherent fiber bundle collects the reflected light and relays the image to a detector or eyepiece [8]. In modern systems, miniature distal CCD cameras are usually used instead of imaging fiber bundles due to the higher resolution they provide. Medical endoscopes permit wide-field, reflected light imaging with white light illumination and, as such, provide the clinician with morphological and limited (i.e. three-color) spectroscopic information. For this reason, endoscopy is used as a tool to aid clinicians, but does not provide complete diagnoses. As an example, in a typical colonoscopy, endoscopic imaging is used to locate suspicious regions of tissue, which are then excised using biopsy forceps and sent for histological examination in order to confirm the clinical diagnosis. Not only is this process invasive, it also often leads to the unnecessary removal of benign/healthy tissue. Hence there is significant interest in the development of techniques that can provide a so-called optical biopsy, where a diagnosis is made at the point of care (i.e. during endoscopy) and tissue is only removed when necessary. These techniques include more advanced imaging modalities such as endomicroscopy and OCT, as well as single-point spectroscopic approaches. Devices based on these methods can be incorporated not only into endoscopes, but also into other medical devices, such as catheters and needles. Thus, when deployed using optical fibers, instruments using these methods have the potential to be applied as tethered optical diagnostic implants in the future.

6.3.2 Endomicroscopy

One technique that aims to provide an optical biopsy during endoscopy is endomicroscopy, which involves the microscopic investigation of tissue using optical fibers [9]. The concepts behind endomicroscopy are the same as those in a standard scanning (e.g. confocal or multiphoton) microscope, with optical fibers also used to provide light delivery and collection, permitting remote imaging. Endomicroscopy is currently in clinical use and in some systems the microscopic imaging device is incorporated into the medical endoscope itself (e.g. EG-3870 and EC-3870, Pentax, Japan), while in others a separate probe-based endomicroscope can be inserted into the working channel of the endoscope (e.g. Cellvizio GI, Mauna Kea Technologies, France). In both cases, endomicroscopy is typically used to microscopically examine regions of tissue that have first been identified as suspicious by the clinician during the standard endoscopic procedure. Endomicroscopy provides

sub-cellular resolution (albeit within a much smaller field of view than that provided by standard wide-field endoscopy), and hence presents the clinician with significantly more information with which to make a diagnosis. In the future, endomicroscopic interrogation of this sort may replace (or more likely augment) physical biopsy, and at present much research is directed toward this end.

Endomicroscopes record images by sequentially scanning an illumination spot across a sample and detecting the resultant fluorescent or reflected light. They work in much the same way as a confocal or multiphoton microscope [10, 11], and use optical fibers to deliver light to and collect light from a remote sample. Endomicroscopes can also be designed to provide optical sectioning (i.e. confocal imaging), where light is only collected from a thin focal plane. This is important in the context of medical applications, as optical sectioning can provide information analogous to that obtained from the physical sectioning of excised tissue that is performed during histological examination. Typically, the resolution obtained during endomicroscopy is of the order of a micron and the field of view can extend up to approximately 600 μm^2. Additionally, it is worth noting that contrast agents such as methylene blue, fluorescein, or toluidine blue are often used to provide optimum image quality.

At the distal end of the endomicroscope, scanning of the illumination spot is usually achieved using one of two techniques: either distal or proximal scanning [9]. These approaches derive their names from the location of their scanning mechanism and more details on both methods can be found in [12] (proximal scanning) and [13–15] (distal scanning). Both proximal and distal scanning systems are in clinical use (proximal scanning—Cellvizio GI, Mauna Kea Technologies, France; distal scanning—EG-3870 and EC-3870, Pentax, Japan) and these systems have been applied widely to medical diagnostic studies.

6.3.2.1 Advanced Endomicroscopy Systems

Beyond the standard approaches to endomicroscopy, there is also significant research being directed toward the development of more advanced systems. These include the incorporation of multiphoton excitation, adaptations to the standard design in order to allow measurement of additional optical parameters, and the development of novel scanning techniques or imaging modalities to provide improvements over the standard approaches (e.g. in terms of minimum size, imaging speed or sampling rate).

Multiphoton excitation can be achieved simply through the use of a pulsed infrared (IR) laser in place of the standard excitation source—which is typically a continuous wave (CW) laser or a light emitting diode (LED)—and an alternative optical fiber with low dispersion characteristics (such as a dual clad photonic crystal fiber) to account for pulse dispersion (e.g. [16–19]). The adaptation of endomicroscopes to allow measurement of additional optical parameters is also relatively straightforward and examples include multi-spectral detection [20] as well as fluorescence lifetime imaging endomicroscopy [21, 22]. There have also been

multiple attempts to improve the sampling rate (and image quality in general) provided by proximal scanning systems while maintaining the small size of the distal tip. Several similar approaches involve the use of a spatial light modulator (SLM) to control the phase of light propagating through the optical fiber that is used for light delivery and collection (either in each individual core of a fiber bundle or in a single multimode optical fiber) in order to synthesize a focused scanning beam at the distal end [23–26]. Alternative approaches to address undersampling use additional optical or mechanical components to "fill the gaps" between the fiber cores in a proximal scanning endomicroscope. This can involve spectrally dispersing the distal light such that it reaches the otherwise unsampled regions of the object [27] or collecting multiple images as the object is shifted relative to the endomicroscope [28].

In practice, faster imaging is always desirable and significant work has been directed toward this end. On the one hand this has involved the development of a number of proximal line-scanning endomicroscopes, which permit faster imaging at the expense of optical sectioning strength [29–31]. Additionally, endocytoscopy [32, 33]—which provides fast, wide-field imaging without optical sectioning—has been widely used clinically and a number of commercial systems are available (e.g. XEC-300, XEC-120, XGIF-Q260EC1 and XCF-Q260EC1, Olympus, Japan). Another approach that provides fast, wide-field microscopic imaging is high-resolution micro-endoscopy [34, 35], which has also recently been modified to permit optically sectioned imaging [36]. One interesting alternative technique to improve imaging speed is spectrally encoded confocal microscopy (SECM), which involves spectrally dispersing white light illumination at the sample such that a line of illumination is obtained with each position in the line corresponding to a different wavelength [37]. By using a spectral detector at the proximal end rather than a simple single-channel detector, it is possible to measure the reflected light intensity at all points along the illumination line simultaneously. This allows the imaging speed to be doubled without compromising image quality, and much research is now being dedicated to optimizing such systems and minimizing the size of the required distal components (e.g. [38–40]). This technique is particularly relevant to this book, as it is has been used in the fabrication of a miniature capsule endomicroscope (see Sect. 6.3.3) that can be swallowed by the patient.

Overall, significant research is still in progress into the development of novel or improved endomicroscopes. Nonetheless, current commercial systems are already in clinical use and many studies have been published discussing the potential for endomicroscopy to be used as an in vivo diagnostic tool.

6.3.2.2 Clinical Applications of Endomicroscopy

Both distal and proximal scanning endomicroscopy have been applied clinically and their use is becoming more widespread. Many research articles have discussed the application of endomicroscopy to a variety of diseases and the possibility of its use as a tool for optical biopsy. This section highlights and summarizes some

important studies. This discussion is not exhaustive, however, and for more information readers are directed towards review articles that describe the use of endomicroscopy in specific diseases or tissues, for example [41–47].

Most commonly, endomicroscopy has been used to study the GI tract and diseases that have been investigated include neoplasia [48–50], colonic polyps [48, 51–53], Barrett's Esophagus (BE) [50, 54–57], inflammatory bowel disease (IBD) [49, 58–60], Crohn's Disease [59], and ulcerative colitis [49, 58, 60]. There have been multiple studies evaluating the utility of endomicroscopy for the characterization of colonic polyps [48, 51–53, 61]. While some of these have suggested that endomicroscopy does not improve upon the sensitivity and specificity provided by alternative endoscopic imaging modalities (e.g. narrowband imaging [52]), others have presented significantly improved diagnostic accuracies [48, 51]. One particularly promising study showed that neoplastic and non-neoplastic polyps could be differentiated in vivo with a sensitivity of 97% and a specificity of 99% [48]. These results suggest that endomicroscopy has the potential to become widely used in endoscopy for the examination of colorectal polyps. However, the current conflict in the literature over diagnostic accuracy means that further studies will be required before this occurs.

IBD—including Crohn's disease and ulcerative colitis—is another gastro-intestinal condition that has been widely studied with endomicroscopy [49, 58–60]. Kiesslich et al. [49] showed that dysplastic lesions could be diagnosed with an accuracy of 97% using endomicroscopy, while van den Broek et al. [58] were able to correctly predict the presence of neoplasia in 81% of cases when combining confocal endomicroscopy with high-definition narrowband imaging endoscopy. As a brief aside, it is worth noting here that one of the important features of endomicroscopy is the fact that the images obtained contain similar details to those observed in histology, which means that clinicians can make diagnoses without the need for significant additional training. This is demonstrated for ulcerative colitis in Fig. 6.1, where three regions of tissue have been imaged using both endomicroscopy (top row) and standard histology (bottom row) [49].

Endomicroscopy has also been applied extensively to the examination of suspicious lesions in patients suffering from BE [42, 50, 54–57, 62, 63]. High sensitivity and/or specificity of diagnosis have been reported in a number of studies, for example in the articles by Kiesslich et al. (92% sensitivity, 98% specificity) [50], Sharma et al. (94% sensitivity, 69% specificity) [56], and Bajbouj et al. (60% sensitivity, 95% specificity) [55]. As well as producing good diagnostic accuracy, it has also been shown that endomicroscopy can provide improvements in sensitivity relative to standard white light imaging and narrowband imaging [56], and that it can reduce the number of biopsies required when screening BE patients for neoplastic regions of tissue [54, 56]. Taken together, this implies that endomicroscopy will become increasingly widespread in the inspection of patients with BE.

While it has been mainly applied to the study and diagnosis of GI conditions, endomicroscopy has also been used to investigate other areas and ailments such as the bile duct [64], head and neck cancers [41], and brain tumors [47, 65, 66]. In these cases, most studies are at much more preliminary stages than the GI

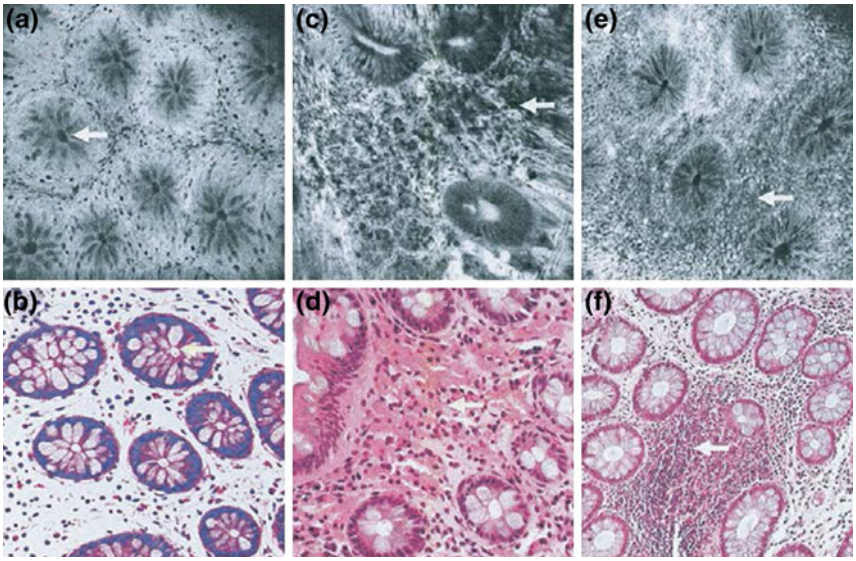

Fig. 6.1 Comparison of images of colon tissue obtained using endomicroscopy (top row) and standard histopathology (bottom row). Note the similar contrast obtained with the two techniques. Images **a** and **b** show normal crypt architecture with regular lumen indicated by the white arrows. Tissue affected by ulcerative colitis is shown in (**c**) and (**d**), where capillaries are distorted and the crypt architecture is altered. In particular, the spacing between crypts is larger than in healthy tissue. **e** and **f** show mixed cellular infiltration of disease with the crypts remaining unaffected. Cellular infiltration is indicated by the white arrows. Figure reproduced from [49], © 2007, with permission from Elsevier

investigations discussed above, and as such, the current focus is on presenting exemplar images rather than carrying out extensive experiments and reporting diagnostic accuracies. Nonetheless, the fact that such studies are under way demonstrates the growing clinical applications of endomicroscopy.

6.3.3 Capsule Endoscopy and Endomicroscopy

An important advancement of endoscopy and endomicroscopy in terms of implantable or ingestible medical devices is the development of capsule-based systems that are swallowed by the patient and provide imaging as they pass through the GI tract. Wireless capsule endoscopy [5] provides wide-field imaging using a small, untethered capsule (approximately 10 mm $\times$ 30 mm) that is ingested by the patient. Video images are recorded and transmitted for live viewing as the capsule passes through the patient's body and the image data obtained is similar to that provided by standard endoscopy (i.e. the images are not high resolution and high magnification as provided by endomicroscopy). Importantly, unlike

endomicroscopes, capsule endoscopes can be considered as (transiently) implantable. They have also become very useful in the investigation of the small intestine —which is difficult to access using standard endoscopes for the upper or lower GI tract—and are now widely used clinically (e.g. PillCam SB, Given Imaging Ltd., USA; MiroCam, Medivators Inc., USA; Endocapsule 10, Olympus Europa, Germany). In particular, wireless capsule endoscopy has been used to study small intestinal bleeding [67–70]. Photographs of clinically used capsule endoscopes are shown in Fig. 6.2, where the implantable/ingestible nature of this method is evident.

Further research in the area of capsule endoscopy is now mainly focused on the production of systems with additional sensing capabilities or higher imaging resolution. One important technique that was recently reported by Tabatabaei et al. [71] uses a tethered capsule (which is considerably less invasive than a standard endoscope) to provide confocal endomicroscopy. The capsule contains all the necessary optics and scanning mechanics to achieve SECM. A diffraction grating disperses broadband IR light into its constituent wavelengths to provide a line of illumination. A motor then drives rotation of the optics in order to allow an image to be collected from around the circumference of the capsule. The capsule is connected to a thin tether that houses an optical fiber that is used for light delivery and collection, and images covering a field of view of 22 mm × 223 μm can be recorded at a frame rate of 6 Hz. The lateral and axial resolutions provided by this system are respectively 2.1 and 14 μm, and its use has been demonstrated in swine esophagus in vivo as well as in ex vivo human biopsy samples. As such, this system represents a significant step towards the development of truly implantable/ingestible probes for confocal endomicroscopy.

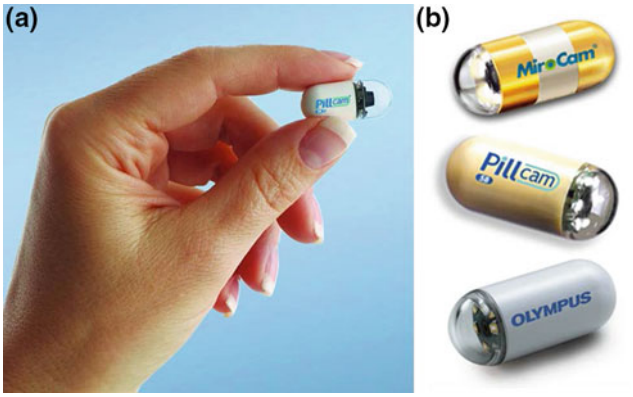

Fig. 6.2 Images of commercially available capsule endoscopy systems. The small size is illustrated in **a** while **b** shows capsules (all of which have very similar features) manufactured by three different companies. **a** PillCam™ SB 2 (Given Imaging, USA). **b** From top: MiroCam™ (IntroMedic Co., Republic of Korea); PillCam™ SB (Given Imaging, USA); EndoCapsule™ (Olympus, Japan)

6.3.4 Optical Coherence Tomography (OCT)

Optical coherence tomography (OCT) is an interferometric imaging technique that was first reported by Huang et al. in 1991 [72]. It relies upon the use of low coherence interferometry to provide depth-resolved images. A low-coherence light source (such as a superluminescent diode, an ultrashort pulsed laser, or a supercontinuum source) is used to illuminate the sample. The illumination is split into a reference and a sample arm, which are recombined at the detector to generate an interference pattern. Due to the short coherence length of the illumination source, interference fringes are only observed when the sample and reference arm lengths are very closely matched. This means that interference fringes are only detected at a specific imaging depth. By filtering the recorded signal such that only regions exhibiting interference (i.e. those with high spatial frequencies) are included, it is possible to obtain a measurement of the light intensity at a single specific depth within the sample. By using a CCD camera to record the light intensity across a wide field of view or by using scanning mirrors, it is then possible to obtain an image of the chosen z-plane (i.e. an optical section). Importantly, the optical sectioning strength in OCT is determined by the coherence length of the light source and, with appropriate illumination, axial resolutions as low as 1 μm can be achieved. Traditionally, depth scanning is then realized through a simple adjustment of the length of the reference arm, which acts to alter the imaging depth at which interference is observed. In more modern systems, however, three-dimensional (3D) imaging is often achieved by rapidly scanning the wavelength of the illumination or by using spectrally resolved detection [73–75]. In both cases, the reference arm length remains fixed and depth-resolved imaging is achieved by calculating the Fourier transform of the spectral data in order to reconstruct the depth information. This approach is referred to as frequency domain OCT, Fourier domain OCT, swept source OCT (in the case of rapid illumination wavelength scanning), or optical frequency domain imaging (OFDI).

Using either approach, OCT can provide 3D imaging at very high frame rates, and for this reason it is now widely used in clinical environments, often using optical fiber-based formats [76]. Its clinical uses include retinal imaging [77–83], vascular imaging for the diagnosis of atherosclerosis [84–94] and endoscopic imaging of the GI tract [95–100]. These medical applications of OCT are reviewed in the following section.

6.3.4.1 Clinical Applications of OCT

As discussed briefly above, there have been myriad medical studies using OCT and it is widely used clinically, with multiple commercial systems now available (e.g. NvisionVLE, NinePoint Medical, USA; Cirrus HD-OCT, Zeiss, Germany; Envisu Clinical SDOCT, Bioptigen, USA). The clinical applications of OCT have been wide-ranging and include (but are not limited to): imaging of the skin [101–104];

retinal imaging for studies on glaucoma, diabetic retinopathy, and neurodegeneration [73, 77–83, 105–109]; vascular imaging for the study and diagnosis of atherosclerosis [84–94, 110, 111]; breast cancer detection [112–114]; prostate cancer detection [115]; optical biopsy in the urinary tract [115, 116]; and optical biopsy in the GI tract (for example, in BE) [95–100, 117]. It is beyond the scope of this review to discuss all of these applications. Instead, the text below focuses on those studies that comprise approaches that fall under the broad remit of techniques that could be considered implantable—i.e. catheter-based probes for vascular imaging, endoscopic probes for GI and urinary tract imaging, and needle-based probes. While none of these devices are currently implantable, it is conceivable that they could be deployed as implants in the future, especially in the case of needles and catheters, which are often left within patients' bodies for long periods of time.

As with endomicroscopy, a number of OCT probes have been developed that can be deployed through the working channel of standard medical endoscopes. Such systems (and others) have been used to investigate the potential for OCT in the diagnosis of various conditions in the GI tract. One example is BE, where OCT has been used to assess neoplastic changes in esophageal tissue [100]. Additionally, a number of studies have also reported the use of OCT to investigate specialized intestinal metaplasia [96, 98, 117]. Beyond BE and specialized intestinal metaplasia, OCT has also been applied to the detection of esophageal adenocarcinomas and colonic polyps [95], as well as to the study of cancers of the urinary tract [116].

One of the most common applications of OCT has been in the study and diagnosis of coronary diseases, such as atherosclerosis [86, 89, 118]. In this case, side viewing OCT probes have been incorporated into arterial and venous catheters, and cross-sectional images of the vasculature are typically recorded by rotating the probe (e.g. [119]). 3D imaging of entire blood vessels can then be realized simply through pullback of the probe, allowing it to record cross-sectional images as it moves backward through the vein or artery (e.g. [91, 111, 120]). Cross-sectional images and a 3D rendered volume dataset of vascular tissue are shown in Fig. 6.3 as examples.

Vascular probes like those described above have found multiple applications in coronary medicine. In terms of atherosclerosis, OCT has been used to identify the chemical composition of plaques and to determine their risk of rupture. It has also been used to measure the thickness of the fibrous caps that cover the lipid-rich cores in atherosclerotic plaques, and at present it is the only technique capable of making such measurements. Moreover, it has been used to study acute intracoronary thrombosis, to guide angioplasties, and to assess percutaneous coronary interventions (i.e. the implantation of stents to improve blood flow) [85, 88, 89, 121–123]. Thus, OCT has become widely used in coronary medicine and its applications are likely to grow further in the future as the technology continues to improve.

A further important use of OCT for the purpose of this chapter is its application in needle probes. While less common than the vascular methods described above, several needle-based OCT systems have been reported in recent years. These devices have been developed with the aim of permitting imaging below the tissue surface and have been applied to ex vivo studies of freshly resected tissue from both

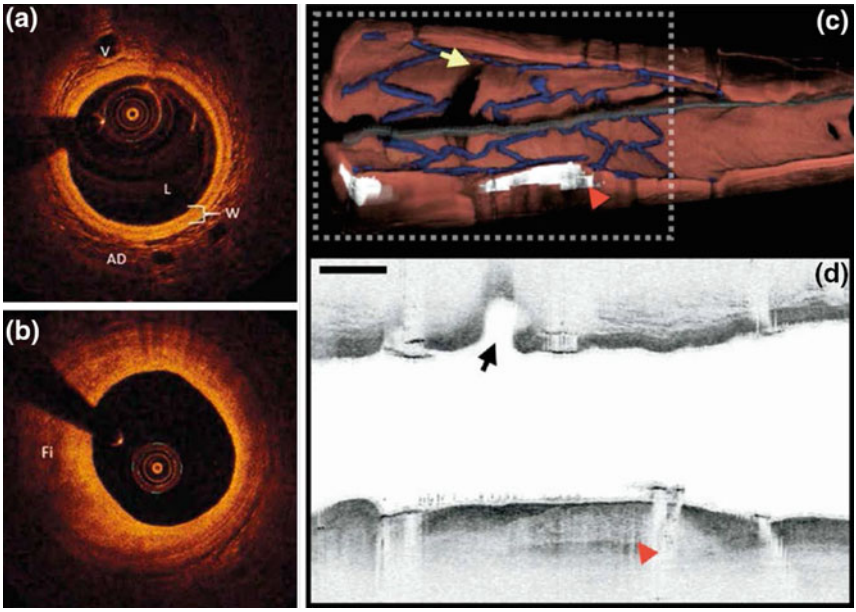

Fig. 6.3 Exemplar intravascular OCT data. **a** Radial cross-sectional image of a healthy blood vessel showing the lumen (L), vessel wall (W) and adventitia (AD) with vasa vasorum (V). **b** Radial cross-section of a blood vessel with a fibrotic atheroma (Fi). **c** 3D reconstruction of a blood vessel containing a stent (blue). A side branch (yellow arrow) and a calcified nodule (white region, highlighted by the red arrowhead) are also indicated. **d** Longitudinal section through the dataset shown in (**c**). Black arrow and red arrowhead indicate the side branch and calcified nodule respectively. **a**, **b** Reproduced with permission from [89], © 2015. **c**, **d** Reproduced from [91], © 2008, with permission from Elsevier

animals and humans. Specifically, imaging of deep skeletal mouse muscle tissue [124] and of the alveoli and other small airways in sheep's lung [125] have been demonstrated using OCT needle probes. In addition, a dual-modality OCT/fluorescence needle probe was recently presented by Scolaro et al. [7], where the fluorescence capability was used to detect fluorescently labeled antibodies in an excised mouse liver. More importantly, freshly resected human tissue samples from patients suffering from breast [112] and prostate cancer [115] have also been successfully imaged using needle-based OCT. Significantly, OCT was able to accurately reproduce the tumor margins obtained from histology in both cases.

OCT needle probes are also minimally invasive: typically, the reported needle diameters are below 1 mm, and the thinnest system presented to date was incorporated into a 310 μm diameter (30-gauge) needle [124, 126]. For illustration, this system is shown in Fig. 6.4 along with a volumetric OCT dataset acquired in ex vivo mouse tissue. Such devices will provide clinicians with the opportunity to image below the tissue surface, hence permitting deeper imaging than is usually

available with OCT (or other optical techniques). For these reasons, they are likely to become clinically useful in the coming years.

Overall, OCT is already widely used clinically—particularly in endoscopic and catheter-based applications—and such devices have shown great potential in their capacity to provide in vivo, real-time disease diagnosis (i.e. optical biopsy). Furthermore, the development of needle-based OCT probes also suggests that further minimally invasive clinical systems will become available in the future. In particular, catheter-based and needle-based probes show considerable promise as potential candidates for implantable devices. With probe tips small enough to cause minimal discomfort to the patient, such systems could be tethered to the necessary external optics and electronics. As an example, this could then allow perpetual imaging of implanted devices, such as central venous catheters, to regularly test for signs of failure.

6.3.4.2 Tethered Capsule OCT

A promising advancement of OCT within the scope of implantable optical sensors is the development of capsule-based OCT. Tethered capsule endomicroscopy (TCE) has been developed for OCT in the GI tract and was first reported by Gora et al. in 2013 [6]. In this approach, the patient swallows a small pill that contains all of the distal scanning mechanics necessary to achieve frequency domain OCT. The pill includes a rotary scanning mechanism and is connected to a 1 mm diameter tether that houses an optical fiber that collects the light from the tissue. As such, a

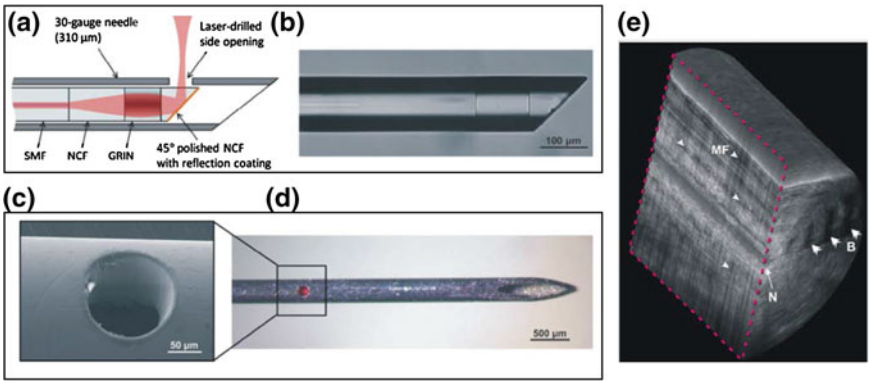

Fig. 6.4 Needle-based OCT. **a** Schematic of 310 μm diameter OCT needle probe. **b** Microscope image of the fiber probe used within the needle. **c** Scanning electron microscopy (SEM) image of the opening in the needle that allows imaging (fabricated using laser drilling). **d** Image of the fully assembled needle probe where red laser light can be seen emerging from the laser-drilled opening. **e** 3D rendered volumetric dataset from normal mouse muscle acquired with the OCT needle probe. Needle tract (N), myofibers (MF) and birefringence artefacts (B) are indicated by the white arrows. Reproduced with permission from [124], © 2014

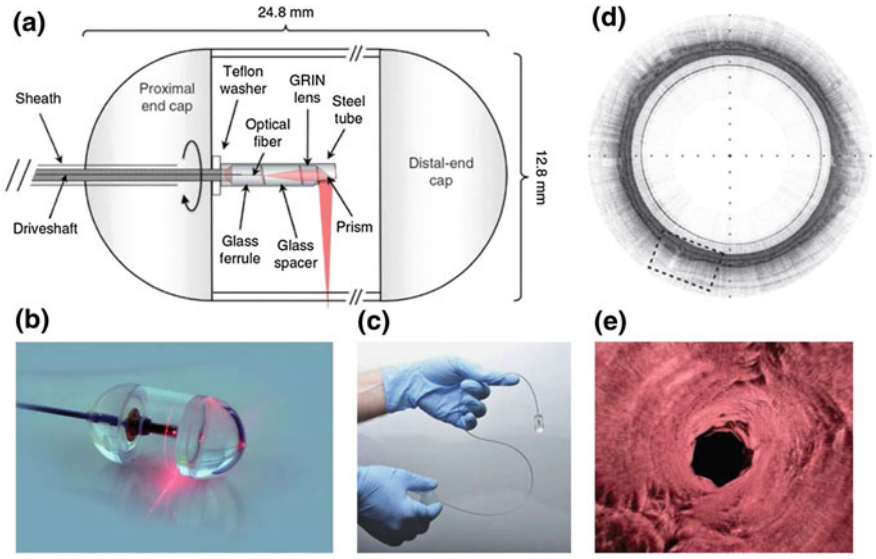

Fig. 6.5 Tethered capsule OCT. **a** Schematic of the tethered capsule OCT probe presented by Gora et al. [6]. Photographs of the tethered capsule system are shown in (**b**) and (**c**), where its small size and minimally invasive nature are evident. **d** Radial cross-sectional OCT image of normal esophageal tissue obtained from a healthy volunteer in vivo. **e** 3D rendered 'flythrough' view of a Barrett's segment of esophagus, also obtained in vivo. Reproduced with permission from Macmillan Publishers Ltd: Nature Medicine [6], © 2013

typical GI imaging procedure is considerably more comfortable for a patient than standard endoscope-based approaches. In general, the pill is swallowed by the patient and allowed to reach the stomach before recording volumetric OCT images while being pulled back through the esophagus. Using this method, imaging of the entire esophagus is possible in 5–6 min and this has been demonstrated in vivo in unsedated patients with BE [6, 127]. A diagram and two photographs of a capsule-based OCT device are shown in Fig. 6.5, along with example data obtained in the esophagi of a healthy patient (d) and a patient suffering from BE (e).

A further tethered capsule OCT device has been reported by Liang et al. [128]. This system has a dual scanning mechanism that allows both high-speed rotary scanning for fast *en face* volumetric imaging (similar to that reported by Gora et al. [6]) as well as slower, accurate 2D scanning to permit high-resolution imaging. The use of this device has been demonstrated in pigs in vivo and its dual scanning mechanisms mean that it may be compatible with both screening applications (which require wide-field imaging) and surveillance applications (which require high-resolution imaging of small, pre-determined regions of tissue) [128]. Interestingly, the 2D distal scanning mechanism means that this capsule could also be utilized for other types of scanning microscopy (e.g. distal scanning endomicroscopy). Its potential for future use as a tool for GI imaging is clear.

Overall, capsule-based OCT is clearly an exciting new methodology that allows in vivo GI imaging in a manner that is much more comfortable for patients than current endoscopic methods. It is likely to become more widely used in the future and may also find applications in imaging of the small intestine, where standard endoscopy is challenging.

6.4 Other Optical Sensors

As discussed above, both endomicroscopy and OCT have been used in a number of different clinical applications—ranging from GI endoscopy for the detection of premalignant tissue changes to intravascular imaging for the diagnosis of atherosclerosis—and their use is continually increasing. While they have shown considerable promise in terms of the potential to provide an optical biopsy, research is still ongoing into the use of other imaging and spectroscopic techniques. In general, this research comprises the use of optical fibers to permit imaging or single point measurements using alternative optical methods. However, a number of capsule- and integrated chip-based devices have also been reported. In both cases, an important aim of the research is to provide the clinician with functional information (e.g. the rate of metabolism at a specific imaging location) rather than simply offering morphological information, as is the case in endomicroscopy or OCT. In some cases, these additional optical approaches have been incorporated into endomicroscopy (see Sect. 6.3.2.1) or OCT probes to provide dual modality imaging systems. This section focuses on research in which the "advanced" optical technique is the central theme of the work (i.e. rather than discussing research involving the incorporation of an additional imaging/sensing modality into an OCT probe or an endomicroscope).

Many optical techniques have been investigated for this purpose and the remainder of this section addresses some of the most common methods. These include laser speckle imaging (LSI), diffuse reflectance spectroscopy, fluorescence spectroscopy (including time resolved fluorescence measurements), and Raman spectroscopy. While LSI (as its name suggests) is typically deployed in an imaging setup, the latter three techniques have mainly been applied in single-point measurement arrangements (although a small number of imaging experiments are also discussed herein). In these single-point approaches, morphological information is dispensed with and light is generally collected from a small (typically less than 1 mm $\times$ 1 mm) field of view. This means that data can be collected in shorter acquisition times without the need for expensive, highly sensitive detectors. Such methods are useful in optical modalities where the required acquisition times can be long due to low signal levels or the incorporation of additional dimensionality (e.g. in wavelength-resolved or time-resolved measurements). They often serve as preliminary research to ascertain whether an imaging modality (which can be used in a more intuitive manner by a clinician) would have any merit.

When considering the development of an implantable optical sensor, however, single-point measurements may in fact hold advantages over imaging techniques. The reason for this is that the data collected by the sensor is less complex and is more suitable for automated analysis and diagnosis. While automatic, computerized processing of 2D or 3D image data can be very complicated (often involving image segmentation and recognition techniques), automated analysis of 1D single-point data can be much simpler. Multiple approaches that allow computer-based diagnosis using spectral data have been reported and these typically employ spectral decomposition techniques (such as principal component analysis—PCA) followed by a form of discriminant analysis. The spectral decomposition acts to break the recorded data down into a small number of base components that accurately describe all measurements, and the discriminant analysis then uses the relative contributions of these base components to make a diagnosis for each measurement site based solely on its spectrum. This type of automated data analysis and diagnosis will be vitally important in any implanted sensor, as it will not be feasible to manually assess data that is being collected continuously. Furthermore, the electrical power used in single-point measurements is considerably lower than that required for imaging, which implies that single point approaches will be preferable when developing an untethered implantable device that cannot be wired to an external power source. Thus, single-point measurement techniques are likely to play an important role in the development of optical implants due to their low power requirements and the potential to analyze the data they provide in an automated fashion.

Lastly, it is worth noting that all of the optical techniques discussed below are readily compatible with optical fibers, and hence have the potential to be deployed as minimally invasive, or even tethered, implantable diagnostic devices. In addition, a number of untethered sensors—based on integrated chips and/or capsules—have also been reported, indicating the possible development of fully implantable devices. The following sections provide a description of the various (pre)clinical studies that have been carried out using these approaches.

6.4.1 Laser Speckle Imaging (LSI)

6.4.1.1 Theoretical Background

Laser speckle imaging (LSI) is most often used to produce spatial maps of blood flow in tissue, for example in the retina or brain. A precursor to LSI is laser Doppler flowmetry, which provides measurements of flow rate based on the Doppler shift of backscattered photons [129]. While Doppler approaches to flow measurements provide accurate and reliable assessment of the flow rate, they rarely provide images or spatial maps of flow due to high data processing requirements. For this reason, LSI was developed in order to provide a technique with less intensive data processing that could enable spatial imaging of tissue blood flow.

In LSI, a coherent laser source diffusely illuminates a sample, and a CCD camera is typically used to image the backscattered light. Due to the non-uniformity of the sample surface and the coherent nature of the illumination, a random interference pattern is recorded by the detector. This interference pattern is known as a speckle pattern and, importantly, speckle patterns have been shown to vary due to sub-surface blood flow (as blood flow effects changes in the surface morphology). In LSI, speckle patterns are converted to flow maps (often referred to as speckle contrast images) by assessing the rate of change of the speckle pattern in either time or space. As such, LSI can provide images of vasculature—including relative or absolute flow rates—with mm to cm fields of view [130].

In a typical measurement procedure, a (series of) speckle pattern(s) is recorded and the speckle contrast, K, at all image pixels is calculated as

$$K = \frac{\sigma}{\langle I \rangle} \tag{6.1}$$

where σ is the standard deviation of the speckle intensity fluctuations and $\langle I \rangle$ is the mean intensity value. The mean and standard deviation of the speckle variations can be measured temporally by recording a series of speckle patterns and calculating the mean and standard deviation of subsequent images. Alternatively, they can be calculated from a single image using a spatial approach. In this case, for every image pixel, $\langle I \rangle$ and σ are obtained in a small window (typically 5×5 or 7×7 pixels) around the central pixel. This method sacrifices spatial resolution (as the window introduces an averaging effect), but improves temporal resolution (as only a single image is required).

The speckle contrast, K, can be related to the image acquisition time, T, and the speckle decorrelation time (τ_c—the characteristic time over which the speckle pattern changes) according to

$$K = \beta^{0.5} \left\{ \frac{\tau_c}{T} + \frac{\tau_c^2}{2T^2} \left[\exp\left(\frac{-2T}{\tau_c} \right) - 1 \right] \right\}^{0.5}. \tag{6.2}$$

Here, β is a constant of proportionality that accounts for the loss of speckle contrast related to the size ratio of the detector and the individual speckles, and due to polarization effects. A complete derivation of this equation can be found in [130, 131]. Nonetheless, it is clear from (6.2) that the speckle contrast is directly related to the rate of decorrelation of the speckle pattern (τ_c). In the case of blood flow measurements, the decorrelation will occur faster in regions of high flow rate, and, as expected, τ_c is inversely related to the flow rate (v):

$$\tau_c = \frac{1}{a k_0 v}. \tag{6.3}$$

In (6.3), k_0 represents the wavenumber while a is a proportionality factor dependent on the scattering properties of the tissue. It is clear from the above equations then

that the speckle contrast can be directly related to the absolute flow rate. However, this often proves difficult in practice, as the number of moving particles and their orientations are unknown (i.e. the parameter a is difficult to calculate). For this reason, relative flow rates are most often reported based on ratios of the decorrelation times (or speckle contrast values) at different times or in different spatial locations. This is not always the case though, and some more complex analysis procedures have been presented that allow calculation of the absolute flow rate (e.g. [132]). Despite the challenges involved in the measurement of absolute flow velocities, LSI has still found multiple biomedical applications, and these are described in detail below.

6.4.1.2 Biomedical Applications of LSI

LSI was first described by Fercher and Briers [131] in 1981, where it was used to generate maps of blood flow in the retina. Since then it has found various biomedical applications—which are reviewed extensively in [130]—and these are discussed below.

As described above, the most common application of LSI has been in blood flow mapping. One example of this is in retinal imaging, where LSI has been applied numerous times (e.g. [131, 133–135]). Most studies have been carried out in animals; however, a small number of investigations have now also been published that report on the in vivo measurement of blood flow rates in human retinas [135, 136]. LSI has also been used to monitor skin perfusion (e.g. [137, 138]). While it is difficult to measure flow in individual vessels in the skin (as the top layer of skin contains very few blood vessels and obscures the signal from below), LSI has instead been used to monitor the overall perfusion [139]. In one interesting application, LSI was used to provide feedback during laser therapy of port wine stains [140]. In this study, in vivo imaging was reported in humans and LSI was used to assess the efficacy of laser therapy of port wine stains in real time. A further application of LSI is in small animal brain imaging, where it has been used to study the relative cerebral blood flow in a number of scenarios. These include the study of the brain's response to external stimuli (for example, after electrical stimulation of the paws of rats [141]) as well as the investigation of cortical spreading depressions (the underlying cause of migraine aura) [142–144] and stroke physiology [145–147]. Example LSI data from the brain of a rat is shown in Fig. 6.6, where a raw speckle pattern and a speckle contrast image are presented. The sensitivity to blood flow is clear in the speckle contrast image, with different vessels showing markedly different speckle contrast values.

One particularly interesting use of LSI within the scope of this book is its application to the measurement of the viscoelastic properties of blood [148]. This approach—known as laser speckle rheology (LSR)—has been used in the characterization of blood coagulation [149, 150] and atherosclerotic plaques [151–153]. Both have obvious clinical uses and the assessment of atherosclerosis ties in well with the catheter-based OCT probes discussed previously (see Sect. 6.3.4.1).

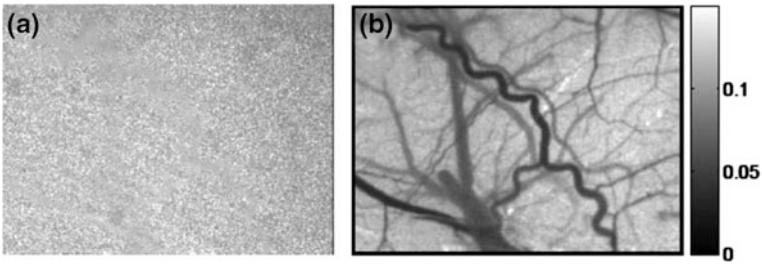

Fig. 6.6 Laser speckle imaging of blood flow in the brain of a rat. **a** Raw speckle image. **b** Speckle contrast image calculated using the spatial speckle approach with a 7 × 7 pixel window. Blood vessels are clearly visualized in the speckle contrast image, as are differences in flow rate. Dark regions with low speckle contrast correspond to high flow rates, while light regions (with higher speckle contrast values) indicate lower flow rates. Figure reproduced with permission from [130], © 2010

Indeed, Wang et al. [154] have reported on the development of fiber bundle-based LSI, and this has the potential to permit speckle measurements in endoscopic or catheter-based systems. Combined with the simplicity and low cost of most LSI setups, the incorporation of optical fiber-based measurements provides a route towards the development of clinically viable (tethered) implantable devices.

6.4.2 Diffuse Reflectance Spectroscopy

When light impinges on biological tissue, reflection can take place in either a specular or a diffuse fashion. Specular reflections return directly from the tissue surface, while the diffusely reflected light undergoes several elastic scattering events within the tissue before re-emerging from the tissue surface. Diffuse reflectance spectroscopy involves the study of this elastically scattered light, and hence provides information about the absorptive and scattering properties of a sample.

In a typical diffuse reflectance spectrometer, a white light source is employed for illumination and spectrally resolved detection is provided by the combination of a dispersive optical element (i.e. a prism or a diffraction grating) and a large area detector (such as a CCD array). Optical fibers are also often used for light delivery and collection, and the positioning of the delivery and collection fibers can be chosen in order to selectively reject specular reflections (see Fig. 6.7a, b).

Optical fiber-based diffuse reflectance spectrometers have been applied to a multitude of clinical studies investigating a variety of different diseases and pathologies. These range from cancers of the skin [156–158], cervix [159–161], bladder [162], and colon [163, 164] to stroke and epilepsy [165–167]. In some cases, diffuse reflectance spectra are used to directly assess disease state. However, in the majority of studies, the measured spectra are used to calculate the tissue or

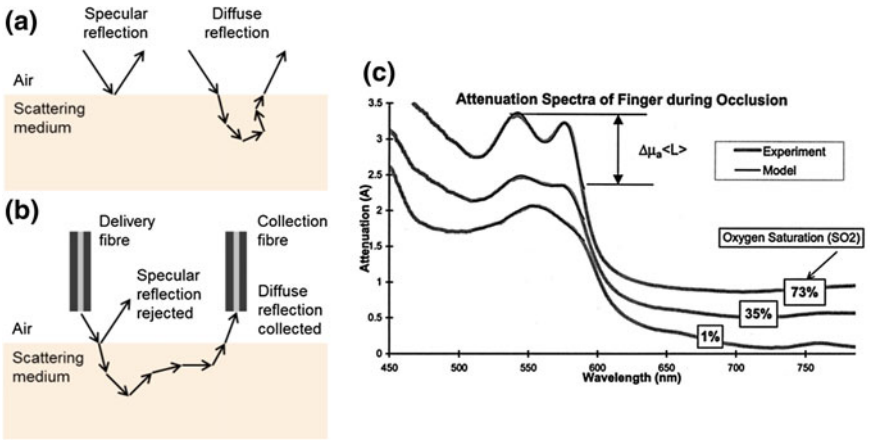

Fig. 6.7 Diffuse reflectance spectroscopy. **a** Diagram illustrating the difference between specular and diffuse reflection. Specular reflection involves direct backscattering of light from the surface of a medium, while diffuse reflection involves multiple scattering events within the medium. Hence, diffusely reflected light carries information about the absorptive and scattering properties of the sample. **b** In fiber-optic diffuse reflectance spectroscopy, the optical fibers used for light delivery and collection can be positioned such that the diffusely reflected light is collected while specular reflections are rejected. **c** Example diffuse reflectance spectral data (in this case, attenuation data is shown) illustrating how the spectra depend upon the tissue oxygen saturation. Graph shown in (**c**) has been reproduced with permission from [155], © 2001

blood oxygen saturation, which can be correlated with the state of health of the tissue (or patient). Three example diffuse reflectance spectra are shown in Fig. 6.7c, where the effect of oxygen saturation on the spectra is clear [155].

In vivo evaluation of the oxygen saturation from diffuse reflectance spectra can be achieved using a number of approaches (e.g. [155, 168–173]) and a detailed description of the relevant mathematics can be found in [174]. Briefly, it is first necessary to calculate the absorption coefficient (μ_a) of the sample according to

$$\mu_a = \varepsilon[C] = -\frac{1}{L}\log\frac{I}{I_0} \tag{6.4}$$

where ε is the extinction coefficient, $[C]$ is the concentration of the absorber, I and I_0 are respectively the detected and incident light intensity, and L is the propagation distance within the sample. If the exact path length (L) is not known, it can be calculated by measuring spectra with multiple different source–detector separations or by employing time- or frequency-resolved techniques (which use pulsed illumination and time-resolved detection or frequency-modulated illumination and detection respectively) [174]. The measured absorption coefficient can then be related to the concentrations and extinction coefficients of oxy- and deoxy-hemoglobin as

$$\mu_a(\lambda) = \varepsilon_{Hb}(\lambda)[Hb] + \varepsilon_{HbO_2}(\lambda)[HbO_2] + f(\lambda) \tag{6.5}$$

where λ represents the wavelength, ε_{Hb} and ε_{HbO2} are the extinction coefficients for deoxy- and oxy-hemoglobin respectively, [Hb] and [HbO_2] are the respective concentrations of deoxy- and oxy-hemoglobin, and $f(\lambda)$ represents the absorption profile due to tissue chromophores other than hemoglobin. The extinction coefficients for oxy-hemoglobin (HbO_2) and deoxy-hemoglobin (Hb) are known, and $f(\lambda)$ is generally assumed to be constant (in the near IR wavelength range) or a linear function (at visible wavelengths). By measuring the absorbance at multiple wavelengths (i.e. by recording a spectrum) it is possible to solve (6.5) for [Hb] and [HbO_2]. The oxygen saturation (SO_2) can then be calculated as the ratio of the oxy-hemoglobin concentration to the total hemoglobin concentration:

$$SO_2 = \frac{[HbO_2]}{[Hb] + [HbO_2]}. \tag{6.6}$$

Blood and tissue oxygen saturation measurements have been used in many clinical studies and it is beyond the scope of this chapter to review all of these. However, examples of the use of SO_2 measurements include the study of stroke physiology [165], monitoring photodynamic therapy [155, 175] and cerebral ischemia [166], as well as the investigation of various cancers [159–163, 176].

A number of commercial devices exist that permit clinical oxygen saturation measurements in vivo. These are typically deployed during or after surgery to ascertain whether the operated tissue is receiving a sufficient blood supply, or to monitor the resuscitation process. Examples of these clinical devices include the O2C (LEA Medizintechnik GmbH, Germany) and a number of finger clip systems (for both clinical and home use) such as the GO_2 (Nonin Medical Inc., USA). Such systems typically provide measurements of the pulse as well as the oxygen saturation, and some devices (e.g. the O2C) also incorporate blood flow monitoring using the laser Doppler approach.

As discussed above, SO_2 measurements are often carried out using optical fiber-based devices (e.g. the O2C is in clinical use) and, as such, their use in a tethered implantable format is not difficult to envisage. Furthermore, the relatively simple device requirements (i.e. a minimum of two illumination wavelengths and a single-point detector) mean that miniaturization for the development of fully implantable devices is also possible. Indeed, work to this end is under way and Chen et al. [1] recently presented a tissue oxygen saturation monitor in which all of the optical and electronic components required for illumination and detection were contained within a single 1.5 × 2 cm integrated chip. Devices of this sort can also be used to make pulse measurements, and in that case only a single illumination wavelength is required. These systems allow the pulse rate to be obtained by monitoring the variations in the reflected or transmitted light intensity that occur as the volume of the vessel or the oxygen content of the blood change in a pulsatile

nature. This approach to pulse measurement is commonly referred to as photoplethysmography (PPG).

Optical pulse and SO_2 sensors have also been extended to provide systolic blood pressure measurements through combination with ECG probes, and a number of implantable systems have recently been reported [2, 3]. In these devices the pulse transit time (PTT) is first calculated as the difference between the arrival times of the peak of the ECG signal (the R-wave) and the rising edge (the systolic slope) of the PPG signal. PTT can then be converted to pulse wave velocity (PWV) through knowledge of the distance that the pulse has traveled (i.e. the distance from the heart to the measurement location), which is directly related to blood pressure. The relationship between the PWV and the blood pressure is linear in the physiologically relevant pressure range, but is also dependent on a number of unknown parameters, such as the blood density, the thickness of the vessel wall, and the inner diameter of the vessel [3]. Thus, PTT-based blood pressure measurements require a calibration procedure to be carried out for each individual patient (as the blood density, vessel wall thickness, etc. will vary from patient to patient) and this represents a significant drawback to techniques of this sort. In addition, research in this area is in its early stages, and as such there is considerable variation across the different reported devices due to (among other factors) the choice of the point in the PPG signal from which the transit time is measured. Nonetheless, these devices provide an opportunity to measure a highly important physiological variable (blood pressure) in a continuous and minimally invasive manner. For this reason, they are likely to be developed further in the near future.

An additional format that is of interest when considering implants is the ingestible capsule, and a device of this sort (HemoPill, Ovesco Endoscopy AG, Germany) has recently been launched that permits detection of blood in the GI tract. This untethered pill is swallowed by the patient and blood is detected based on the relative absorbance of light from blue and red LEDs. This system permits rapid diagnosis of internal bleeding at a much lower cost than with standard or capsule-based endoscopes due to the fact that an image sensor is not required. This demonstrates that the development of untethered, ingestible/implantable probes that can detect blood, measure SO_2, or make other optical measurements is entirely feasible.

Due to its ease of miniaturization and compatibility with optical fibers, the development of implantable SO_2 monitors (and other diffuse reflectance-based probes) is likely to continue. Furthermore, as SO_2 measurements have already been shown to have important clinical applications and can be extended to allow detection of additional physiologically useful parameters, such as pulse and blood pressure, the development and use of such devices is almost certain to be successful. For this reason, an increasing number of implantable or minimally invasive SO_2 devices are likely to be presented in the coming years, and these will offer new opportunities to accurately monitor resuscitation, ischemia, tissue viability during/after surgery, and many other important clinical targets.

6.4.3 Fluorescence Spectroscopy

In a fluorescent molecule, the absorption of an incident photon acts to promote an electron within the molecule to a higher energy state (i.e. a higher energy molecular orbital). When the electron later relaxes back into its (lower energy) ground state, energy can be released in the form of light. This emissive behavior is known as fluorescence and has been widely studied in the context of medicine.

A fluorescence spectrometer has a very similar layout to a diffuse reflectance system. However, narrowband excitation is typically employed (using a laser source or a lamp with a narrow excitation filter), as is an emission filter, which ensures that no elastically scattered (reflected) excitation light reaches the detector. Most often the collected light is recorded as a function of wavelength (i.e. as a spectrum), but alternative parameters can also be measured, such as the polarization of the emitted light or the fluorescence lifetime [177].

Fluorescence measurements have been applied to many biomedical studies and some fluorescence-based systems are already in clinical use. One such approach is autofluorescence imaging (AFI) [178–181], which is used during endoscopy to help guide GI biopsies. Furthermore, as described previously, endomicroscopy has been used in conjunction with contrast agents to allow microscopic fluorescence imaging for in vivo assessment of GI disorders. As with many of the techniques described above, optical fibers are often used for light delivery and collection in clinical investigations, as these provide a minimally invasive measurement modality. In the future, such systems could also become useful as tethered implanted devices. As fluorescence measurements are clinically compatible, many studies have reported the investigation of fluorescence as a diagnostic parameter in a variety of diseases. One important example is in the study and diagnosis of cancer, where both spectrally [182–188] and temporally [158, 189–198] resolved fluorescence measurements have been investigated extensively. This has involved single-point measurements [158, 185–190] as well as imaging modalities [193, 194, 199–202] and has entailed the study of the signals from intrinsic tissue fluorophores (referred to as autofluorescence) as well as the use of fluorescent contrast agents [203]. In terms of autofluorescence measurements, observed changes in fluorescence between healthy and diseased tissues have been correlated to metabolic state or to changes in the constituent fluorophores that are present. In other cases, the fluorescence spectrum or lifetime is simply used as a diagnostic parameter with no attempt made to make a link to the physiological changes occurring. In studies where contrast agents are used, a fluorescent dye or stain is chosen to optimize the image contrast. In some cases the chosen stain preferentially accumulates in cancerous cells and one important example is 5-aminolevulinic acid (5-ALA)—a precursor to protoporphyrin IX (PpIX), which accumulates in tumors [203].

The final goal of research into fluorescence as a clinical tool for cancer diagnosis is usually aimed at producing screening systems that can be used to test high-risk patients. Another option, however, is to develop implantable devices that can continually monitor tumors during treatment. Such a system could entail a

fiber-optic tethered device, and these are likely to become more prevalent once the size of the required optical apparatus has been sufficiently miniaturized.

Another important use of implantable medical devices is in the diagnosis of infection (for example, during recovery from surgical procedures). As such, optical systems capable of detecting the presence of infection or of specific bacteria would be very useful clinically. Limited studies into the use of fluorescence for this purpose have been reported in the literature and these have typically used contrast agents. One example study was presented by Yamashita et al. [204], where the authors used a chymotrypsin-activated fluorescent probe to optically monitor for signs of pancreatic fistula (a common complication after digestive surgery that can lead to infection) after resection of the pancreas. The results of this study were positive, with high diagnostic sensitivity and specificity reported as well as real-time visualization of pancreatic leakage during surgery. However, while an approach that requires the use of a contrast agent may be feasible during surgery, it is much more difficult to envisage the use of a contrast agent as part of a long-term implantable sensing modality. One option here would be to chemically immobilize the contrast agent on the tip of an optical fiber. However, for some fluorescent dyes this would entail complex chemical synthesis and such a technique would also require a foreign chemical to be implanted within the patient. Although this would involve a very small amount of fluorescent dye implanted for a relatively short amount of time (days, weeks, or months), it is still a sub-optimal arrangement. Research into the use of alternative optical techniques that can report on the presence of infection or bacteria without the need for contrast agents is currently under way. One technique under investigation for this purpose is Raman spectroscopy, which is described in the following section.

6.4.4 Raman Spectroscopy

Beyond absorption, reflection (elastic scattering) and fluorescence, another transition that can occur when light is incident upon an optically active molecule is Raman (inelastic) scattering. As discussed above, in the case of absorption, photons incident on a molecule act to promote electrons within that molecule to electronically excited states. When those electrons decay back to their ground energy state, fluorescence photons are emitted. In the case of elastic scattering (which is also referred to as Rayleigh scattering or reflection), the incident photon perturbs the scattering molecule but does not have sufficient energy to promote an electron to its first (or higher) excited state. Instead, an electron is instantaneously promoted to a so-called ‘virtual state’ before immediately decaying back to the ground state. No energy transfer occurs between the photon and the molecule; hence the wavelength of the scattered photon remains unchanged. Inelastic scattering—also referred to as Raman scattering—also involves the instantaneous promotion of an electron to a virtual state. However, in this case, the excited electron decays back into a different vibrational energy level (vibronic mode) to the one that it started in. Due to this

change in the vibronic mode of the molecule there is a concomitant transfer of energy between the molecule and the scattered photon, which can be detected as a change in the wavelength of the photon. Most often the energy is transferred from the photon to the scattering molecule: the molecule gains vibrational energy and the photon loses energy, leading to an increase in its wavelength (known as a Stokes shift). Alternatively, the opposite can also occur when a photon impinges on a molecule that is already in an excited vibrational state. In this case, the perturbation of the molecule caused by the scattering event can lead to the molecule falling into a lower energy vibronic mode. Energy is then transferred from the molecule to the photon and a reduction in the wavelength of the photon—known as an anti-Stokes shift—is observed. The relevant electronic and vibrational transitions that can occur in an optically active (i.e. scattering/absorbing/fluorescent) molecule are shown in the Jablonski diagram in Fig. 6.8.

In theory, the instrumentation required for Raman spectroscopy is identical to that used in fluorescence spectroscopy. Typically, however, Raman signal levels are orders of magnitude lower than those observed in fluorescence measurements. For this reason, high throughput diffraction gratings as well as cooled, high quantum efficiency CCD detectors are often used for Raman measurements, even though these are not necessarily required for fluorescence experiments. They provide improved detection efficiency and allow data to be collected in reasonable acquisition times and with acceptable excitation laser powers. Additionally, a notch (or band-stop) filter (rather than a long pass filter) is often used to block the excitation

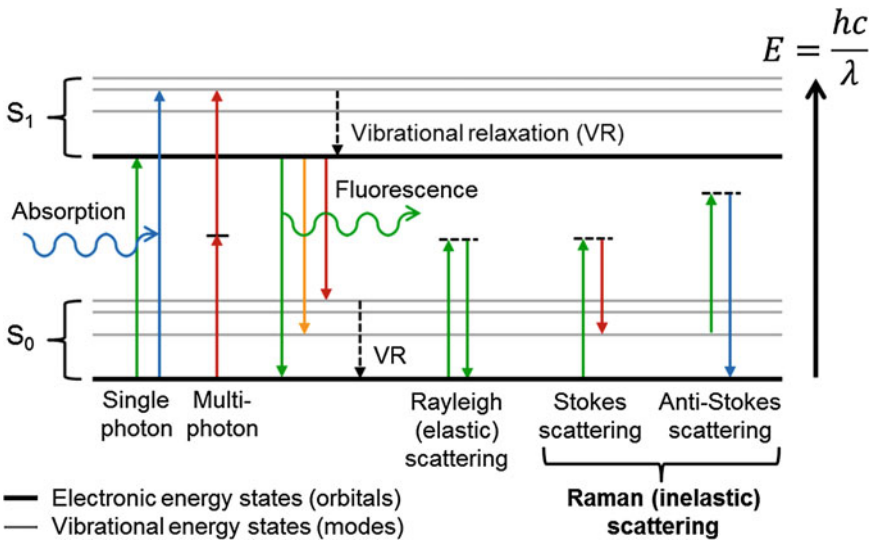

Fig. 6.8 Jablonski energy level diagram showing some electronic and vibrational transitions that can occur in an optically active molecule, including absorption (both single photon and multi-photon), fluorescence, elastic scattering, and Raman (inelastic) scattering. E energy; h Planck's constant; c speed of light; λ wavelength

light. This then allows wavelengths both above and below the excitation wavelength to reach the detector meaning that both the Stokes and anti-Stokes signals can be collected.

Raman spectroscopy is becoming widely used in a variety of different fields and the main reason for this is that it provides very specific signals. In fact, the observed signals are so specific that they can even be used to characterize chemical compounds in terms of their constituent molecular bonds (due to the different bond vibrations that can be excited). Thus, Raman spectroscopy is becoming increasingly common in chemistry, where it is often used for chemical identification [205]. The specificity of the spectra obtained has also meant that Raman spectroscopy has been investigated as a potential clinical tool and this has involved its application to the study of—among many other things—retinal inflammation [206], gastric [207] and oral neoplasia [208], colonic polyps [209], lung cancer [210, 211], brain tumors [212], and dengue virus [213].

As with the techniques described above, Raman spectroscopy is directly compatible with optical fibers, and this compatibility is vital in terms of developing a clinical modality. While the use of optical fibers does present significant hurdles—such as reduced signal collection efficiency and the introduction of background signal (in the form of fluorescence or Raman scattering from the optical fiber itself)—optical fiber-based Raman spectroscopy is now becoming more widespread, with a number of commercial spectrometers and delivery/collection optical fibers now available. Typically, the optical fibers used have optical filters incorporated into them in order to reject both elastically scattered excitation light and any Raman or fluorescence signal from the fiber itself (e.g. RPB Fiber Optic Raman Probe, InPhotonics Inc., USA). Despite the potential limitations imposed by optical fibers, a number of research groups have developed and used optical fiber-based Raman spectrometers (e.g. [214]) for medical applications. Additionally, Raman spectroscopy has been deployed using both endoscopes and catheters [209–211, 215, 216]. Combined with promising results involving the use of Raman spectroscopy for disease diagnosis (e.g. [206–213]), this implies that Raman measurements may well become useful in the clinic in the future.

One particularly promising application of Raman spectroscopy for implantable sensing is in the detection of bacteria for the diagnosis of infection. Raman spectroscopy has been applied to the investigation of bacteria many times, with an important early study being reported by Howard et al. in 1980 [217]. Since then, many bacterial Raman studies have been conducted, showing that Raman spectra can be used to detect the presence of bacteria and to differentiate between different bacterial species (e.g. [218–228]). This has been presented in the context of the food industry where the detection of bacteria is vitally important in terms of food preservation (e.g. [229]). Furthermore, a number of (pre)clinical studies have been reported discussing the use of Raman spectroscopy in the detection of infection. Teh et al. [207] reported the detection of *Helicobacter pylori* infection (a precursor to stomach cancer) in freshly excised gastric tissue samples using a fiber-optic Raman probe, while detection of the bacterium *Shewanella oneidensis* MR-1 using a fiber-optic surface enhanced Raman spectroscopy (SERS) probe was reported by

Yang et al. [226]. In addition, de Siqueira e Oliveira et al. [230] recorded Raman spectra from multiple bacterial species responsible for urinary tract infections (UTIs) using a fiber-based system and demonstrated discrimination of those bacteria by applying PCA to the measured spectra (and this approach is discussed in more detail below).

Considerable work in this area has also been undertaken by the research group of Costas Pitris [218–222]. This group has further demonstrated that Raman spectra can be used to discriminate between multiple bacteria that are relevant to UTIs in an in vitro setting. This was achieved using spectral decomposition techniques and is illustrated in Fig. 6.9. Specifically, it involved the use of PCA to break the spectra down into a small number of base spectral components, followed by the use of linear discriminant analysis (LDA) in order to use the relative contributions of those base spectra to provide an 'optical diagnosis' for each spectrum. In this case, the diagnosis entailed an assessment of the species of bacteria present. This is quite a common approach in optical spectroscopy and has also been used in numerous fluorescence and diffuse reflectance studies. Importantly, it provides a method of automated diagnosis (in this case, automated identification of bacteria), which would be vital in any implanted optical sensor. Interestingly, the authors were also able to use Raman spectra to successfully carry out an antibiogram—i.e. they were able to successfully identify the antibiotic that was best suited to treatment of a specific infection [218–221]. While this work was carried out in vitro, it shows considerable promise as an alternative, improved method for UTI diagnosis and antibiogram, where standard techniques currently require up to two days for a full diagnosis and antibiotic selection.

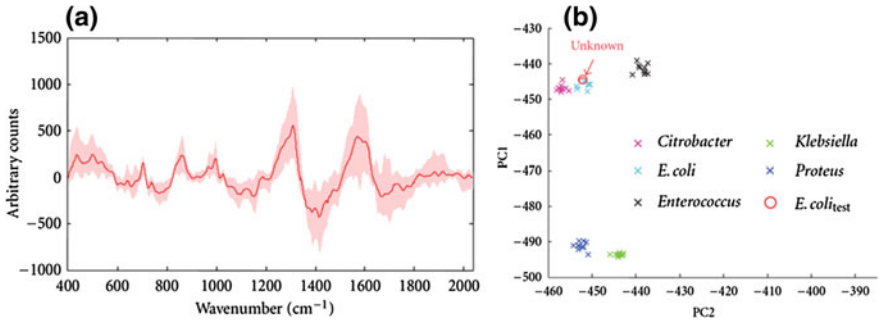

Fig. 6.9 Data illustrating the use of Raman spectroscopy to detect and discriminate between multiple bacteria relevant to urinary tract infections (UTIs). **a** Surface enhanced Raman (SERS) spectra recorded from multiple *Escherichia coli* samples showing the mean spectrum (red line) and the intersample variability (pink). **b** PCA of Raman spectra from multiple bacteria permits accurate classification of each sample. This is illustrated using a plot of the first and second principal components of the spectra calculated using PCA. On this graph, the locations of each of the bacterial species are clearly separated allowing accurate classification. Graphs reproduced from [220] under the terms of the Creative Commons Attribution license CC BY 3.0 (https://creativecommons.org/licenses/by/3.0/), © 2012

An inherent drawback of Raman measurements, discussed briefly above, is the low signal level that is often obtained. This means that long acquisition times and high excitation powers are frequently required in order to obtain an acceptable signal-to-noise ratio (SNR). Neither of these is likely to be compatible with a clinical embodiment; hence much research is currently directed toward the development of methods that provide improved SNRs. One such method is SERS (surface-enhanced Raman spectroscopy, mentioned briefly above) [231], which was first observed (although not initially recognized) by Fleischmann et al. [232]. Typically, SERS involves the use of surface immobilized metal nanostructures to provide an enhancement of the Raman signal. This enhancement is a result of surface plasmons that are excited in the nanostructures and act to amplify the Raman signal, with this amplification being strongest when the plasmon frequency is resonant with the optical radiation (i.e. the excitation light and/or the Raman scattering). A variety of SERS devices have been presented in the literature (e.g. [233–239]). However, enhancement factors (relative to standard Raman scattering measurements) vary greatly between different configurations, and for this reason commercial SERS systems have not yet gained significant market penetration. Nonetheless, and importantly from the perspective of this book, a number of optical fiber-based SERS devices have been reported. These have mostly involved the deposition or immobilization of silver or gold nanoparticles on the tip of an optical fiber, with the fiber then being used to allow fluid measurements via immersion of the fiber tip in the analyte [226, 240–243]. One interesting approach that was recently reported used two-photon lithography to fabricate a 3D structure on an optical fiber tip that provided both surface enhancement and optical focusing, thus also improving the collection efficiency of the probe [244]. Furthermore, optical fiber-based SERS devices have been applied to the measurement and detection of bacteria [226] and it is easy to see how this type of device could become useful clinically in the future. Particularly useful clinical embodiments could include fiber-optic SERS devices incorporated into urinary or central venous catheters. The fiber-optic tip of such a device would be minimally invasive and could feasibly be implanted as a tethered format. SERS could then be used to monitor for signs of infection, and UTIs appear to be a particularly promising target, as these are especially common in patients using urinary catheters and in vitro research has already been published reporting the use of Raman spectra to detect the relevant bacteria (see above and [218–222, 230]). Of course, the external housing of such a tethered implantable device would also need to be miniaturized in order that it could be worn or easily carried by the patient. However, portable handheld Raman spectrometers are available commercially and further miniaturization to produce clinically useful devices should be possible.

Overall, Raman spectroscopy and SERS are promising modalities for clinical applications with many potential diagnostic uses. In particular, the application of Raman measurements to the detection and discrimination of bacteria appears to provide a promising avenue for the development of tethered implantable devices based on optical fibers. Such devices could be used in patients recovering from surgery or in those requiring the use of catheters, for which infections are especially

prevalent. In these circumstances, a minimally invasive implanted device that is capable of detecting infections early, before symptoms become severe, would provide considerable clinical benefit. Raman spectroscopy has the potential to be used for this purpose, and research in this area is likely to continue and increase in the coming years.

6.4.5 *Other Optical Fiber-Based Sensing Modalities*

Beyond the methods described above, there are also many further optical fiber-based sensing techniques—some of which have potential applications in healthcare—and these are described briefly in this section.

Fiber Bragg gratings [245, 246] have been widely used for environmental sensing purposes, for example in the measurement of strain and temperature. However these are typically used in industrial applications and are not particularly relevant here (although a number of fiber Bragg grating sensors have been applied to in vivo monitoring of peristalsis, e.g. [247, 248]). A more promising technique for medical applications is optical fiber-based Fabry–Perot interferometry [249], in which a small Fabry–Perot etalon is deposited on the tip of an optical fiber. The wavelength of the light reflected back from this etalon can then be used to determine a number of parameters, including temperature, pressure, refractive index and even acoustic wave frequency. As with fiber Bragg gratings, Fabry–Perot systems have mainly been developed for industrial applications; however, they are more versatile and could certainly be used clinically due to their forward viewing arrangement. Furthermore, the range of sensing targets is higher, and some—including pressure and acoustic wave frequency—have more obvious clinical applications, for example in minimally invasive ultrasound measurements or blood pressure monitoring. Indeed, a fiber-optic Fabry–Perot blood pressure sensor was recently reported by Wu et al. with in vivo use demonstrated in the aortic arch and right coronary artery of a pig by introducing the probe into the artery through a catheter [250].

Finally, there are several further optical fiber-based sensing modalities that rely upon the immobilization of a sensing layer or membrane on the tip of an optical fiber. This sensing layer exhibits changes in its optical properties (for example, its refractive index, its absorption profile, or its fluorescence emission wavelength) when it comes into contact with a specific chemical compound or biological species. Fiber-optic devices of this sort have been used as chemical sensors (to detect the presence or concentration of particular elements or compounds) [251–255], biosensors (for example, for the detection of glucose [256]), and ion sensors (which allow measurement of ion concentrations and, hence, pH) [251, 254, 257–263]. One approach that has been particularly useful in the development of these types of fiber-optic sensors is the production of so-called sol-gel films [4, 264]. Sol-gel technology allows the fabrication of thin, porous glass layers on the tips of optical fibers using a relatively simple polymerization reaction. The resulting films can

have high homogeneity and purity and are also chemically inert. Furthermore, it is possible to encapsulate sensing molecules into the sol-gel glass via simple modifications of the polymerization protocol. This technology has become widely used in the development of optical fiber sensors and one particularly prevalent application has been in pH sensing. For this reason, sol-gel based optical fiber sensing technology has the potential to become useful medically where measurements of pH or other ion concentrations could be very valuable. Additionally, biosensing could also be very useful medically and this has been achieved using modified sol-gel preparation procedures that allow the encapsulation of chosen biomolecules within the sol-gel matrix.

While the sensing modalities addressed in this section are still under development, they certainly have potential merit as medical sensors. Moreover, some can be applied using a single fiber with a (relatively) simple modification (i.e. the production of a Fabry–Perot etalon or a sol-gel film) to the optical fiber tip. For this reason, it is again easy to envisage the use of these techniques as tethered implantable sensors, where the tip of the optical fiber sensor could be incorporated into a clinical catheter or needle in a straightforward manner. Of course, other fiber-optic sensing modalities exist and this review is certainly not exhaustive. However, the techniques reported above should provide a reasonably complete summary of approaches that could be used clinically—perhaps as (tethered) implants—in the future.

6.5 Implantable Visual Prosthetics

In addition to the diagnostic devices described above, implantable optical systems have also been deployed for therapeutic purposes, in particular for the treatment of vision loss. Such implants are used in the treatment of cataracts, retinitis pigmentosa (RP), and age-related macular degeneration (AMD), and are described briefly in the following sections.

6.5.1 Intraocular Lens Implants

Cataracts—clouding of the lens in the eye leading to impaired vision—have long been treated by surgically removing the lens and replacing it with a synthetic implant known as an intraocular lens (IOL). This procedure was first reported in 1949, and found more widespread applications from the late 1970s and early 1980s [265]. Traditionally, the implanted lenses had a single focal length, providing good distance vision but poor near-field sight. Thus, patients with so-called monofocal IOL implants would typically require reading glasses after surgery. To combat this issue, accommodating and multifocal IOLs have been developed over the last 20–30 years, with the latter now widely used clinically [266–268]. Accommodating

IOLs interact with the ciliary muscles within the eye to provide forward and backward movement of the implanted lens, hence allowing the patient to focus on both near and distant objects. While in theory this approach will offer clear vision over all distances, in practice the range of accommodation (i.e. the range of movement of the lens, and hence the range of focal lengths that it provides) often remains insufficient to provide truly spectacle-free post-operative sight [267, 268].

Multifocal IOLs, on the other hand, focus light to multiple points using diffractive or refractive effects (or a combination of both in the case of hybrid multifocal IOLs). Refractive IOLs feature two or more spherical zones with different radii of curvature, which each focus light to a different focal point [267, 268]. As the pupil dilates or constricts, more or less light is focused to each of the discrete focal points. In the majority of patients, pupil diameter changes as they focus on near or distant objects [269] and this effect helps the function of refractive IOLs. When focusing on a distant object the pupil dilates, allowing more light to pass through the outer portion of the IOL, which is optimized for distance vision. Similarly, the pupil constricts when the eye is focused on a near object, causing the light to pass through the central region of the lens, which has a shorter focal length designed for near-field vision. Diffractive IOLs generate multiple points of focus in a different manner. A series of concentric rings of different heights acts as a phase mask that diffracts light to two or more different points simultaneously. In contrast to refractive systems, the foci generated by diffractive IOLs are independent of pupil diameter [268]. Despite this, they can still provide clear vision at multiple focal distances, as patients will primarily perceive only the focused image [268, 270–272].

Both refractive and diffractive multifocal IOLs provide improved near vision relative to their monofocal counterparts [266–268]. However, both also have drawbacks. For example, halos and glare are more common than in monofocal IOLs [268, 273, 274] and the contrast of the retinal image is typically poorer [266, 267]. This is an effect of the defocused images reaching the retina as well as aberrations within the lens itself, and it can be further exacerbated by tilt or displacement of the implanted lens [275]. Several hybrid IOLs have been and are being developed, which combine both refractive and diffractive features into single lenses with the aim of improving image clarity while maintaining good vision over all distances [268]. Despite their limitations, both multifocal and monofocal IOL implants are in widespread clinical use, with surgeons often recommending different lenses for different patients in order to best address the needs of the individual. Indeed, in some cases patients will even have a different type of IOL implanted in each eye in order to obtain the best possible tradeoff between near and distance vision.

6.5.2 Visual Prostheses

Further ocular implants are also used in the treatment of RP and AMD, both of which cause the onset of blindness through degradation of the photoreceptors (the

rods and cones) in the retina. Importantly, in both diseases, the inner nerve cells in the retina—the bipolar cells, the retinal ganglion cells (RGCs), and the axons—as well as the tissues responsible for transmission and processing of visual signals in the eye and brain (such as the optic nerve and the visual cortex) remain functional [276–278] (although there is some secondary degeneration and remodeling of the retinal neurons [277, 279–282]). In the healthy retina, the photoreceptive rods and cones absorb light and then send electrical signals to the bipolar cells that are transmitted to the brain via the RGCs, the axons, and the optic nerve. Thus, as only the photoreceptors are damaged in RP and AMD, it should theoretically be possible to induce visual signals (phosphenes) in patients with these conditions by electrically stimulating the bipolar cells, RGCs, axons, or the optic nerve [276–278]. Alternatively, phosphenes can also be generated by stimulating the regions of the brain that are responsible for processing and interpreting visual information, for example, the visual cortex [283, 284]. Indeed, several studies have reported the development of devices that can be implanted in the eye and instigate a degree of vision in blind patients by electrically stimulating the retina (detailed reviews can be found in [276–278]). Furthermore, a small number of systems have also been commercialized and are now available clinically (e.g. Argus II (Second Sight Medical Products, USA) [285], Alpha-IMS (Retina Implant AG, Germany) [286–288], Iris II (Pixium Vision, France) [289]).

These devices are known as visual or retinal prostheses and they can be broadly categorized according to the technology on which they are based or the region of the retina in which they are implanted. The majority of systems require implantation in or on the retina, although stimulation of the brain and optic nerve have also been reported [276–278]. Of the more common retinal implants, the smallest systems consist of an array of photodiodes that is placed close to or within the retina. The eye focuses light onto the photodiodes, which then convert that light into electrical impulses that stimulate (depolarize) the bipolar cells and/or RGCs, hence inducing a visual signal [286]. Photodiodes have the advantage of containing all the necessary electronics to provide synthetic vision within the implant itself, and thus do not theoretically require wires, batteries, or external components. A significant drawback, however, is that photodiodes alone are often incapable of providing sufficient current to efficiently activate the retinal neurons. To circumvent this problem, an example device has been reported that incorporates an amplification circuit within each pixel along with an external head-mounted power source that is used to inductively drive the implant (Fig. 6.10a). This system delivers larger currents to the retinal neurons and more efficiently stimulates the visual pathway [286, 287]. Photodiode-based systems are typically implanted within the retina at the location of the degenerated photoreceptors such that the photodiodes directly replace the photosensitive cells and stimulate the bipolar cells. This approach has the advantage of requiring little or no processing of the stimulation signal as the targeted neurons are those directly proximal to the photoreceptors. Due to the implantation location, these devices are referred to as subretinal implants.

In the most common alternative, the implant contains only the stimulation electronics, and the sensing elements are dispensed with. Instead, a camera mounted

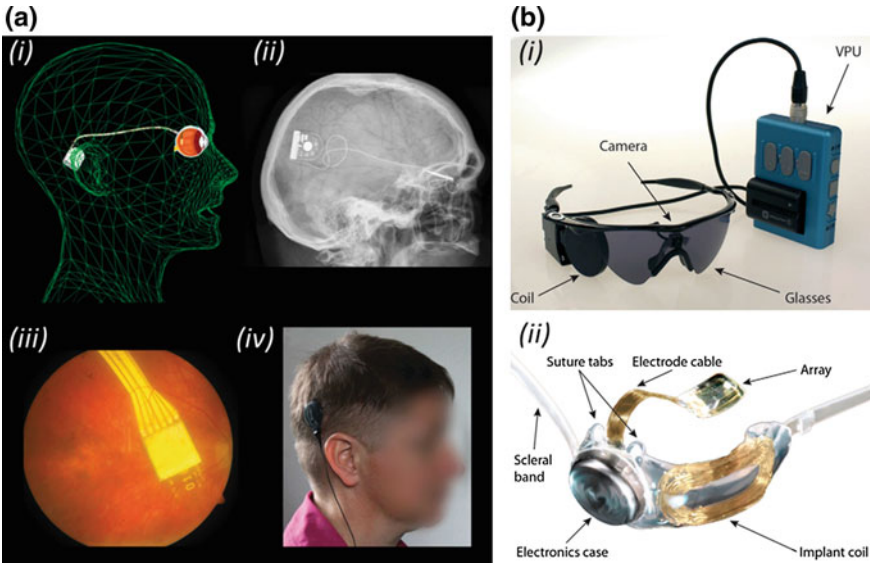

Fig. 6.10 Implantable retinal prostheses: **a** the Alpha-IMS subretinal implant and **b** the Argus II epiretinal implant. **a** Diagrams and images of the Alpha-IMS system showing: (i) 3D diagram and (ii) X-ray image of the retinal prosthesis and the coil implanted behind the ear to allow external control and powering; (iii) photograph of the retina after implantation of the 3 mm × 3 mm chip beneath the fovea; (iv) photograph of the primary external coil, which is magnetically mounted above the implanted coil shown in (i) and (ii), and provides power and signals to the implant via electrical induction. **b** Images of the Argus II visual prosthesis: (i) external components including glasses (with mounted camera and external powering coil) and visual processing unit (VPU); (ii) internal components, including the electrode array, the internal coil for wireless power delivery, the electronics casing, and the suture tabs and scleral band used to fix the implant in place on the retinal surface. **a** Reproduced from [287] under the terms of the Creative Commons Attribution license CC BY 4.0 (https://creativecommons.org/licenses/by/4.0/), © 2013. **b** Reproduced from [290], © 2012, with permission from Elsevier

on a pair of glasses is used to capture the image and an external processing unit converts the visual information into an electrical signal to be delivered by the electrodes in the implant (Fig. 6.10b). This signal is transmitted to the implant by an external power source and a transcutaneous telemetry link very similar to that used in the wirelessly powered photodiode-based system described above [290–292]. In this case, the implants are typically fixed onto the outer surface of the retina (i.e. on the vitreal side, the side closer to the front of the eye) and are thus known as epiretinal implants. This means that the stimulation signal is delivered to more distal parts of the retinal neural processing network—either the RGCs or the axons. In turn, this acts as both an advantage and a disadvantage. On the one hand, stimulating more distal neurons means that lower threshold currents are required to elicit visual signals. On the other hand, addressing the RGCs or axons means that more advanced processing of the visual signal is required (as the bypassed

photoreceptors and bipolar cells provide a degree of processing in the healthy eye) and this explains the use of an external visual processing unit (VPU).

Of course, both approaches have pros and cons. The subretinal photodiode-based implants represent the system with the smallest impact on the patient, with the only necessary external component being a wireless power source, which consists of a small telemetry link worn on the head and a battery pack [287]. The external constituents of epiretinal prostheses, on the other hand, typically also entail a pair of glasses to mount a camera as well as a VPU. While this increases the external footprint of the device, it also acts to simplify the electronics of the implanted chip (which entails only stimulation electrodes and not photodiodes or amplification circuits). Furthermore, as epiretinal implants are positioned on—rather than below—the surface of the retina, the implantation procedure is simpler than for subretinal systems and the constraints on the size of the chip are less stringent. This represents a clear advantage of epiretinal implants, but also brings an important drawback: using a head-mounted camera to capture the image rather than an implanted array of photodiodes means that the phosphenes (or the image) perceived by the patient will change only in response to head movements and not as a result of changes in the direction of the patient's gaze (i.e. the direction in which their eyes are looking).

Despite the current limitations of the two methods, commercial systems have been released based on both [276], and devices based on other concepts and/or implant locations have also been reported (and in some cases commercialized) [278]. The Argus II device was recently brought to market by Second Sight Medical Products [285] and has been approved for use in the treatment of late-stage RP in both Europe and the USA. It is an epiretinal system consisting of an implantable array of 60 electrodes, a pair of glasses with a mounted camera and wireless powering unit, and a VPU. A similar system is also available from Pixium Vision—the Iris II Bionic Vision Restoration System—which is CE marked (i.e. it has European regulatory approval) for use in RP and is currently undergoing clinical trials [289]. In addition, the Alpha-IMS is a subretinal device that entails an implantable array of 1500 photodiodes/electrodes and an external power source to drive amplification circuits within the chip [287]. This system has been commercialized by Retina Implant AG [288] and has recently received regulatory approval for the treatment of late-stage RP in Europe.

Naturally, further systems are also under investigation that do not fall perfectly into either of the two categories discussed above. For example, Pixium Vision are developing a subretinal implant [293, 294] that uses an external camera for image detection in combination with an implanted photovoltaic array and a near IR image projection system that is integrated into the goggles that house the camera (PRIMA Bionic Vision Restoration System [295]). This system is effectively a hybrid of the photodiode and camera-based approaches discussed above and has the advantage that the implant does not require a power supply, as the near IR image projection system provides a high enough light intensity to generate sufficient current in the implanted photodiodes to efficiently activate the retinal neurons. As a result, the necessary surgery is much simpler than for implants with extra-ocular wireless powering links. Furthermore, the connection between eye movement and image

perception is maintained, as this device uses the eye's optical system to transmit information from the image projector to the retinal implant. However, despite the potential advances offered by this system, it is at a considerably earlier stage of development than the three commercially available devices described above.

In addition to the PRIMA system from Pixium, several other visual prostheses have been reported that generate synthetic vision with alternate approaches to the epiretinal and subretinal implants discussed above. Suprachoroidal implants are typically positioned between the choroid and the sclera. The greater distance from the retina renders the surgery simpler and safer; however, this also acts to increase the stimulation thresholds. Nonetheless, there have been reports of safe stimulation in animals using this approach [296, 297] and recent clinical studies have demonstrated that suprachoroidal systems can stimulate visual percepts in blind patients [298, 299]. Further alternative approaches involve placing the electrodes further from the retina, with the aim of stimulating deeper layers of the visual pathway. Example devices of this kind have been reported for stimulation of the optic nerve [300–302] and the visual cortex [303–305]. While these latter methods offer opportunities to treat blindness caused by degeneration of more than just the photoreceptive cells in the retina, clinical research is at a much earlier stage than for retinal prostheses [276].

For the more common epiretinal and subretinal implants, clinical trials have reached a more advanced stage and several studies have demonstrated improvements in the vision of blind patients. With the Argus II and Alpha-IMS devices (as well as with several other systems including earlier embodiments such as the Argus I), improvements have been reported in the ability of patients to perform simple tasks such as object identification and localization. In addition, patients' visual acuities (a common measure of the clarity of vision) have been shown to improve when using the prostheses [276–278, 286, 287, 290]. While these early results are of course very promising, it is worth noting that the visual acuities reported to date are still well below the level at which patients are classified as legally blind. For this reason, significant work in this field is still required, and this will involve further device development alongside physiological studies aimed at better elucidating the relationship between the electrical stimulation protocol and the phosphenes that are invoked in the patient. Indeed, some particularly interesting questions remain in this area, with one important example being how to increase the number of image pixels perceived by the patient (which is not currently believed to be a simple function of the number of stimulating electrodes [277]). Nonetheless, despite the many outstanding challenges, the use of visual prostheses can be expected to increase significantly in the future as more advanced devices are developed that provide more profound enhancements to the vision of blind patients.

6.6 Optogenetics

As a further example of optical techniques used as implants, this section presents a discussion of the current progress in optogenetics. Optogenetics involves the genetic modification of nerve cells—most often neurons in the brain—in order to render them sensitive to light. Subsequently, the sensitized neurons can be addressed optically (by focusing light onto chosen cells) allowing control of particular functions or events [306, 307]. This is analogous to the electrical activation of neurons used in the visual prostheses described in Sect. 6.5.2. In recent years, optogenetics has been widely applied in the field of neuroscience, where many in vitro cell studies and in vivo animal experiments have been conducted aimed at elucidating and understanding signaling pathways in the brain. Experiments such as these have shown great promise, not only in the study of neurological function, but also in the investigation of the causes and effects of a multitude of brain disorders (including Parkinson's disease [308]). Importantly, this has provided many valuable new insights into possible modes of treatment for such disorders. Furthermore, the growing use of optogenetic techniques has triggered much discussion about the potential development of neural implants based on optogenetics that would allow treatment of a wide range of ailments, including brain injuries, depression, and even drug/alcohol dependency. While this field does not have particular significance in the area of optical sensing, it is certainly relevant in terms of the development of optical implants. For this reason, optogenetics is discussed in this chapter and the following sections describe the basic principles, the development of miniaturized devices suitable for implantation in animals, and progress towards medical optogenetic systems for use in humans. The latter section has a focus on optogenetic retinal prostheses—which aim to restore vision to the blind—but also discusses the possible future development of more ambitious fully implantable systems for use in the brain.

6.6.1 Theoretical Background

Optogenetics involves the combination of the genetic modification of neurons (or other nerve cells) to render them sensitive to light with the subsequent use of optical techniques to address the sensitized neurons. It relies heavily on the discovery of light-sensitive ion channels and ion pumps such as Channelrhodopsin-2 (ChR2) [309], Halorhodopsin (NpHR) [310], and Archaerhodopsin (Arch) [311]. If a neuron expresses one (or more) of these light-sensitive opsin proteins then its membrane will be depolarized (for neural excitation) or hyperpolarized (for neural inhibition) when illuminated with light of the appropriate wavelength and intensity [312, 313]. Depolarization of neuronal membranes involves the transfer of positively charged ions (Na^+ or Ca^{2+}) from the extracellular space into the cell cytoplasm. The charge within the cells then becomes more positive, and importantly this

induces the firing of action potentials, which are central to cell–cell communication. Conversely, hyperpolarization involves a cell's membrane potential becoming more negative and occurs either through an efflux of potassium (K^+) ions or an influx of chloride (Cl^-) ions. This inhibits action potentials by effectively increasing the threshold for depolarization (by making the cell's resting potential more negative). Thus, by modulating ion channels/pumps it is possible to control certain signaling pathways in the nervous system and hence influence the behavior of tissues or even live, freely moving animals. Using light-sensitive ion channels/pumps (such as ChR2, NpHR, and Arch) it is possible to achieve this neuronal control using optics and this concept is illustrated in Fig. 6.11 [306, 307, 313, 314].

In order to carry out any optogenetic study it is first necessary to modify specific cells in order that they express one (or more) of the light-sensitive opsin proteins discussed above. These proteins allow control of ion flows as they can reversibly bind to the co-factor retinal, with this binding reaction reliant upon the incident light intensity (and wavelength). Depending on their binding state, the proteins will then provide either an "open" or "closed" configuration for the ion channel/pump. Significantly, vertebrate tissues contain naturally occurring retinal, which means that optogenetic control can be permitted simply through the expression of an appropriate opsin protein and without the need for any additional chemicals or components (i.e. without the separate and additional introduction of retinal, for which it would be considerably more difficult to obtain cellular specificity) [306].

The expression of opsins in mammalian cells can be achieved in a number of ways. One option is to use transgenic animals that have been genetically engineered to express the appropriate opsins in specific cells, and a number of transgenic opsin-expressing mouse lines have now been reported (e.g. [315, 316]). An alternative approach is to use a viral expression system. In this case a virus is injected into the host animal, which causes rapid production of a particular opsin. With viral expression, cellular specificity can be obtained by using particular promoters (viral receptors) that act to target the virus to specific types of cells (although this

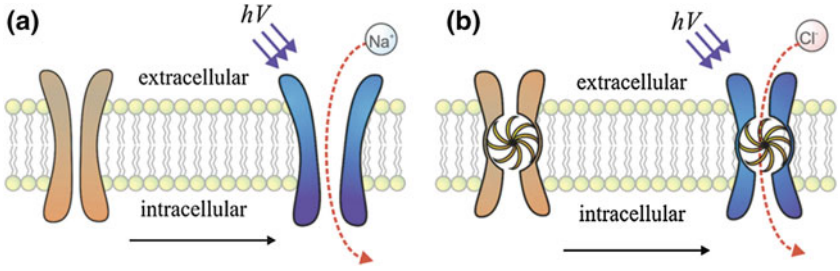

Fig. 6.11 Schematics explaining the function of light-sensitive ion channels (**a**) and ion pumps (**b**). **a** The light-sensitive ion channel ChR2 opens upon irradiation allowing positively charged ions (Na^+) to diffuse into the cell leading to depolarization. **b** The light-sensitive ion pump NpHR is activated when irradiated with light of the appropriate wavelength and induces an influx of Cl^- ions. This leads to hyperpolarization, which inhibits the neuron. Diagrams reproduced with permission from [314], © 2014

approach is actually more efficient in transgenic animals than it is in viral expression in wild type animals). Alternatively, the virus can simply be spatially targeted by injecting a small quantity into a chosen region of tissue, and in practice both techniques are often used in conjunction. Viral expression systems have now been used in multiple live mammals (including mice, rats, and primates) and in all cases the introduced viral vectors have been well tolerated, the proteins have been highly expressed over long periods of time, and no adverse effects have been reported [317]. Interestingly, this reveals the possibility of the use of optogenetics in human subjects, where it could be applied in retinal prostheses or for the treatment of conditions such as depression (see Sect. 6.6.3). Further discussion of the genetic expression of opsin proteins is beyond the scope of this chapter; however, the interested reader can find more details in [307].

With opsin expression successfully achieved, optogenetics then relies solely on optics for the illumination of specific neurons at chosen times in order to elicit a particular response in the subject. This has been realized with a number of different optical systems using filtered lamps, lasers, or LEDs as light sources and with optical fibers often used for light delivery [307, 313]. Using such systems, many researchers have now reported behavioral control in freely moving animals as well as the study of neuronal function and the causes/effects of multiple neurological conditions (e.g. [308, 317–321]). As such, optogenetics is an exciting field of study that has the potential to provide medical advances as well as vital tools for the study of numerous brain disorders. For this reason, considerable research is now directed towards the production of smaller systems that can be used as implants so that truly freely moving animals can be studied. Such implantable systems may also be useful medically in the future and progress towards these miniature systems is discussed in the following section.

6.6.2 Towards Miniaturized Optogenetic Implants

As mentioned above, optogenetics is a promising tool for the study of many neurological disorders and may also hold potential for the treatment of such conditions in the form of medical implants. In order to carry out optogenetic studies in animals it is necessary to mount or implant an optical system on (or inside) the skull of the animal to allow control of the photosensitized neurons. To monitor the effects of the optogenetic excitation/inhibition of neurons in the most physiologically relevant manner it is desirable to have an optical illumination system that does not impair the movement of the animal in any way. To this end, much work has been undertaken aimed at miniaturizing the optical systems used in optogenetics. Ideally, fully implantable wireless systems should be used where the animal is not tethered to any nearby device and can be studied during normal behavior while moving around freely without any restrictions. Such systems will allow high-fidelity optogenetic studies to be carried out and will also provide a potential route for the production of future optogenetic implants for medical use in humans. Progress towards the

development of miniaturized optogenetic implants is discussed below and is also reviewed in detail in [313].

The first report of optogenetic control of intact animal brains was published by Aravanis et al. in 2007 [321]. In this study, motor control in living rodents was stimulated using an intracranial multimode optical fiber coupled to a solid state diode laser. Several similar systems using lasers or LEDs coupled to optical fibers for light delivery were reported subsequently (e.g. [327–329]); however, the drawback of this approach is that it is non-specific due to the diffuse illumination, which activates many surrounding neurons. To improve upon this, many further devices have since been developed that allow selective activation of individual neurons. As with less advanced systems, these use either lasers or LEDs as illumination sources, but have more complex methods of light delivery. One such approach involves the use of optical fibers with sharpened tips (produced through chemical etching techniques), which was reported, for example, in [330]. The thinner tips of these sharpened fibers provide improved spatial resolution and also reduce the risk of tissue damage as the probe is inserted into the brain. Additionally, they permit stimulation of deep-lying neurons and provide flexibility of the chosen illumination depth as the etched optical fiber can be inserted into areas below the tissue surface. The drawback, however, is that this method only allows single-site stimulation. An illustration of an example sharpened optical fiber-based optogenetic probe is shown in Fig. 6.12a, where measurement of the neuronal activity is also provided by a second hollow core fiber filled with NaCl, which acts as an electrode [322].

An illumination modality that can provide multi-site stimulation is the use of micro-waveguide arrays. These have a variety of forms, but usually allow laser light to be coupled into a small waveguide that is inserted at a fixed depth in the brain. In some cases numerous waveguides are incorporated into a single device such that simultaneous (or rapid sequential) stimulation of multiple spatially distinct sites is possible. Examples of micro-waveguide array-based optogenetic devices are presented in [323, 331] and one such system is shown in Fig. 6.12b.

The above approaches—based on the use of sharpened optical fibers or waveguide arrays—have typically used lasers as illumination sources due to their high light intensity and narrow spectral bandwidth. Beyond these, a number of devices have also been reported that use LEDs. An obvious advantage is the small size of LEDs (relative to lasers), which means that they can be incorporated into the implantable device itself, precluding the requirement for optical fibers to deliver light from the illumination source to the optogenetic implant. Combined with the low power consumption of LEDs, this means that they are suitable for integration into fully wireless, untethered devices for applications in freely behaving animals. A number of LED-based implantable optogenetic devices have been presented in the literature, with some early systems using standard commercial LEDs [332–334]. In order to reduce size and improve spatial resolution, micro-scale LEDs (μLEDs) have since been used and the formats of these systems have generally been designed to mimic the features of either Utah-style (e.g. [324–326]) or Michigan-style (e.g. [335, 336]) electrode arrays. Both surface-mounted μLED

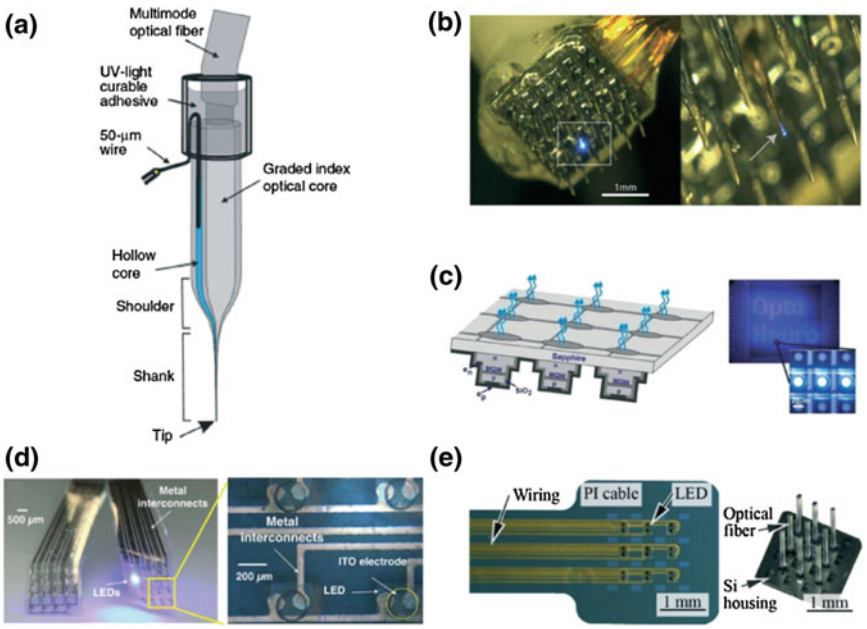

Fig. 6.12 Example implantable stimulation and measurement devices for optogenetics. **a** A dual core optical fiber system with a sharpened tip allowing deep implantation. One fiber core provides optical stimulation while the second is a hollow core fiber that is filled with NaCl. This second fiber core acts as an electrode for measurement of neural activity. Reproduced with permission from Macmillan Publishers Ltd: Nature Methods [322], © 2011. **b** An electrode measurement array in which one electrode has been replaced with a multimode optical fiber to allow optical stimulation. Reproduced with permission from [323]. © IOP Publishing 2012. All rights reserved. **c** A high-density μLED array that permits multi-site surface stimulation. Reproduced with permission from [324]. © IOP Publishing 2010. All rights reserved. **d** A combined μLED and micro-electrode array on a transparent platform allowing both optical stimulation and electrical recording of cortical activity. Reproduced with permission from [325]. © IEEE 2013. **e** A μLED-coupled optical fiber array permitting sub-surface multi-site optical stimulation. Reproduced with permission from [326]. © IEEE 2015

arrays [324, 325] and optical fiber- or waveguide-coupled μLED arrays [326, 337, 338] have been reported, with the latter utilizing short sections of optical fiber or other waveguiding material to permit neural stimulation below the surface of the brain. Importantly, both approaches allow the generation of optical stimulation patterns with high temporal and spatial resolution (on the order of milliseconds and micrometers respectively). Some example implantable μLED-based optogentic devices are shown in Fig. 6.12c–e.

While the techniques described above allow for carefully controlled, multi-site optical stimulation of neurons with high temporal and spatial resolution, there is also a need to read out the effects of the stimulation. For this reason, many of the systems discussed above have also incorporated neural readout electrodes. On the one hand this has involved the addition of measurement electrodes to optogenetic

stimulation systems based on sharpened optical fibers [322, 329] (for example, see Fig. 6.12a). Alternatively, micro-waveguides or μLEDs have been incorporated into electrode arrays to allow both stimulation and measurement at multiple sites simultaneously (e.g., [323, 325]). An example system that uses a micro-waveguide for excitation is shown in Fig. 6.12b, where one measurement electrode in an array has been replaced by a multimode optical fiber allowing optical stimulation at a single fixed location along with measurement of multiple surrounding areas [323].

Finally, it is also worth noting that a number of truly wireless optogenetic stimulation devices have been developed, and these can be divided into two distinct categories of neural implants: battery-powered [339–341] and battery-free [342, 343]. As the name suggests, battery-powered neural implants dispense with external powering through the incorporation of a battery in the implant. This provides a straightforward method for the development of entirely untethered devices, but drawbacks include the limited operation time of the implant and the additional weight that the battery imparts to the head of the animal. Battery-free approaches, on the other hand, do not incorporate batteries in the implants and instead rely upon wireless transmission of power. For optogenetic applications this has been achieved using both inductive coupling and radio-frequency (RF) scavenging techniques. A particularly interesting device was recently reported by Park et al. [344] in which wireless RF powering was combined with the use of flexible electronics to produce a soft, stretchable implant that was used for stimulation of the spinal cord or the sciatic nerve in mice. Importantly, these devices remained functional for up to six months after implantation (with at least one use per month). More information on both inductive coupling and RF scavenging can be found in Chap. 7, which discusses progress towards battery-less medical implants and wireless powering telemetries in detail.

Overall, marked progress has been made in recent years on the development of miniature implantable devices for optogenetic stimulation. Alongside this research, much work has also been directed towards the production of more advanced light-sensitive proteins that provide higher transfection efficiencies, improved specificity, or lower activation thresholds. Further discussion of this biological work is beyond the scope of this chapter, but more details can be found in the review published by Fenno et al. [307]. Taken together, these developments have driven significant advances in the field of optogenetics, permitting studies to be carried out in less and less invasive fashions. This research is likely to continue and will provide many useful tools that may be used in biomedical studies of neural function and disease. In the future, this technology may even be used to develop medical devices and/or implants for use in humans. Indeed, work towards this goal is already under way and this is addressed in the following section.

6.6.3 Clinical Optogenetics

The development of optogenetics—particularly miniaturized optogenetic devices suitable for implantation in animals—has raised many interesting questions about the potential use of optogenetics in humans. In terms of neural implants this could entail the treatment of a vast range of disorders, including depression and even substance abuse. However, the development of such medical implants is still only in the conceptual stage. A medical application of optogenetics that has reached a much later stage of development is its use as a form of visual prosthesis, which is aimed at restoring sight in those who suffer from blindness. Importantly, as the eye is transparent, photo-stimulation can be achieved externally, without the need for an implant. Additionally (as discussed in Sect. 6.5.2), in many cases of blindness the photoreceptors in the retina degenerate, causing a complete loss of vision; however, a functional neural link from the retina to the brain is still maintained. In such scenarios, it should be possible to (optically) stimulate those remaining neural links and hence restore the patient's vision.

The basic concept behind the use of optogenetics for visual prostheses—or more specifically, retinal prostheses—would first involve photosensitizing a remaining neural layer in the retina using one of the opsins discussed above. In an ideal case, this alone would lead to complete visual restoration. In reality, however, this may prove very difficult for a number of reasons. Firstly, in a typical case, the patient may have suffered a loss of function in the light-sensitive rods and cones in their retina, meaning that neurons in secondary layers would need to be photosensitized. During normal vision in a healthy subject, a significant degree of retinal processing occurs as signals are transmitted through several layers of nerve cells. Due to this processing, the stimulation that is required in secondary (or higher) retinal nerve layers to produce a specific visual effect will be significantly different to that required in the primary layers (i.e. in the rods and cones). Secondly, the optical powers required for stimulation of most opsin proteins can be quite high (up to several mW mm^{-2}) meaning that ambient light would not be sufficient for photo-stimulation. Thus, an optogenetic retinal prosthesis would most likely also involve the use of a headset or pair of glasses that projects light into the eye in order to stimulate the photosensitized cells.

Considerable research has been undertaken aimed at the development of retinal prostheses based on optogenetics. On the one hand, this has involved studies of the effects of photosensitizing the retinas of animals (typically mice and rats) with degenerative visual conditions. Promising results have been obtained in a number of investigations where the stimulation of action potentials and visual-evoked potentials (VEPs) has been achieved in live, blind animals after transfection with a chosen opsin. The first such study was reported by Bi et al. in 2006 [345], and since then a number of articles have been published discussing similar results in different animals or using different combinations of opsins, promoters, and expression methods [346–349].

Complementary to this research, much work has also been directed towards the development of appropriate display technology for use in optogenetic headsets or glasses. Primarily this entails the production of displays with appropriate resolutions to provide a reasonably complete restoration of vision and with optical powers high enough to permit efficient photo-stimulation of the sensitized retinal cells. The display techniques investigated have included: spatial light modulation (for example, using micro-mirror or liquid crystal arrays) with compact lasers or high-luminance LEDs as light sources; mechanical laser beam scanning; holography, also using laser excitation [350]; and high-power LED arrays [324, 351, 352]. Each has benefits and drawbacks, but the main requirement is that the display can be small enough to be comfortably mounted on a headset or pair of glasses while still providing sufficient resolution and excitation power. Beyond this, an optogenetic headset would also need to incorporate a small camera with which to obtain the visual information to be projected and it would need to provide processing of the recorded image such that the necessary optical stimulation signal can be calculated (i.e. the external components of the prosthesis would be similar to those used in the camera-based visual prostheses described in Sect. 6.5.2).

Of course, research into the development of display systems and transfection techniques for optogenetic retinal prostheses is still under way, and a detailed review of the work carried out to date can be found in [314]. Overall, the use of optogenetics for visual restoration via retinal prosthesis is an exciting field of study with the potential for considerable impact in medicine. Much work is still required before this can be realized though, and this must first involve the evaluation of the safety of virally transfecting human retinas with light-sensitive opsins. Once this work is complete, first-in-human retinal prosthesis trials can begin and these may act as precursors to later investigations into the use of more complex implantable optogenetic systems for neural stimulation in the brain. In the nearer term, however, the true impact of optogenetics is likely to be found not in medical implants and prostheses, but rather in the fundamental biological and neurological studies that it permits. Such investigations have already provided considerable advances in our understanding of a number of diseases (including Parkinson's) and will continue to do so in the future as the optogenetic toolbox is expanded further.

6.7 Conclusions

In this chapter, a variety of optical techniques have been discussed that are being developed with potential future applications as medical implants. The bulk of the chapter is focused on the development of implantable optical sensing modalities that may become useful in disease diagnosis and patient health monitoring. A particularly promising application of miniaturized implantable optical sensors would be in the detection of surgical site infection (SSI), which is a common post-surgical complication that can cause increased patient recovery times and even

increased patient mortality [353, 354]. Thus, an implantable or minimally invasive optical device that can provide early detection of SSI would be highly desirable.

Following the discussion of optical diagnostic tools in Sects. 6.3 and 6.4, the fields of both implantable visual prosthetics (6.5) and optogenetics (6.6) were covered. Visual prostheses in current clinical use include IOL implants for the treatment of cataracts and retinal (visual) prostheses for the restoration of sight in patients suffering with RP or AMD. The latter entail electronic devices that are implanted within the eye and provide electrical stimulation of neurons in the visual pathway. While these devices do not provide diagnostic functions, they have been presented in this chapter as they represent an interesting example of an implantable optical technology that is commercially available.

Optogenetics involves the combination of the genetic modification of neurons (such that they express light-sensitive proteins) with the use of photonics in order to permit photo-stimulation of the modified neurons in a minimally invasive manner. Optogenetics is a rapidly growing field that has provided a novel means by which to study neurological and nervous function. For this reason it is becoming widely used within the neuroscience community and the work carried out to date indicates many potential future uses of optogenetics in medicine. These include further optical prostheses for the restoration of vision in the blind—for which considerable work is already underway—as well as the development of more futuristic neural implants for the treatment of illnesses including depression and drug dependency.

When considering the development of diagnostic/therapeutic implants, optogenetics may provide exciting opportunities in the future. However, progress towards this goal can only be expected to take place over a long period of time, as the translation of optogenetics into medical use in humans is likely to face numerous technological and ethical hurdles along the way. The electrical visual prostheses described in Sect. 6.5.2 hold considerable potential for the treatment of blindness, but have not been designed for diagnostic use. On the other hand, the optical imaging and sensing modalities discussed in Sects. 6.3 and 6.4 have a variety of diagnostic applications and are considerably closer to medically deployable formats than optogenetic systems. Indeed, almost all of these methods have been employed for in vivo clinical measurements using optical fibers and some are already available commercially. The commercially available techniques include confocal endomicroscopy and OCT, both of which are finding increasing application owing to their capability to provide in situ diagnoses of a number of medical disorders. Moreover, research continues in these areas and is driven towards the development of smaller, less-invasive devices, including tethered capsule systems, which offer a more comfortable experience for the patient as they undergo endoscopy. Despite this, no long-term (i.e. more than one day) implantable optical systems have yet been reported for use in humans that can provide continuous imaging or sensing capabilities that would permit perpetual monitoring of a patient's state of health.

Any fiber-optic sensing modality has the potential to be deployed as a tethered implant, and many of the techniques discussed in this chapter could be used in this fashion. OCT and endomicroscopy have been incorporated into medical catheters and this could be extended to allow long-term imaging over a number of days (as

catheters often remain implanted for days, weeks, or even months). However, such systems provide image data, which is complex and (at least at the present time) typically requires expert analysis before a diagnosis can be made. For this reason, single-point spectroscopic systems—which allow measurement of, for example, diffuse reflectance, fluorescence or Raman spectra—may provide a more feasible route towards the production of tethered, implantable optical sensors. The data acquired with these systems consist of wavelength-resolved intensity measurements that can often provide diagnoses through combination with automated analysis techniques (such as PCA followed by LDA). For this reason they are immediately more compatible with an implant-based format, where it will be impossible for the perpetually recorded data to be analyzed manually. Instead, changes in the spectra corresponding to poor health outcomes could be detected automatically prior to an alert being sent to a clinician.

Many of the spectroscopic techniques described in this chapter have potential applications in this area and all have shown promise in medical diagnostics. For example, diffuse reflectance spectra offer reliable measurements of blood oxygen saturation, which could in turn be used as an indicator of tissue health or viability after surgery. Research has also shown that fluorescence can report on tissue disease state, for example in the detection of pre-cancerous lesions or to monitor infection (albeit with the use of a contrast agent). Raman spectroscopy has also been applied to the detection of various maladies and, importantly, clinical Raman spectra are typically recorded in a label-free manner. In particular, Raman spectra have been shown to effectively detect and discriminate multiple bacteria that are relevant to UTIs, and this capability may be useful in the detection of SSI, which is caused by many of the same bacteria. The development of optical spectroscopic techniques for the detection of bacteria is likely to continue in the future and current research implies that Raman scattering may provide a useful contrast mechanism for this purpose. Once available, such technology could be deployed as a tethered implant and would have the potential to significantly improve patient outcomes. This will be true for monitoring and detecting a number of diseases. SSI, however, will be especially relevant, where an implantable sensor capable of providing early detection would vastly improve patient outcomes by allowing successful treatment of infection using antibiotics rather than requiring repeated additional surgical interventions. Such tethered devices could terminate at a bedside device kept near to the patient, although this would impair mobility. A more desirable format could incorporate miniaturized detection optics into a patch that could be worn by the patient, thus minimizing the impact on everyday activity.

While tethered optical implants like those described above have the potential to provide significant improvements in healthcare, they clearly do not offer an optimum solution, simply due to their tethered format. In an ideal case, a patient should not be attached to any external device, whether portable or not. To this end, the development of fully implantable medical sensors is under way, and this involves optical systems as well as a variety of alternative sensing modalities (some of which are discussed in other chapters of this book). Within optogenetics much research has been undertaken into the development of optical implants, with the main aim

being to develop systems suitable for implantation in small animals to allow free behavior during neurological research. This progress is also relevant to the development of fully implantable, untethered optical sensors for healthcare and a small number of devices of this sort have indeed been reported. For example, integrated chips that allow measurements of tissue oxygenation and blood pressure have been developed, and an ingestible capsule for the detection of GI bleeding was also launched recently (see Sect. 6.4.2 for further details). Several technical challenges remain, however, and these include the questions of biocompatibility and the production of battery-free wireless sensors that can be powered externally (also discussed elsewhere in this book). Nonetheless, the development of implantable optical systems for applications in medicine—for both sensing and treatment—will certainly continue. Importantly, this is likely to lead to many exciting medical advances in the future, providing improvements in disease detection rates and reducing patient morbidity and mortality.

Overall, optical sensing modalities offer minimally invasive diagnosis of a number of diseases. Combined with the miniaturization of optical systems, this provides an opportunity for the development of implantable devices that have the potential to revolutionize certain areas of healthcare. In particular, the treatment of SSI would benefit significantly from the development of novel and improved detection modalities that allow continuous patient monitoring via an implant. Early devices are likely to involve tethered formats, where optical fibers will be used for light delivery and collection, with the external optics contained within a wearable patch. Beyond this, the development of fully implantable wireless systems will also continue, with important current research challenges including the questions of biocompatibility, biofouling, and, of course, sufficient miniaturization. Both tethered devices and fully implantable systems offer the prospect of radical advances in medicine and their development will almost certainly bring about significant changes. In conclusion, implantable optical sensing is an exciting field of study, which will attract considerable attention in the coming years. It is likely to witness further advances and to undergo substantial expansion in the near future, and this will doubtless lead to the development of a range of novel devices that can provide vast improvements in the field of healthcare.

References

1. C.M. Chen, R. Kwasnicki, B. Lo, G.Z. Yang, Wearable tissue oxygenation monitoring sensor and a forearm vascular phantom design for data validation, in *2014 11th International Conference on Wearable and Implantable Body Sensor Networks* (*BSN*) (2014), pp. 64–68
2. J. Fiala, P. Bingger, D. Ruh, K. Foerster, C. Heilmann, F. Beyersdorf, H. Zappe, A. Seifert, An implantable optical blood pressure sensor based on pulse transit time. Biomed. Microdev. **15**(1), 73–81 (2013)
3. M. Theodor, D. Ruh, J. Fiala, K. Forster, C. Heilmann, Y. Manoli, F. Beyersdorf, H. Zappe, A. Seifert, Subcutaneous blood pressure monitoring with an implantable optical sensor. Biomed. Microdev. **15**(5), 811–820 (2013)

4. P.C.A. Jeronimo, A.N. Araujo, M. Montenegro, Optical sensors and biosensors based on sol-gel films. Talanta **72**(1), 13–27 (2007)
5. G. Iddan, G. Meron, A. Glukhovsky, P. Swain, Wireless capsule endoscopy. Nature **405** (6785), 417 (2000)
6. M.J. Gora, J.S. Sauk, R.W. Carruth, K.A. Gallagher, M.J. Suter, N.S. Nishioka, L.E. Kava, M. Rosenberg, B.E. Bouma, G.J. Tearney, Tethered capsule endomicroscopy enables less invasive imaging of gastrointestinal tract microstructure. Nat. Med. **19**(2), 238–240 (2013)
7. L. Scolaro, D. Lorenser, W.-J. Madore, R.W. Kirk, A.S. Kramer, G.C. Yeoh, N. Godbout, D. D. Sampson, C. Boudoux, R.A. McLaughlin, Molecular imaging needles: dual-modality optical coherence tomography and fluorescence imaging of labeled antibodies deep in tissue. Biomed. Opt. Express **6**(5), 1767–1781 (2015)
8. G. Berci, K.A. Forde, History of endoscopy: what lessons have we learned from the past? Surg. Endosc. **14**(1), 5–15 (2000)
9. F. Helmchen, Miniaturization of fluorescence microscopes using fibre optics. Exp. Physiol. **87**(6), 737–745 (2002)
10. T. Wilson, Confocal microscopy, in *Confocal Microscopy*, ed. by T. Wilson (Academic Press Limited, London, 1990), pp. 1–60
11. T. Wilson, Resolution and optical sectioning in the confocal microscope. J. Microsc. **244**(2), 113–121 (2011)
12. A.F. Gmitro, D. Aziz, Confocal microscopy through a fiberoptic imaging bundle. Opt. Lett. **18**(8), 565–567 (1993)
13. D.L. Dickensheets, G.S. Kino, Micromachined scanning confocal optical microscope. Opt. Lett. **21**(10), 764–766 (1996)
14. F. Helmchen, M.S. Fee, D.W. Tank, W. Denk, A miniature head-mounted two-photon microscope. High-resolution brain imaging in freely moving animals. Neuron **31**(6), 903–912 (2001)
15. A. Polglase, W. McLaren, S. Skinner, R. Kiesslich, M. Neurath, P. Delaney, A fluorescence confocal endomicroscope for in vivo microscopy of the upper- and the lower-GI tract. Gastrointest. Endosc. **62**(5), 686–695 (2005)
16. W. Gobel, J.N. Kerr, A. Nimmerjahn, F. Helmchen, Miniaturized two-photon microscope based on a flexible coherent fiber bundle and a gradient-index lens objective. Opt. Lett. **29** (21), 2521–2523 (2004)
17. M.T. Myaing, D.J. MacDonald, X. Li, Fiber-optic scanning two-photon fluorescence endoscope. Opt. Lett. **31**(8), 1076–1078 (2006)
18. S. Tang, W. Jung, D. McCormick, T. Xie, J. Su, Y.C. Ahn, B.J. Tromberg, Z. Chen, Design and implementation of fiber-based multiphoton endoscopy with microelectromechanical systems scanning. J. Biomed. Opt. **14**(3), 034005 (2009)
19. H. Bao, M. Gu, Reduction of self-phase modulation in double-clad photonic crystal fiber for nonlinear optical endoscopy. Opt. Lett. **34**(2), 148–150 (2009)
20. F. Jean, G. Bourg-Heckly, B. Viellerobe, Fibered confocal spectroscopy and multicolor imaging system for in vivo fluorescence analysis. Opt. Express **15**(7), 4008–4017 (2007)
21. G.T. Kennedy, H.B. Manning, D.S. Elson, M.A.A. Neil, G.W. Stamp, B. Viellerobe, F. Lacombe, C. Dunsby, P.M.W. French, A fluorescence lifetime imaging scanning confocal endomicroscope. J. Biophoton. **3**(1–2), 103–107 (2010)
22. G.O. Fruhwirth, S. Ameer-Beg, R. Cook, T. Watson, T. Ng, F. Festy, Fluorescence lifetime endoscopy using TCSPC for the measurement of fret in live cells. Opt. Express **18**(11), 11148–11158 (2010)
23. A.J. Thompson, C. Paterson, M.A. Neil, C. Dunsby, P.M. French, Adaptive phase compensation for ultracompact laser scanning endomicroscopy. Opt. Lett. **36**(9), 1707–1709 (2011)
24. T. Cizmar, M. Mazilu, K. Dholakia, In situ wavefront correction and its application to micromanipulation. Nat. Photonics **4**(6), 388–394 (2010)
25. M. Ploschner, T. Tyc, T. Cizmar, Seeing through chaos in multimode fibres. Nat. Photonics **9**(8), 529 (2015)

26. Y. Kim, S.C. Warren, J.M. Stone, J.C. Knight, M.A.A. Neil, C. Paterson, C.W. Dunsby, P. M.W. French, Adaptive multiphoton endomicroscope incorporating a polarization-maintaining multicore optical fibre. IEEE J. Sel. Top. Quantum Electron. **11** (99), 1 (2015)
27. N. Bedard, T.S. Tkaczyk, Snapshot spectrally encoded fluorescence imaging through a fiber bundle. J. Biomed. Opt. **17**(8) (2012)
28. M. Kyrish, R. Kester, R. Richards-Kortum, T. Tkaczyk, Improving spatial resolution of a fiber bundle optical biopsy system. Endoscopic Microsc. V, **7558** (2010)
29. Y.S. Sabharwal, A.R. Rouse, L. Donaldson, M.F. Hopkins, A.F. Gmitro, Slit-scanning confocal microendoscope for high-resolution in vivo imaging. Appl. Opt. **38**(34), 7133–7144 (1999)
30. A. Rouse, A. Gmitro, Multispectral imaging with a confocal microendoscope. Opt. Lett. **25** (23), 1708–1710 (2000)
31. M. Hughes, G.Z. Yang, High speed, line-scanning, fiber bundle fluorescence confocal endomicroscopy for improved mosaicking. Biomed. Opt. Express **6**(4), 1241–1252 (2015)
32. H. Neumann, F.S. Fuchs, M. Vieth, R. Atreya, J. Siebler, R. Kiesslich, M.F. Neurath, Review article: in vivo imaging by endocytoscopy. Aliment. Pharmacol. Ther. **33**(11), 1183–1193 (2011)
33. M. Hughes, T.P. Chang, G.-Z. Yang, Fiber bundle endocytoscopy. Biomed. Opt. Express **4** (12), 2781–2794 (2013)
34. J.S. Louie, R. Richards-Kortum, S. Anandasabapathy, Applications and advancements in the use of high-resolution microendoscopy for detection of gastrointestinal neoplasia. Clin. Gastroenterol. Hepatol. **12**(11), 1789–1792 (2014)
35. M.-A. Protano, H. Xu, G. Wang, A.D. Polydorides, S.M. Dawsey, J. Cui, L. Xue, F. Zhang, T. Quang, M.C. Pierce, D. Shin, R.A. Schwarz, M.S. Bhutani, M. Lee, N. Parikh, C. Hur, W. Xu, E. Moshier, J. Godbold, J. Mitcham, C. Hudson, R.R. Richards-Kortum, S. Anandasabapathy, Low-cost high-resolution microendoscopy for the detection of esophageal squamous cell neoplasia: an international trial. Gastroenterology **149**(2), 321–329 (2015)
36. P.A. Keahey, T.S. Tkaczyk, K.M. Schmeler, R.R. Richards-Kortum, Optimizing modulation frequency for structured illumination in a fiber-optic microendoscope to image nuclear morphometry in columnar epithelium. Biomed. Opt. Express **6**(3), 870–880 (2015)
37. G.J. Tearney, R.H. Webb, B.E. Bouma, Spectrally encoded confocal microscopy. Opt. Lett. **23**(15), 1152–1154 (1998)
38. C. Boudoux, S.H. Yun, W.Y. Oh, W.M. White, N.V. Iftimia, M. Shishkov, B.E. Bouma, G. J. Tearney, Rapid wavelength-swept spectrally encoded confocal microscopy. Opt. Express **13**(20), 8214–8221 (2005)
39. D. Kang, R.W. Carruth, M. Kim, S.C. Schlachter, M. Shishkov, K. Woods, N. Tabatabaei, T. Wu, G.J. Tearney, Endoscopic probe optics for spectrally encoded confocal microscopy. Biomed. Opt. Express **4**(10), 1925–1936 (2013)
40. A. Zeidan, D. Yelin, Miniature forward-viewing spectrally encoded endoscopic probe. Opt. Lett. **39**(16), 4871–4874 (2014)
41. M. Abbaci, I. Breuskin, O. Casiraghi, F. De Leeu, M. Ferchiou, S. Temam, C. Laplace-Builhe, Confocal laser endomicroscopy for non-invasive head and neck cancer imaging: a comprehensive review. Oral Oncol. **50**(8), 711–716 (2014)
42. A. Gupta, B.M. Attar, P. Koduru, A.R. Murali, B.T. Go, R. Agarwal, Utility of confocal laser endomicroscopy in identifying high-grade dysplasia and adenocarcinoma in Barrett's esophagus: a systematic review and meta-analysis. Eur. J. Gastroenterol. Hepatol. **26**(4), 369–377 (2014)
43. F. Salvatori, S. Siciliano, F. Maione, D. Esposito, S. Masone, M. Persico, G.D. De Palma, Confocal laser endomicroscopy in the study of colonic mucosa in IBD patients: a review. Gastroenterol. Res. Pract. (2012)
44. P. Su, Y. Liu, S. Lin, K. Xiao, P. Chen, S. An, J. He, Y. Bai, Efficacy of confocal laser endomicroscopy for discriminating colorectal neoplasms from non-neoplasms: a systematic review and meta-analysis. Colorectal Dis. **15**(1), E1–E12 (2013)

45. V. Subramanian, K. Ragunath, Advanced endoscopic imaging: a review of commercially available technologies. Clin. Gastroenterol. Hepatol. **12**(3), 368 (2014)
46. P.S.-P. Thong, M. Olivo, S.S. Tandjung, M.M. Movania, F. Lin, K. Qian, H.-S. Seah, K.-C. Soo, Review of confocal fluorescence endomicroscopy for cancer detection. IEEE J. Sel. Top. Quantum Electron. **18**(4), 1355–1366 (2012)
47. A.H. Zehri, W. Ramey, J.F. Georges, M.A. Mooney, N.L. Martirosyan, M.C. Preul, P. Nakaji, Neurosurgical confocal endomicroscopy: a review of contrast agents, confocal systems, and future imaging modalities. Surg. Neurol. Int. **5**, 60 (2014)
48. R. Kiesslich, J. Burg, M. Vieth, J. Gnaendiger, M. Enders, P. Delaney, A. Polglase, W. McLaren, D. Janell, S. Thomas, B. Nafe, P.R. Galle, M.F. Neurath, Confocal laser endoscopy for diagnosing intraepithelial neoplasias and colorectal cancer in vivo. Gastroenterology **127**(3), 706–713 (2004)
49. R. Kiesslich, M. Goetz, K. Lammersdorf, C. Schneider, J. Burg, M. Stolte, M. Vieth, B. Nafe, P.R. Galle, M.F. Neurath, Chromoscopy-guided endomicroscopy increases the diagnostic yield of intraepithelial neoplasia in ulcerative colitis. Gastroenterology **132**(3), 874–882 (2007)
50. R. Kiesslich, L. Gossner, M. Goetz, A. Dahlmann, M. Vieth, M. Stolte, A. Hoffman, M. Jung, B. Nafe, P.R. Galle, M.F. Neurath, In vivo histology of Barrett's esophagus and associated neoplasia by confocal laser endomicroscopy. Clin. Gastroenterol. Hepatol. **4**(8), 979–987 (2006)
51. A.M. Buchner, M.W. Shahid, M.G. Heckman, M. Krishna, M. Ghabril, M. Hasan, J.E. Crook, V. Gomez, M. Raimondo, T. Woodward, H.C. Wolfsen, M.B. Wallace, Comparison of probe-based confocal laser endomicroscopy with virtual chromoendoscopy for classification of colon polyps. Gastroenterology **138**(3), 834–842 (2010)
52. T. Kuiper, F.J.C. van den Broek, S. van Eeden, P. Fockens, E. Dekker, Feasibility and accuracy of confocal endomicroscopy in comparison with narrow-band imaging and chromoendoscopy for the differentiation of colorectal lesions. Am. J. Gastroenterol. **107**(4), 543–550 (2012)
53. V. Gomez, A.M. Buchner, E. Dekker, F.J.C. van den Broek, A. Meining, M.W. Shahid, M. S. Ghabril, P. Fockens, M.G. Heckman, M.B. Wallace, Interobserver agreement and accuracy among international experts with probe-based confocal laser endomicroscopy in predicting colorectal neoplasia. Endoscopy **42**(4), 286–291 (2010)
54. K.B. Dunbar, P. Okolo III, E. Montgomery, M.I. Canto, Confocal laser endomicroscopy in Barrett's esophagus and endoscopically inapparent Barrett's neoplasia: a prospective, randomized, double-blind, controlled, crossover trial. Gastrointest. Endosc. **70**(4), 645–654 (2009)
55. M. Bajbouj, M. Vieth, T. Roesch, S. Miehlke, V. Becker, M. Anders, H. Pohl, A. Madisch, T. Schuster, R.M. Schmid, A. Meining, Probe-based confocal laser endomicroscopy compared with standard four-quadrant biopsy for evaluation of neoplasia in Barrett's esophagus. Endoscopy **42**(6), 435–440 (2010)
56. P. Sharma, A.R. Meining, E. Coron, C.J. Lightdale, H.C. Wolfsen, A. Bansal, M. Bajbouj, J.-P. Galiniche, J.A. Abrams, A. Rastogi, N. Gupta, J.E. Michalek, G.Y. Lauwers, M.B. Wallace, Real-time increased detection of neoplastic tissue in Barrett's esophagus with probe-based confocal laser endomicroscopy: final results of an international multicenter, prospective, randomized, controlled trial. Gastrointest. Endosc. **74**(3), 465–472 (2011)
57. M.B. Wallace, P. Sharma, C. Lightdale, H. Wolfsen, E. Coron, A. Buchner, M. Bajbouj, A. Bansal, A. Rastogi, J. Abrams, J.E. Crook, A. Meining, Preliminary accuracy and interobserver agreement for the detection of intraepithelial neoplasia in Barrett's esophagus with probe-based confocal laser endomicroscopy. Gastrointest. Endosc. **72**(1), 19–24 (2010)
58. F.J.C. van den Broek, J.A. van Es, S. van Eeden, P.C.F. Stokkers, C.Y. Ponsioen, J.B. Reitsma, P. Fockens, E. Dekker, Pilot study of probe-based confocal laser endomicroscopy during colonoscopic surveillance of patients with longstanding ulcerative colitis. Endoscopy **43**(2), 116–122 (2011)

59. H. Neumann, M. Vieth, R. Atreya, M. Grauer, J. Siebler, T. Bernatik, M.F. Neurath, J. Mudter, Assessment of Crohn's disease activity by confocal laser endomicroscopy. Inflammat. Bowel Dis. **18**(12), 2261–2269 (2012)
60. C.-Q. Li, X.-J. Xie, T. Yu, X.-M. Gu, X.-L. Zuo, C.-J. Zhou, W.-Q. Huang, H. Chen, Y.-Q. Li, Classification of inflammation activity in ulcerative colitis by confocal laser endomicroscopy. Am. J. Gastroenterol. **105**(6), 1391–1396 (2010)
61. B. Andre, T. Vercauteren, A.M. Buchner, M. Krishna, N. Ayache, M.B. Wallace, Software for automated classification of probe-based confocal laser endomicroscopy videos of colorectal polyps. World J. Gastroenterol. **18**(39), 5560–5569 (2012)
62. S. Gaddam, S.C. Mathur, M. Singh, J. Arora, S.B. Wani, N. Gupta, A. Overhiser, A. Rastogi, V. Singh, N. Desai, S.B. Hall, A. Bansal, P. Sharma, Novel probe-based confocal laser endomicroscopy criteria and interobserver agreement for the detection of dysplasia in Barrett's esophagus. Am. J. Gastroenterol. **106**(11), 1961–1969 (2011)
63. H. Neumann, C. Langner, M.F. Neurath, M. Vieth, Confocal laser endomicroscopy for diagnosis of Barrett's esophagus. Front. Oncol. **2**, 42 (2012)
64. I. Smith, P.E. Kline, M. Gaidhane, M. Kahaleh, A review on the use of confocal laser endomicroscopy in the bile duct. Gastroenterol. Res. Pract. (2012)
65. M. Behbahaninia, N.L. Martirosyan, J. Georges, J.A. Udovich, M.Y.S. Kalani, B.G. Feuerstein, P. Nakaji, R.F. Spetzler, M.C. Preul, Intraoperative fluorescent imaging of intracranial tumors: a review. Clin. Neurol. Neurosurg. **115**(5), 517–528 (2013)
66. F. Acerbi, C. Cavallo, M. Broggi, R. Cordella, E. Anghileri, M. Eoli, M. Schiariti, G. Broggi, P. Ferroli, Fluorescein-guided surgery for malignant gliomas: a review. Neurosurg. Rev. **37**(4), 547–555 (2014)
67. C. Ell, S. Remke, A. May, L. Helou, R. Henrich, G. Mayer, The first prospective controlled trial comparing wireless capsule endoscopy with push enteroscopy in chronic gastrointestinal bleeding. Endoscopy **34**(9), 685–689 (2002)
68. B.S. Lewis, P. Swain, Capsule endoscopy in the evaluation of patients with suspected small intestinal bleeding: results of a pilot study. Gastrointest. Endosc. **56**(3), 349–353 (2002)
69. M. Mylonaki, A. Fritscher-Ravens, P. Swain, Wireless capsule endoscopy: a comparison with push enteroscopy in patients with gastroscopy and colonoscopy negative gastrointestinal bleeding. Gut **52**(8), 1122–1126 (2003)
70. M. Pennazio, R. Santucci, E. Rondonotti, C. Abbiati, G. Beccari, F.P. Rossini, R. de Franchis, Outcome of patients with obscure gastrointestinal bleeding after capsule endoscopy: report of 100 consecutive cases. Gastroenterology **126**(3), 643–653 (2004)
71. N. Tabatabaei, D. Kang, T. Wu, M. Kim, R.W. Carruth, J. Leung, J.S. Sauk, W. Shreffler, Q. Yuan, A. Katz, N.S. Nishioka, G.J. Tearney, Tethered confocal endomicroscopy capsule for diagnosis and monitoring of eosinophilic esophagitis. Biomed. Opt. Express **5**(1), 197–207 (2014)
72. D. Huang, E.A. Swanson, C.P. Lin, J.S. Schuman, W.G. Stinson, W. Chang, M.R. Hee, T. Flotte, K. Gregory, C.A. Puliafito, J.G. Fujimoto, Optical coherence tomography. Science **254**(5035), 1178–1181 (1991)
73. B. Cense, N.A. Nassif, T. Chen, M. Pierce, S.H. Yun, B.H. Park, B.E. Bouma, G.J. Tearney, J.F. de Boer, Ultrahigh-resolution high-speed retinal imaging using spectral-domain optical coherence tomography. Opt. Express **12**(11), 2435–2447 (2004)
74. M.A. Choma, M.V. Sarunic, C.H. Yang, J.A. Izatt, Sensitivity advantage of swept source and Fourier domain optical coherence tomography. Opt. Express **11**(18), 2183–2189 (2003)
75. S.H. Yun, G.J. Tearney, B.E. Bouma, B.H. Park, J.F. de Boer, High-speed spectral-domain optical coherence tomography at 1.3 μm wavelength. Opt. Express **11**(26), 3598–3604 (2003)
76. P.H. Tomlins, R.K. Wang, Theory, developments and applications of optical coherence tomography. J. Phys. D Appl. Phys. **38**(15), 2519–2535 (2005)
77. T. Alasil, P.A. Keane, D.A. Sim, A. Tufail, M.E. Rauser, Optical coherence tomography in pediatric ophthalmology: current roles and future directions. Ophthalm. Surg. Lasers Imaging Retina **44**(6), S19–S29 (2013)

78. J.P. Ehlers, Y.K. Tao, S.K. Srivastava, The value of intraoperative optical coherence tomography imaging in vitreoretinal surgery. Curr. Opin. Ophthalmol. **25**(3), 221–227 (2014)
79. T. Garcia, A. Tourbah, E. Setrouk, A. Ducasse, C. Arndt, Optical coherence tomography in neuro-ophthalmology. J. Francais D: Ophtalmol. **35**(6), 454–466 (2012)
80. B.E. Goldhagen, M.T. Bhatti, P.P. Srinivasan, S.J. Chiu, S. Farsiu, M.A. El-Dairi, Retinal atrophy in eyes with resolved papilledema detected by optical coherence tomography. J. Neuro-Ophthalmol. **35**(2), 122–126 (2015)
81. G.J. Jaffe, J. Caprioli, Optical coherence tomography to detect and manage retinal disease and glaucoma. Am. J. Ophthalmol. **137**(1), 156–169 (2004)
82. N.A. Nassif, B. Cense, B.H. Park, M.C. Pierce, S.H. Yun, B.E. Bouma, G.J. Tearney, T.C. Chen, J.F. de Boer, In vivo high-resolution video-rate spectral-domain optical coherence tomography of the human retina and optic nerve. Opt. Express **12**(3), 367–376 (2004)
83. G. Virgili, F. Menchini, G. Casazza, R. Hogg, R. R. Das, X. Wang, M. Michelessi, Optical coherence tomography (OCT) for detection of macular oedema in patients with diabetic retinopathy. Cochrane Database Syst. Rev. **1** (2015)
84. M.E. Brezinski, G.J. Tearney, N.J. Weissman, S.A. Boppart, B.E. Bouma, M.R. Hee, A.E. Weyman, E.A. Swanson, J.F. Southern, J.G. Fujimoto, Assessing atherosclerotic plaque morphology: comparison of optical coherence tomography and high frequency intravascular ultrasound. Heart **77**(5), 397–403 (1997)
85. A.H. Chau, R.C. Chan, M. Shishkov, B. MacNeill, N. Iftimiia, G.J. Tearney, R.D. Kamm, B. E. Bouma, M.R. Kaazempur-Mofrad, Mechanical analysis of atherosclerotic plaques based on optical coherence tomography. Ann. Biomed. Eng. **32**(11), 1494–1503 (2004)
86. G. Ferrante, P. Presbitero, R. Whitbourn, P. Barlis, Current applications of optical coherence tomography for coronary intervention. Int. J. Cardiol. **165**(1), 7–16 (2013)
87. I.K. Jang, B.E. Bouma, D.H. Kang, S.J. Park, S.W. Park, K.B. Seung, K.B. Choi, M. Shishkov, K. Schlendorf, E. Pomerantsev, S.L. Houser, H.T. Aretz, G.J. Tearney, Visualization of coronary atherosclerotic plaques in patients using optical coherence tomography: comparison with intravascular ultrasound. J. Am. College Cardiol. **39**(4), 604–609 (2002)
88. O.C. Raffel, G.J. Tearney, D.D. Gauthier, E.F. Halpern, B.E. Bouma, I.-K. Jang, Relationship between a systemic inflammatory marker, plaque inflammation, and plaque characteristics determined by intravascular optical coherence tomography. Arterioscler. Thromb. Vasc. Biol. **27**(8), 1820–1827 (2007)
89. T. Roleder, J. Jakala, G.L. Kaluza, L. Partyka, K. Proniewska, E. Pociask, W. Zasada, W. Wojakowski, Z. Gasior, D. Dudek, The basics of intravascular optical coherence tomography. Postepy W Kardiologii Interwencyjnej **11**(2), 74–83 (2015)
90. A. Tanaka, G. J. Tearney, B.E. Bouma, Challenges on the frontier of intracoronary imaging: atherosclerotic plaque macrophage measurement by optical coherence tomography. J. Biomed. Opt. **15**(1) (2010)
91. G.J. Tearney, S. Waxman, M. Shishkov, B.J. Vakoc, M.J. Suter, M.I. Freilich, A.E. Desjardins, W.-Y. Oh, L.A. Bartlett, M. Rosenberg, B.E. Bouma, Three-dimensional coronary artery microscopy by intracoronary optical frequency domain imaging. JACC-Cardiovasc. Imag. **1**(6), 752–761 (2008)
92. G.J. Tearney, H. Yabushita, S.L. Houser, H.T. Aretz, I.K. Jang, K.H. Schlendorf, C.R. Kauffman, M. Shishkov, E.F. Halpern, B.E. Bouma, Quantification of macrophage content in atherosclerotic plaques by optical coherence tomography. Circulation **107**(1), 113–119 (2003)
93. L. Vignali, E. Solinas, E. Emanuele, Research and clinical applications of optical coherence tomography in invasive cardiology: a review. Curr. Cardiol. Rev. **10**(4), 369–376 (2014)
94. H. Yabushita, B.E. Bourna, S.L. Houser, T. Aretz, I.K. Jang, K.H. Schlendorf, C.R. Kauffman, M. Shishkov, D.H. Kang, E.F. Halpern, G.J. Tearney, Characterization of human atherosclerosis by optical coherence tomography. Circulation **106**(13), 1640–1645 (2002)

95. S. Brand, J.M. Poneros, B.E. Bouma, G.J. Tearney, C.C. Compton, N.S. Nishioka, Optical coherence tomography in the gastrointestinal tract. Endoscopy **32**(10), 796–803 (2000)
96. J.A. Evans, B.E. Bouma, J. Bressner, M. Shishkov, G.Y. Lauwers, M. Mino-Kenudson, N.S. Nishioka, G.J. Tearney, Identifying intestinal metaplasia at the squamocolumnar junction by using optical coherence tomography. Gastrointest. Endosc. **65**(1), 50–56 (2007)
97. C.-P. Liang, C.-W. Chen, J. Wierwille, J. Desai, R. Gullapalli, R. Mezrich, C.-M. Tang, Y. Chen, Endoscopic microscopy using optical coherence tomography. Curr. Med. Imag. Rev. **8**(3), 174–193 (2012)
98. M.J. Suter, B.J. Vakoc, P.S. Yachimski, M. Shishkov, G.Y. Lauwers, M. Mino-Kenudson, B.E. Bouma, N.S. Nishioka, G.J. Tearney, Comprehensive microscopy of the esophagus in human patients with optical frequency domain imaging. Gastrointest. Endosc. **68**(4), 745–753 (2008)
99. G.J. Tearney, M.E. Brezinski, J.F. Southern, B.E. Bouma, S.A. Boppart, J.G. Fujimoto, Optical biopsy in human gastrointestinal tissue using optical coherence tomography. Am. J. Gastroenterol. **92**(10), 1800–1804 (1997)
100. B.J. Vakoc, M. Shishko, S.H. Yun, W.-Y. Oh, M.J. Suter, A.E. Desjardins, J.A. Evans, N.S. Nishioka, G.J. Tearney, B.E. Bouma, Comprehensive esophageal microscopy by using optical frequency-domain imaging (with video). Gastrointest. Endosc. **65**(6), 898–905 (2007)
101. S.A. Coulman, J.C. Birchall, A. Alex, M. Pearton, B. Hofer, C. O'Mahony, W. Drexler, B. Povazay, In vivo, in situ imaging of microneedle insertion into the skin of human volunteers using optical coherence tomography. Pharma. Res. **28**(1), 66–81 (2011)
102. T. Gambichler, V. Jaedicke, S. Terras, Optical coherence tomography in dermatology: technical and clinical aspects. Arch. Dermatol. Res. **303**(7), 457–473 (2011)
103. T. Gambichler, A. Pljakic, L. Schmitz, Recent advances in clinical application of optical coherence tomography of human skin. Clin. Cosmet. Investig. Dermatol. **8**, 345–354 (2015)
104. J. Welzel, Optical coherence tomography in dermatology: a review. Skin Res. Tech. **7**(1), 1–9 (2001)
105. A.S. Fjeldstad, N.G. Carlson, J.W. Rose, Optical coherence tomography as a biomarker in multiple sclerosis. Expert Opinion Med. Diagnost. **6**(6), 593–604 (2012)
106. L.M. Simao, The contribution of optical coherence tomography in neurodegenerative diseases. Curr. Opinion Ophthalmol. **24**(6), 521–527 (2013)
107. A. Vidal-Jordana, J. Sastre-Garriga, X. Montalban, Optical coherence tomography in multiple sclerosis. Rev. Neurol. **54**(9), 556–563 (2012)
108. A. Vinekar, S. Mangalesh, C. Jayadev, R.S. Maldonado, N. Bauer, C.A. Toth, Retinal imaging of infants on spectral domain optical coherence tomography. Biomed. Res. Int. (2015)
109. K.A. Townsend, G. Wollstein, J.S. Schuman, Imaging of the retinal nerve fibre layer for glaucoma. Br. J. Ophthalmol. **93**(2), 139–143 (2009)
110. G.J. Tearney, OCT imaging of macrophages a bright spot in the study of inflammation in human atherosclerosis. JACC Cardiovasc. Imag. **8**(1), 73–75 (2015)
111. K. Toutouzas, Y.S. Chatzizisis, M. Riga, A. Giannopoulos, A.P. Antoniadis, S. Tu, Y. Fujino, D. Mitsouras, C. Doulaverakis, I. Tsampoulatidis, V.G. Koutkias, K. Bouki, Y. Li, I. Chouvarda, G. Cheimariotis, N. Maglaveras, I. Kompatsiaris, S. Nakamura, J.H.C. Reiber, F. Rybicki, H. Karvounis, C. Stefanadis, D. Tousoulis, G.D. Giannoglou, Accurate and reproducible reconstruction of coronary arteries and endothelial shear stress calculation using 3D OCT: comparative study to 3D IVUS and 3D QCA. Atherosclerosis **240**(2), 510–519 (2015)
112. R.A. McLaughlin, B.C. Quirk, A. Curatolo, R.W. Kirk, L. Scolaro, D. Lorenser, P.D. Robbins, B.A. Wood, C.M. Saunders, D.D. Sampson, Imaging of breast cancer with optical coherence tomography needle probes: feasibility and initial results. IEEE J. Sel. Top. Quantum Electron. **18**(3), 1184–1191 (2012)
113. C. Zhou, D.W. Cohen, Y. Wang, H.-C. Lee, A.E. Mondelblatt, T.-H. Tsai, A.D. Aguirre, J. G. Fujimoto, J.L. Connolly, Integrated optical coherence tomography and microscopy for

ex vivo multiscale evaluation of human breast tissues. Cancer Res. **70**(24), 10071–10079 (2010)
114. A.M. Zysk, S.A. Boppart, Computational methods for analysis of human breast tumor tissue in optical coherence tomography images. J. Biomed. Opt. **11**(5) (2006)
115. B.G. Muller, D.M. de Bruin, W. van den Bos, M.J. Brandt, J.F. Velu, M.T.J. Bus, D. J. Faber, D. Savci, P.J. Zondervan, T.M. de Reijke, P.L. Pes, J. de la Rosette, T.G. van Leeuwen, Prostate cancer diagnosis: the feasibility of needle-based optical coherence tomography. J. Med Imag. (Bellingham, Wash.) **2**(3), 037501 (2015)
116. M.T.J. Bus, D.M. de Bruin, D.J. Faber, G.M. Kamphuis, P.J. Zondervan, M.P.L. Pes, T.M. de Reijke, O. Traxer, T.G. van Leeuwen, J.J.M.C.H. de la Rosette, Optical diagnostics for upper urinary tract urothelial cancer: technology, thresholds, and clinical applications. J. Endourol. **29**(2), 113–123 (2015)
117. J.M. Poneros, S. Brand, B.E. Bouma, G.J. Tearney, C.C. Compton, N.S. Nishioka, Diagnosis of specialized intestinal metaplasia by optical coherence tomography. Gastroenterology **120**(1), 7–12 (2001)
118. H.G. Bezerra, M.A. Costa, G. Guagliumi, A.M. Rollins, D.I. Simon, Intracoronary optical coherence tomography: a comprehensive review clinical and research applications. JACC Cardiovasc. Interven. **2**(11), 1035–1046 (2009)
119. G.J. Tearney, M.E. Brezinski, B.E. Bouma, S.A. Boppart, C. Pitris, J.F. Southern, J.G. Fujimoto, In vivo endoscopic optical biopsy with optical coherence tomography. Science **276**(5321), 2037–2039 (1997)
120. J. Ha, H. Yoo, G.J. Tearney, B.E. Bouma, Compensation of motion artifacts in intracoronary optical frequency domain imaging and optical coherence tomography. Int. J. Cardiovasc. Imag. **28**(6), 1299–1304 (2012)
121. I. Ben-Dor, M. Mahmoudi, A.D. Pichard, L.F. Satler, R. Waksman, Optical coherence tomography: a new imaging modality for plaque characterization and stent implantation. J. Interven. Cardiol. **24**(2), 184–192 (2011)
122. B.E. Bouma, G.J. Tearney, H. Yabushita, M. Shishkov, C.R. Kauffman, D.D. Gauthier, B.D. MacNeill, S.L. Houser, H.T. Aretz, E.F. Halpern, I.K. Jang, Evaluation of intracoronary stenting by intravascular optical coherence tomography. Heart **89**(3), 317–320 (2003)
123. R.C. Chan, A.H. Chau, W.C. Karl, S. Nadkarni, A.S. Khalil, N. Iftimia, M. Shishkov, G. J. Tearney, M.R. Kaazempur-Mofrad, B.E. Bouma, OCT-based arterial elastography: robust estimation exploiting tissue biomechanics. Opt. Express **12**(19), 4558–4572 (2004)
124. X. Yang, D. Lorenser, R.A. McLaughlin, R.W. Kirk, M. Edmond, M.C. Simpson, M.D. Grounds, D.D. Sampson, Imaging deep skeletal muscle structure using a high-sensitivity ultrathin side-viewing optical coherence tomography needle probe. Biomed. Opt. Express **5** (1), 136–148 (2014)
125. B.C. Quirk, R.A. McLaughlin, A. Curatolo, R.W. Kirk, P.B. Noble, D.D. Sampson, In situ imaging of lung alveoli with an optical coherence tomography needle probe. J. Biomed. Opt. **16**(3) (2011)
126. D. Lorenser, X. Yang, R.W. Kirk, B.C. Quirk, R.A. McLaughlin, D.D. Sampson, Ultrathin side-viewing needle probe for optical coherence tomography. Opt. Lett. **36**(19), 3894–3896 (2011)
127. M.J. Gora, J.S. Sauk, R.W. Carruth, W. Lu, D.T. Carlton, A. Soomro, M. Rosenberg, N.S. Nishioka, G.J. Tearney, Imaging the upper gastrointestinal tract in unsedated patients using tethered capsule endomicroscopy. Gastroenterology **145**(4), 723–725 (2013)
128. K. Liang, G. Traverso, H.-C. Lee, O.O. Ahsen, Z. Wang, B. Potsaid, M. Giacomelli, V. Jayaraman, R. Barman, A. Cable, H. Mashimo, R. Langer, J.G. Fujimoto, Ultrahigh speed *en face* OCT capsule for endoscopic imaging. Biomed. Opt. Express **6**(4), 1146–1163 (2015)
129. M.D. Stern, In vivo evaluation of microcirculation by coherent light scattering. Nature **254** (5495), 56–58 (1975)
130. D.A. Boas, A.K. Dunn, Laser speckle contrast imaging in biomedical optics. J. Biomed. Opt. **15**(1), 011109 (2010)

131. A.F. Fercher, J.D. Briers, Flow visualization by means of single-exposure speckle photography. Opt. Commun. **37**(5), 326–330 (1981)
132. H. Li, Q. Liu, H.Y. Lu, Y. Li, H.F. Zhang, S.B. Tong, Directly measuring absolute flow speed by frequency-domain laser speckle imaging. Opt. Express **22**(17), 21079–21087 (2014)
133. Y. Tamaki, M. Araie, E. Kawamoto, S. Eguchi, H. Fujii, Noncontact, two-dimensional measurement of retinal microcirculation using laser speckle phenomenon. Invest. Ophthalmol. Vis. Sci. **35**(11), 3825–3834 (1994)
134. Y. Tamaki, M. Araie, E. Kawamoto, S. Eguchi, H. Fujii, Non-contact, two-dimensional measurement of tissue circulation in choroid and optic nerve head using laser speckle phenomenon. Exp. Eye Res. **60**(4), 373–383 (1995)
135. M. Nagahara, Y. Tamaki, A. Tomidokoro, M. Araie, In vivo measurement of blood velocity in human major retinal vessels using the laser speckle method. Invest. Ophthalmol. Vis. Sci. **52**(1), 87–92 (2011)
136. H. Isono, S. Kishi, Y. Kimura, N. Hagiwara, N. Konishi, H. Fujii, Observation of choroidal circulation using index of erythrocytic velocity. Arch. Ophthalmol. **121**(2), 225–231 (2003)
137. B. Choi, N.M. Kang, J.S. Nelson, Laser speckle imaging for monitoring blood flow dynamics in the in vivo rodent dorsal skin fold model. Microvasc. Res. **68**(2), 143–146 (2004)
138. B. Choi, J.C. Ramirez-San-Juan, J. Lotfi, J. Stuart Nelson, Linear response range characterization and in vivo application of laser speckle imaging of blood flow dynamics. J. Biomed. Opt. **11**(4), 041129 (2006)
139. K.R. Forrester, J. Tulip, C. Leonard, C. Stewart, R.C. Bray, A laser speckle imaging technique for measuring tissue perfusion. IEEE Trans. Biomed. Eng. **51**(11), 2074–2084 (2004)
140. Y.C. Huang, T.L. Ringold, J.S. Nelson, B. Choi, Noninvasive blood flow imaging for real-time feedback during laser therapy of port wine stain birthmarks. Lasers Surg. Med. **40**(3), 167–173 (2008)
141. A.K. Dunn, A. Devor, A.M. Dale, D.A. Boas, Spatial extent of oxygen metabolism and hemodynamic changes during functional activation of the rat somatosensory cortex. Neuroimage **27**(2), 279–290 (2005)
142. A.K. Dunn, H. Bolay, M.A. Moskowitz, D.A. Boas, Dynamic imaging of cerebral blood flow using laser speckle. J. Cereb. Blood Flow Metab. **21**(3), 195–201 (2001)
143. H. Bolay, U. Reuter, A.K. Dunn, Z. Huang, D.A. Boas, M.A. Moskowitz, Intrinsic brain activity triggers trigeminal meningeal afferents in a migraine model. Nat. Med. **8**(2), 136–142 (2002)
144. C. Ayata, H.K. Shin, S. Salomone, Y. Ozdemir-Gursoy, D.A. Boas, A.K. Dunn, M.A. Moskowitz, Pronounced hypoperfusion during spreading depression in mouse cortex. J. Cereb. Blood Flow Metab. **24**(10), 1172–1182 (2004)
145. H.K. Shin, A.K. Dunn, P.B. Jones, D.A. Boas, M.A. Moskowitz, C. Ayata, Vasoconstrictive neurovascular coupling during focal ischemic depolarizations. J. Cereb. Blood Flow Metab. **26**(8), 1018–1030 (2006)
146. H.K. Shin, A.K. Dunn, P.B. Jones, D.A. Boas, E.H. Lo, M.A. Moskowitz, C. Ayata, Normobaric hyperoxia improves cerebral blood flow and oxygenation, and inhibits peri-infarct depolarizations in experimental focal ischaemia. Brain **130**(Pt 6), 1631–1642 (2007)
147. S. Zhang, T.H. Murphy, Imaging the impact of cortical microcirculation on synaptic structure and sensory-evoked hemodynamic responses in vivo. PLoS Biol. **5**(5), e119 (2007)
148. Z. Hajjarian, S.K. Nadkarni, Evaluating the viscoelastic properties of tissue from laser speckle fluctuations. Sci. Rep. **2** (2012)
149. M.M. Tripathi, Z. Hajjarian, E.M. Van Cott, S.K. Nadkarni, Assessing blood coagulation status with laser speckle rheology. Biomed. Opt. Express **5**(3), 817–831 (2014)
150. Z. Hajjarian, M.M. Tripathi, S.K. Nadkarni, Optical thromboelastography to evaluate whole blood coagulation. J. Biophotonics **8**(5), 372–381 (2015)

151. S.K. Nadkarni, B.E. Bouma, T. Helg, R. Chan, E. Halpern, A. Chau, M.S. Minsky, J.T. Motz, S.L. Houser, G.J. Tearney, Characterization of atherosclerotic plaques by laser speckle imaging. Circulation **112**(6), 885–892 (2005)
152. S.K. Nadkarni, A. Bilenca, B.E. Bouma, G.J. Tearney, Measurement of fibrous cap thickness in atherosclerotic plaques by spatiotemporal analysis of laser speckle images. J. Biomed. Opt. **11**(2), 8 (2006)
153. S.K. Nadkarni, Optical measurement of arterial mechanical properties: from atherosclerotic plaque initiation to rupture. J. Biomed. Opt. **18**(12), (2013)
154. J. Wang, S.K. Nadkarni, The influence of optical fiber bundle parameters on the transmission of laser speckle patterns. Opt. Express **22**(8), 8908–8918 (2014)
155. A.A. Stratonnikov, V.B. Loschenov, Evaluation of blood oxygen saturation in vivo from diffuse reflectance spectra. J. Biomed. Opt. **6**(4), 457–467 (2001)
156. R. Marchesini, N. Cascinelli, M. Brambilla, C. Clemente, L. Mascheroni, E. Pignoli, A. Testori, D.R. Venturoli, In vivo spectrophotometric evaluation of neoplastic and non-neoplastic skin pigmented lesions. II: discriminant analysis between nevus and melanoma. Photochem. Photobiol. **55**(4), 515–522 (1992)
157. N. Rajaram, T.J. Aramil, K. Lee, J.S. Reichenberg, T.H. Nguyen, J.W. Tunnell, Design and validation of a clinical instrument for spectral diagnosis of cutaneous malignancy. Appl. Opt. **49**(2), 142–152 (2010)
158. A.J. Thompson, S. Coda, M. Brydegaard Sørensen, G. Kennedy, R. Patalay, U. Waitong-Bramming, P.A.A. De Beule, M.A.A. Neil, S. Andersson-Engels, N. Bendsoe, P.M.W. French, K. Svanberg, C. Dunsby, In vivo measurements of diffuse reflectance and time-resolved autofluorescence emission spectra of basal cell carcinomas. J. Biophotonics **5** (3), 240–254 (2012)
159. I.J. Bigio, T.M. Johnson, J.R. Mourant, B.J. Tromberg, Y. Tadir, M. Fehr, H. Nilsson, V.C. Darrow, Determination of the cervical transformation zone using elastic-scattering spectroscopy, in *Advances in Laser and Light Spectroscopy to Diagnose Cancer and Other Diseases III: Optical Biopsy, Proceedings*, vol. 2679 (1996), pp. 85–91
160. J.R. Mourant, T.J. Bocklage, T.M. Powers, H.M. Greene, K.L. Bullock, L.R. Marr-Lyon, M. H. Dorin, A.G. Waxman, M.M. Zsemlye, H.O. Smith, In vivo light scattering measurements for detection of precancerous conditions of the cervix. Gynecol. Oncol. **105**(2), 439–445 (2007)
161. J.R. Mourant, T.J. Bocklage, T.M. Powers, H.M. Greene, M.H. Dorin, A.G. Waxman, M.M. Zsemlye, H.O. Smith, Detection of cervical intraepithelial neoplasias and cancers in cervical tissue by in vivo light scattering. J. Lower Genital Tract Dis. **13**(4), 216–223 (2009)
162. J.R. Mourant, I.J. Bigio, J. Boyer, R.L. Conn, T. Johnson, T. Shimada, Spectroscopic diagnosis of bladder cancer with elastic light scattering. Lasers Surg. Med. **17**(4), 350–357 (1995)
163. J.R. Mourant, J. Boyer, T.M. Johnson, J. Lacey, I.J. Bigio, A. Bohorfoush, M. Mellow, Detection of gastrointestinal cancer by elastic scattering and absorption spectroscopies with the los-alamos optical biopsy system, in *Advances in Laser and Light Spectroscopy to Diagnose Cancer and Other Diseases II, Proceedings*, vol. 2387 (1995), pp. 210–217
164. H.W. Wang, J.K. Jiang, C.H. Lin, J.K. Lin, G.J. Huang, J.S. Yu, Diffuse reflectance spectroscopy detects increased hemoglobin concentration and decreased oxygenation during colon carcinogenesis from normal to malignant tumors. Opt. Express **17**(4), 2805–2817 (2009)
165. J.P. Culver, T. Durduran, T. Furuya, C. Cheung, J.H. Greenberg, A.G. Yodh, Diffuse optical tomography of cerebral blood flow, oxygenation, and metabolism in rat during focal ischemia. J. Cerebral Blood Flow Metabol. **23**(8), 911–924 (2003)
166. H. Levy, D. Ringuette, O. Levi, Rapid monitoring of cerebral ischemia dynamics using laser-based optical imaging of blood oxygenation and flow. Biomed. Opt. Express **3**(4), 777–791 (2012)
167. Y. Shang, L. Chen, M. Toborek, G.Q. Yu, Diffuse optical monitoring of repeated cerebral ischemia in mice. Opt. Express **19**(21), 20301–20315 (2011)

168. F.F. Jobsis, Noninvasive, infrared monitoring of cerebral and myocardial oxygen sufficiency and circulatory parameters. Science **198**(4323), 1264–1267 (1977)
169. N. Sato, T. Kamada, M. Shichiri, S. Kawano, H. Abe, B. Hagihara, Measurement of hemoperfusion and oxygen sufficiency in gastric mucosa in vivo. Evidence of mucosal hypoxia as the cause of hemorrhagic shock-induced gastric mucosal lesion in rats. Gastroenterology **76**(4), 814–819 (1979)
170. G.A. Mook, A. Buursma, A. Gerding, G. Kwant, W.G. Zijlstra, Spectrophotometric determination of oxygen saturation of blood independent of the presence of indocyanine green. Cardiovasc. Res. **13**(4), 233–237 (1979)
171. F.W. Leung, T. Morishita, E.H. Livingston, T. Reedy, P.H. Guth, Reflectance spectrophotometry for the assessment of gastroduodenal mucosal perfusion. Am. J. Physiol. **252**(6 Pt 1), G797–G804 (1987)
172. J.W. Feather, M. Hajizadeh-Saffar, G. Leslie, J.B. Dawson, A portable scanning reflectance spectrophotometer using visible wavelengths for the rapid measurement of skin pigments. Phys. Med. Biol. **34**(7), 807–820 (1989)
173. K.H. Frank, M. Kessler, K. Appelbaum, W. Dummler, The erlangen micro-lightguide spectrophotometer empho I. Phys. Med. Biol. **34**(12), 1883–1900 (1989)
174. E.M. Sevick, B. Chance, J. Leigh, S. Nioka, M. Maris, Quantitation of time- and frequency-resolved optical spectra for the determination of tissue oxygenation. Anal. Biochem. **195**(2), 330–351 (1991)
175. I.J. Bigio, J.R. Mourant, G. Los, Elastic-scattering spectroscopy for quantitative measurement of chemotherapy and PDT drug concentrations in vivo, in *Optical Biopsies and Microscopic Techniques III, Proceedings*, vol. 3568 (1999), pp. 26–30
176. J.R. Mourant, I.J. Bigio, J. Boyer, J. Lacey, T. Johnson, R.L. Conn, Diagnosis of tissue pathology with elastic scattering spectroscopy, in *Leos'94—Conference Proceedings*, vol. 1 (1994), pp. 17–18
177. J.R. Lakowicz, *Principles of Fluorescence Spectroscopy*, 3rd edn. (Springer, New York, 2006)
178. J. Haringsma, G.N.J. Tytgat, H. Yano, H. Iishi, M. Tatsuta, T. Ogihara, H. Watanabe, N. Sato, N. Marcon, B.C. Wilson, R.W. Cline, Autofluorescence endoscopy: feasibility of detection of GI neoplasms unapparent to white light endoscopy with an evolving technology. Gastrointest. Endosc. **53**(6), 642–650 (2001)
179. F.J.C. van den Broek, P. Fockens, S. van Eeden, J.B. Reitsma, J.C.H. Hardwick, P.C.F. Stokkers, E. Dekker, Endoscopic tri-modal imaging for surveillance in ulcerative colitis: randomised comparison of high-resolution endoscopy and autofluorescence imaging for neoplasia detection; and evaluation of narrow-band imaging for classification of lesions. Gut **57**(8), 1083–1089 (2008)
180. W.L. Curvers, R. Singh, L.M.W.-K. Song, H.C. Wolfsen, K. Ragunath, K. Wang, M.B. Wallace, P. Fockens, J.J.G.H.M. Bergman, Endoscopic tri-modal imaging for detection of early neoplasia in Barrett's oesophagus: a multi-centre feasibility study using high-resolution endoscopy, autofluorescence imaging and narrow band imaging incorporated in one endoscopy system. Gut **57**(2), 167–172 (2008)
181. M.A. Kara, F.P. Peters, P. Fockens, F.J.W. ten Kate, J.J.G.H.M. Bergman, Endoscopic video-autofluorescence imaging followed by narrow band imaging for detecting early neoplasia in Barrett's esophagus. Gastrointest. Endosc. **64**(2), 176–185 (2006)
182. N. Rajaram, J.S. Reichenberg, M.R. Migden, T.H. Nguyen, J.W. Tunnell, Pilot clinical study for quantitative spectral diagnosis of non-melanoma skin cancer. Lasers Surg. Med. **42**(10), 716–727 (2010)
183. L. Brancaleon, A.J. Durkin, J.H. Tu, G. Menaker, J.D. Fallon, N. Kollias, In vivo fluorescence spectroscopy of nonmelanoma skin cancer. Photochem. Photobiol. **73**(2), 178–183 (2001)
184. M.A. D'Hallewin, L. Bezdetnaya, F. Guillemin, Fluorescence detection of bladder cancer: a review. Eur. Urol. **42**(5), 417–425 (2002)

185. L. Silveira Jr., J.A. Betiol Filho, F.L. Silveira, R.A. Zangaro, M.T. Pacheco, Laser-induced fluorescence at 488 nm excitation for detecting benign and malignant lesions in stomach mucosa. J. Fluoresc. **18**(1), 35–40 (2008)
186. C.R. Kapadia, F.W. Cutruzzola, K.M. O'Brien, M.L. Stetz, R. Enriquez, L.I. Deckelbaum, Laser-induced fluorescence spectroscopy of human colonic mucosa. Detection of adenomatous transformation. Gastroenterology **99**(1), 150–157 (1990)
187. Y. Yang, G.C. Tang, M. Bessler, R.R. Alfano, Fluorescence spectroscopy as a photonic pathology method for detecting colon cancer. Lasers Life Sci. **6**(4), 259–276 (1995)
188. D.C. De Veld, M. Skurichina, M.J. Witjes, R.P. Duin, H.J. Sterenborg, J.L. Roodenburg, Clinical study for classification of benign, dysplastic, and malignant oral lesions using autofluorescence spectroscopy. J. Biomed. Opt. **9**(5), 940–950 (2004)
189. P.A.A. De Beule, C. Dunsby, N.P. Galletly, G.W. Stamp, A.C. Chu, U. Anand, P. Anand, C. D. Benham, A. Naylor, P.M.W. French, A hyperspectral fluorescence lifetime probe for skin cancer diagnosis. Rev. Sci. Instrum. **78**(12), 123101 (2007)
190. S. Coda, A.J. Thompson, G.T. Kennedy, K.L. Roche, L. Ayaru, D.S. Bansi, G.W. Stamp, A. V. Thillainayagam, P.M. French, C. Dunsby, Fluorescence lifetime spectroscopy of tissue autofluorescence in normal and diseased colon measured ex vivo using a fiber-optic probe. Biomed. Opt. Express **5**(2), 515–538 (2014)
191. P.V. Butte, B.K. Pikul, A. Hever, W.H. Yong, K.L. Black, L. Marcu, Diagnosis of meningioma by time-resolved fluorescence spectroscopy. J. Biomed. Opt. **10**(6), 064026 (2005)
192. L. Marcu, J.A. Jo, P.V. Butte, W.H. Yong, B.K. Pikul, K.L. Black, R.C. Thompson, Fluorescence lifetime spectroscopy of glioblastoma multiforme. Photochem. Photobiol. **80** (1), 98–103 (2004)
193. N.P. Galletly, J. McGinty, C. Dunsby, F. Teixeira, J. Requejo-Isidro, I. Munro, D.S. Elson, M.A.A. Neil, A.C. Chu, P.M.W. French, G.W. Stamp, Fluorescence lifetime imaging distinguishes basal cell carcinoma from surrounding uninvolved skin. Br. J. Dermatol. **159** (1), 152–161 (2008)
194. J. McGinty, N.P. Galletly, C. Dunsby, I. Munro, D.S. Elson, J. Requejo-Isidro, P. Cohen, R. Ahmad, A. Forsyth, A.V. Thillainayagam, M.A.A. Neil, P.M.W. French, G.W. Stamp, Wide-field fluorescence lifetime imaging of cancer. Biomed. Opt. Express **1**(2), 627–640 (2010)
195. H.M. Chen, C.P. Chiang, C. You, T.C. Hsiao, C.Y. Wang, Time-resolved autofluorescence spectroscopy for classifying normal and premalignant oral tissues. Lasers Surg. Med. **37**(1), 37–45 (2005)
196. M. Mycek, K. Schomacker, N. Nishioka, Colonic polyp differentiation using time-resolved autofluorescence spectroscopy. Gastrointest. Endosc. **48**(4), 390–394 (1998)
197. T.J. Pfefer, D.Y. Paithankar, J.M. Poneros, K.T. Schomacker, N.S. Nishioka, Temporally and spectrally resolved fluorescence spectroscopy for the detection of high grade dysplasia in Barrett's esophagus. Lasers Surg. Med. **32**(1), 10–16 (2003)
198. V. De Giorgi, D. Massi, S. Sestini, R. Cicchi, F.S. Pavone, T. Lotti, Combined non-linear laser imaging (two-photon excitation fluorescence microscopy, fluorescence lifetime imaging microscopy, multispectral multiphoton microscopy) in cutaneous tumours: first experiences. J. Eur. Acad. Dermatology Venereol. **23**(3), 314–316 (2009)
199. B.W. Chwirot, S. Chwirot, W. Jedrzejczyk, M. Jackowski, A.M. Raczynska, J. Winczakiewicz, J. Dobber, Ultraviolet laser-induced fluorescence of human stomach tissues: detection of cancer tissues by imaging techniques. Lasers Surg. Med. **21**(2), 149–158 (1997)
200. B.W. Chwirot, Z. Michniewicz, M. Kowalska, J. Nussbeutel, Detection of colonic malignant lesions by digital imaging of UV laser-induced autofluorescence. Photochem. Photobiol. **69** (3), 336–340 (1999)
201. S.D. Xiao, L. Zhong, H.Y. Luo, X.Y. Chen, Y. Shi, Autofluorescence imaging analysis of gastric cancer. Chin. J. Digest. Dis. **3**, 95–98 (2002)

202. J. Mizeret, G. Wagnieres, T. Stepinac, H. VandenBergh, Endoscopic tissue characterization by frequency-domain fluorescence lifetime imaging (FD-FLIM). Lasers Med. Sci. **12**(3), 209–217 (1997)
203. J. Haringsma, G.N.J. Tytgat, Fluorescence and autofluorescence. Best Pract. Res. Clin. Gastroenterol. **13**(1), 1–10 (1999)
204. S. Yamashita, M. Sakabe, T. Ishizawa, K. Hasegawa, Y. Urano, N. Kokudo, Visualization of the leakage of pancreatic juice using a chymotrypsin-activated fluorescent probe. Br. J. Surg. **100**(9), 1220–1228 (2013)
205. R. Petry, M. Schmitt, J. Popp, Raman spectroscopy—a prospective tool in the life sciences. ChemPhysChem **4**(1), 14–30 (2003)
206. M. Marro, A. Taubes, A. Abernathy, S. Balint, B. Moreno, B. Sanchez-Dalmau, E.H. Martínez-Lapiscina, I. Amat-Roldan, D. Petrov, P. Villoslada, Dynamic molecular monitoring of retina inflammation by in vivo Raman spectroscopy coupled with multivariate analysis. J. Biophotonics **7**(9), 724–734 (2014)
207. S.K. Teh, W. Zhene, K.Y. Ho, M. Teh, K.G. Yeoh, Z.W. Huang, Near-infrared Raman spectroscopy for optical diagnosis in the stomach: identification of helicobacter-pylori infection and intestinal metaplasia. Int. J. Cancer **126**(8), 1920–1927 (2010)
208. H. Krishna, S.K. Majumder, P. Chaturvedi, M. Sidramesh, P.K. Gupta, In vivo Raman spectroscopy for detection of oral neoplasia: a pilot clinical study. J. Biophotonics **7**(9), 690–702 (2014)
209. M.S. Bergholt, K. Lin, J. Wang, W. Zheng, H. Xu, Q. Huang, J.L. Ren, K.Y. Ho, M. Teh, S. Srivastava, B. Wong, K.G. Yeoh, Z. Huang, Simultaneous fingerprint and high-wavenumber fiber-optic Raman spectroscopy enhances real-time in vivo diagnosis of adenomatous polyps during colonoscopy. J. Biophotonics **9**(4), 333–342 (2016)
210. M.A. Short, S. Lam, A. McWilliams, J.H. Zhao, H. Lui, H.S. Zeng, Development and preliminary results of an endoscopic Raman probe for potential in vivo diagnosis of lung cancers. Opt. Lett. **33**(7), 711–713 (2008)
211. M.A. Short, S. Lam, A.M. McWilliams, D.N. Ionescu, H.S. Zeng, Using laser Raman spectroscopy to reduce false positives of autofluorescence bronchoscopies a pilot study. J. Thoracic Oncol. **6**(7), 1206–1214 (2011)
212. O. Aydin, M. Altas, M. Kahraman, O.F. Bayrak, M. Culha, Differentiation of healthy brain tissue and tumors using surface-enhanced Raman scattering. Appl. Spectrosc. **63**(10), 1095–1100 (2009)
213. M. Saleem, M. Bilal, S. Anwar, A. Rehman, M. Ahmed, Optical diagnosis of dengue virus infection in human blood serum using Raman spectroscopy. Laser Phys. Lett. **10**(3), 5 (2013)
214. Z. Huang, H. Zeng, I. Hamzavi, D.I. McLean, H. Lui, Rapid near-infrared Raman spectroscopy system for real-time in vivo skin measurements. Opt. Lett. **26**(22), 1782–1784 (2001)
215. Z. Huang, S.K. Teh, W. Zheng, J. Mo, K. Lin, X. Shao, K.Y. Ho, M. Teh, K.G. Yeoh, Integrated Raman spectroscopy and trimodal wide-field imaging techniques for real-time in vivo tissue Raman measurements at endoscopy. Opt. Lett. **34**(6), 758–760 (2009)
216. Y. Komachi, H. Sato, H. Tashiro, Intravascular Raman spectroscopic catheter for molecular diagnosis of atherosclerotic coronary disease. Appl. Opt. **45**(30), 7938–7943 (2006)
217. W.F. Howard, W.H. Nelson, J.F. Sperry, Resonance Raman method for the rapid detection and identification of bacteria in water. Appl. Spectrosc. **34**(1), 72–75 (1980)
218. K. Hadjigeorgiou, E. Kastanos, A. Kyriakides, C. Pitris, Complete urinary tract infection (UTI) diagnosis and antibiogram using surface enhanced Raman spectroscopy (SERS), in *Optical Diagnostics and Sensing XII: Toward Point-of-Care Diagnostics and Design and Performance Validation of Phantoms Used in Conjunction with Optical Measurement of Tissue IV*, vol. 8229 (2012)
219. E. Kastanos, K. Hadjigeorgiou, C. Pitris, Rapid identification of bacterial resistance to ciprofloxacin using surface enhanced Raman spectroscopy, in *Optical Diagnostics and*

Sensing XIV: Toward Point-of-Care Diagnostics, SPIE Photonics West (SPIE, San Francisco, CA, 2014)
220. E. Kastanos, A. Kyriakides, K. Hadjigeorgiou, C. Pitris, A novel method for bacterial UTI diagnosis using Raman spectroscopy. Int. J. Spectrosc. (2012)
221. E.K. Kastanos, A. Kyriakides, K. Hadjigeorgiou, C. Pitris, A novel method for urinary tract infection diagnosis and antibiogram using Raman spectroscopy. J. Raman Spectrosc. **41**(9), 958–963 (2010)
222. A. Kyriakides, E. Kastanos, K. Hadjigeorgiou, C. Pitris, Classification of Raman spectra of bacteria using rank order kernels, in *Advanced Biomedical and Clinical Diagnostic Systems XI*, vol. 8572 (2013)
223. A. Sengupta, M.L. Laucks, E.J. Davis, Surface-enhanced Raman spectroscopy of bacteria and pollen. Appl. Spectrosc. **59**(8), 1016–1023 (2005)
224. A. Sengupta, M. Mujacic, E.J. Davis, Detection of bacteria by surface-enhanced Raman spectroscopy. Anal. Bioanal. Chem. **386**(5), 1379–1386 (2006)
225. W.H. Nelson, J.F. Sperry, *Direct Detection of Bacteria-Antibody Complexes Via UV Resonance Raman Spectroscopy* (The Board of Governors for Higher Education, State of Rhode Island and Providence Plantations, 2005)
226. X. Yang, C. Gu, F. Qian, Y. Li, J.Z. Zhang, Highly sensitive detection of proteins and bacteria in aqueous solution using surface-enhanced Raman scattering and optical fibers. Anal. Chem. **83**(15), 5888–5894 (2011)
227. A. Sivanesan, E. Witkowska, W. Adamkiewicz, L. Dziewit, A. Kaminska, J. Waluk, Nanostructured silver-gold bimetallic SERS substrates for selective identification of bacteria in human blood. Analyst **139**(5), 1037–1043 (2014)
228. A.K. Boardman, W.S. Wong, W.R. Premasiri, L.D. Ziegler, J.C. Lee, M. Miljkovic, C.M. Klapperich, A. Sharon, A.F. Sauer-Budge, Rapid detection of bacteria from blood with surface-enhanced Raman spectroscopy. Anal. Chem. **88**(16), 8026–8035 (2016)
229. M. Harz, P. Rosch, J. Popp, Vibrational spectroscopy—a powerful tool for the rapid identification of microbial cells at the single-cell level. Cytometry. Part A: J. Int. Soc. Anal. Cytol. **75**(2), 104–113 (2009)
230. F.S. de Siqueira e Oliveira, H.E. Giana, L. Silveira, Discrimination of selected species of pathogenic bacteria using near-infrared Raman spectroscopy and principal components analysis. J. Biomed. Opt. **17**(10), 107004 (2012)
231. A. Campion, P. Kambhampati, Surface-enhanced Raman scattering. Chem. Soc. Rev. **27**(4), 241–250 (1998)
232. M. Fleischmann, P.J. Hendra, A.J. McQuillan, Raman-spectra of pyridine adsorbed at a silver electrode. Chem. Phys. Lett. **26**(2), 163–166 (1974)
233. Z.A. Nima, A. Biswas, I.S. Bayer, F.D. Hardcastle, D. Perry, A. Ghosh, E. Dervishi, A.S. Biris, Applications of surface-enhanced Raman scattering in advanced bio-medical technologies and diagnostics. Drug Metabol. Rev. **46**(2), 155–175 (2014)
234. A.K. Singh, S.A. Khan, Z. Fan, T. Demeritte, D. Senapati, R. Kanchanapally, P.C. Ray, Development of a long-range surface-enhanced Raman spectroscopy ruler. J. Am. Chem. Soc. **134**(20), 8662–8669 (2012)
235. B. Yan, A. Thubagere, W.R. Premasiri, L.D. Ziegler, L. Dal Negro, B.M. Reinhard, Engineered SERS substrates with multiscale signal enhancement: nanoparticle cluster arrays. ACS Nano **3**(5), 1190–1202 (2009)
236. E. Temur, I.H. Boyaci, U. Tamer, H. Unsal, N. Aydogan, A highly sensitive detection platform based on surface-enhanced Raman scattering for *Escherichia coli* enumeration. Anal. Bioanal. Chem. **397**(4), 1595–1604 (2010)
237. H.Y. Lin, C.H. Huang, W.H. Hsieh, L.H. Liu, Y.C. Lin, C.C. Chu, S.T. Wang, I.T. Kuo, L. K. Chau, C.Y. Yang, On-line SERS detection of single bacterium using novel SERS nanoprobes and a microfluidic dielectrophoresis device. Small **10**(22), 4700–4710 (2014)
238. C. Yuen, Q. Liu, Towards in vivo intradermal surface enhanced Raman scattering (SERS) measurements: silver coated microneedle based SERS probe. J. Biophotonics **7**(9), 683–689 (2014)

239. Z. Fan, R. Kanchanapally, P.C. Ray, Hybrid graphene oxide based ultrasensitive SERS probe for label-free biosensing. J. Phys. Chem. Lett. **4**(21), 3813–3818 (2013)
240. P.R. Stoddart, D.J. White, Optical fibre SERS sensors. Anal. Bioanal. Chem. **394**(7), 1761–1774 (2009)
241. G.F. Andrade, M. Fan, A.G. Brolo, Multilayer silver nanoparticles-modified optical fiber tip for high performance SERS remote sensing. Biosens. Bioelectron. **25**(10), 2270–2275 (2010)
242. G.F.S. Andrade, J.G. Hayashi, M.M. Rahman, W.J. Salcedo, C.M.B. Cordeiro, A.G. Brolo, Surface-enhanced resonance Raman scattering (SERS) using Au nanohole arrays on optical fiber tips. Plasmonics **8**(2), 1113–1121 (2013)
243. F. Deiss, N. Sojic, D.J. White, P.R. Stoddart, Nanostructured optical fibre arrays for high-density biochemical sensing and remote imaging. Anal. Bioanal. Chem. **396**(1), 53–71 (2010)
244. Z. Xie, S. Feng, P. Wang, L. Zhang, X. Ren, L. Cui, T. Zhai, J. Chen, Y. Wang, X. Wang, W. Sun, J. Ye, P. Han, P.J. Klar, Y. Zhang, Demonstration of a 3D radar-like SERS sensor micro- and nanofabricated on an optical fiber. Adv. Opt. Mater. **3**(9), 1232–1239 (2015)
245. J.L. Kou, M. Ding, J. Feng, Y.Q. Lu, F. Xu, G. Brambilla, Microfiber-based bragg gratings for sensing applications: a review. Sensors **12**(7), 8861–8876 (2012)
246. A.D. Kersey, M.A. Davis, H.J. Patrick, M. LeBlanc, K.P. Koo, C.G. Askins, M.A. Putnam, E.J. Friebele, Fiber grating sensors. J. Lightwave Technol. **15**(8), 1442–1463 (1997)
247. J.W. Arkwright, N.G. Blenman, I.D. Underhill, S.A. Maunder, N.J. Spencer, M. Costa, S. J. Brookes, M.M. Szczesniak, P.G. Dinning, A fibre optic catheter for simultaneous measurement of longitudinal and circumferential muscular activity in the gastrointestinal tract. J. Biophotonics **4**(4), 244–251 (2011)
248. J.W. Arkwright, N.G. Blenman, I.D. Underhill, S.A. Maunder, N.J. Spencer, M. Costa, S. J. Brookes, M.M. Szczesniak, P.G. Dinning, Measurement of muscular activity associated with peristalsis in the human gut using fiber Bragg grating arrays. IEEE Sensors J. **12**(1), 113–117 (2012)
249. M.R. Islam, M.M. Ali, M.H. Lai, K.S. Lim, H. Ahmad, Chronology of Fabry-Perot interferometer fiber-optic sensors and their applications: a review. Sensors (Basel) **14**(4), 7451–7488 (2014)
250. N. Wu, Y. Tian, X.T. Zou, Y. Zhai, K. Barringhaus, X.W. Wang, A miniature fiber optic blood pressure sensor and its application in in vivo blood pressure measurements of a swine model. Sens. Actuators B: Chem. **181**, 172–178 (2013)
251. O.S. Wolfbeis, Fiber-optic chemical sensors and biosensors. Anal. Chem. **76**(12), 3269–3283 (2004)
252. M.T. Carter, R.C. Thomas, M.E. Berton, Fiber waveguide chemical sensors for detection of explosive related vapors, in *Detection and Remediation Technologies for Mines and Minelike Targets VII, Pts 1 and 2*, vol. 4742 (2002), pp. 509–519
253. M. Janotta, A. Katzir, B. Mizaikoff, Sol-gel-coated mid-infrared fiber-optic sensors. Appl. Spectrosc. **57**(7), 823–828 (2003)
254. C.A. Browne, D.H. Tarrant, M.S. Olteanu, J.W. Mullens, E.L. Chronister, Intrinsic sol-gel clad fiber-optic sensors with time-resolved detection. Anal. Chem. **68**(14), 2289–2295 (1996)
255. G. Okeeffe, B.D. Maccraith, A.K. Mcevoy, C.M. Mcdonagh, J.F. Mcgilp, Development of a led-based phase fluorometric oxygen sensor using evanescent-wave excitation of a sol-gel immobilized dye. Sens. Actuators B: Chem. **29**(1–3), 226–230 (1995)
256. O.S. Wolfbeis, M. Schaferling, A. Durkop, Reversible optical sensor membrane for hydrogen peroxide using an immobilized fluorescent probe, and its application to a glucose biosensor. Microchim. Acta **143**(4), 221–227 (2003)
257. Y. Qin, S. Peper, A. Radu, A. Ceresa, E. Bakker, Plasticizer-free polymer containing a covalently immobilized Ca^{2+}-selective ionophore for potentiometric and optical sensors. Anal. Chem. **75**(13), 3038–3045 (2003)

258. A.S. Jeevarajan, S. Vani, T.D. Taylor, M.M. Anderson, Continuous pH monitoring in a perfused bioreactor system using an optical pH sensor. Biotechnol. Bioeng. **78**(4), 467–472 (2002)
259. N.A. Yusof, M. Ahmad, A flow cell optosensor for lead based on immobilized gallocynin in chitosan membrane. Talanta **58**(3), 459–466 (2002)
260. A. Lobnik, I. Oehme, I. Murkovic, O.S. Wolfbeis, Ph optical sensors based on sol-gels: chemical doping versus covalent immobilization. Anal. Chim. Acta **367**(1–3), 159–165 (1998)
261. T.M. Butler, B.D. Maccraith, C.M. Mcdonagh, Development of an extended range fibre optic ph sensor using evanescent wave absorption of sol-gel entrapped pH indicators. Chem. Biochem. Environ. Fiber Sens. VII **2508**, 168–178 (1995)
262. B.D. Gupta, D.K. Sharma, Evanescent wave absorption based fiber optic ph sensor prepared by dye doped sol-gel immobilization technique. Opt. Commun. **140**(1–3), 32–35 (1997)
263. E. Alvarado-Mendez, R. Rojas-Laguna, J.A. Andrade-Lucio, D. Hernandez-Cruz, R.A. Lessard, J.G. Avina-Cervantes, Design and characterization of pH sensor based on sol-gel silica layer on plastic optical fiber. Sens. Actuators B: Chem. **106**(2), 518–522 (2005)
264. B.D. Maccraith, C.M. Mcdonagh, G. Okeeffe, A.K. Mcevoy, T. Butler, F.R. Sheridan, Sol-gel coatings for optical chemical sensors and biosensors. Sens. Actuators B: Chem. **29** (1–3), 51–57 (1995)
265. H.P. Williams, Sir Harold Ridley's vision. Br. J. Ophthalmol. **85**(9), 1022–1023 (2001)
266. M. Leyland, E. Zinicola, Multifocal versus monofocal intraocular lenses in cataract surgery: a systematic review. Ophthalmology **110**(9), 1789–1798 (2003)
267. S.R. de Silva, J.R. Evans, V. Kirthi, M. Ziaei, M. Leyland, Multifocal versus monofocal intraocular lenses after cataract extraction. Cochrane Database Syst. Rev. **12** (2016)
268. D. Madrid-Costa, A. Cervino, T. Ferrer-Blasco, S. Garcia-Lazaro, R. Montes-Mico, Visual and optical performance with hybrid multifocal intraocular lenses. Clin. Exp. Optom. **93**(6), 426–440 (2010)
269. M. Chen, Accommodation in pseudophakic eyes. Taiwan J. Ophthalmol. **2**(4), 117–121 (2012)
270. R.F. Steinert, B.L. Aker, D.J. Trentacost, P.J. Smith, N. Tarantino, A prospective comparative study of the amo array zonal-progressive multifocal silicone intraocular lens and a monofocal intraocular lens. Ophthalmology **106**(7), 1243–1255 (1999)
271. M.C. Knorz, Results of a European multicenter study of the true vista bifocal intraocular lens. J. Cataract Refract. Surg. **19**(5), 626–634 (1993)
272. H.V. Gimbel, D.R. Sanders, M.G. Raanan, Visual and refractive results of multifocal intraocular lenses. Ophthalmology **98**(6), 881–888 (1991)
273. J.D. Hunkeler, T.M. Coffman, J. Paugh, A. Lang, P. Smith, N. Tarantino, Characterization of visual phenomena with the array multifocal intraocular lens. J. Cataract Refract. Surg. **28**(7), 1195–1204 (2002)
274. J.S. Chang, J.C. Ng, S.Y. Lau, Visual outcomes and patient satisfaction after presbyopic lens exchange with a diffractive multifocal intraocular lens. J. Refract. Surg. **28**(7), 468–474 (2012)
275. J.L. Alió, D.P. Piñero, A.B. Plaza-Puche, M.J.R. Chan, Visual outcomes and optical performance of a monofocal intraocular lens and a new-generation multifocal intraocular lens. J. Cataract Refract. Surg. **37**(2), 241–250 (2011)
276. R.K. Shepherd, M.N. Shivdasani, D.A. Nayagam, C.E. Williams, P.J. Blamey, Visual prostheses for the blind. Trends Biotechnol. **31**(10), 562–571 (2013)
277. S. Picaud, J.A. Sahel, Retinal prostheses: clinical results and future challenges. C.R. Biol. **337**(3), 214–222 (2014)
278. A.E. Hadjinicolaou, H. Meffin, M.I. Maturana, S.L. Cloherty, M.R. Ibbotson, Prosthetic vision: devices, patient outcomes and retinal research. Clin. Exper. Optometry **98**(5), 395–410 (2015)
279. A.H. Milam, Z.Y. Li, R.N. Fariss, Histopathology of the human retina in retinitis pigmentosa. Progr. Retinal Eye Res. **17**(2), 175–205 (1998)

280. M.S. Humayun, M. Prince, E. de Juan, Y. Barron, M. Moskowitz, I.B. Klock, A.H. Milam, Morphometric analysis of the extramacular retina from postmortem eyes with retinitis pigmentosa. Invest. Ophthalmol. Vis. Sci. **40**(1), 143–148 (1999)
281. M.P. Villegas-Perez, J.M. Lawrence, M. Vidal-Sanz, M.M. Lavail, R.D. Lund, Ganglion cell loss in RCS rat retina: a result of compression of axons by contracting intraretinal vessels linked to the pigment epithelium. J. Comp. Neurol. **392**(1), 58–77 (1998)
282. R.E. Marc, B.W. Jones, C.B. Watt, E. Strettoi, Neural remodeling in retinal degeneration. Progr. Retinal Eye Res. **22**(5), 607–655 (2003)
283. G.S. Brindley, W.S. Lewin, The sensations produced by electrical stimulation of the visual cortex. J. Physiol. **196**(2), 479–493 (1968)
284. W.H. Dobelle, M.G. Mladejovsky, J.P. Girvin, Artifical vision for the blind: electrical stimulation of visual cortex offers hope for a functional prosthesis. Science **183**(4123), 440–444 (1974)
285. Second Sight Medical Products, The Argus® II retinal prosthesis system. http://www.2-sight.com/argus-ii-rps-pr-en.html (2016)
286. E. Zrenner, K.U. Bartz-Schmidt, H. Benav, D. Besch, A. Bruckmann, V.P. Gabel, F. Gekeler, U. Greppmaier, A. Harscher, S. Kibbel, J. Koch, A. Kusnyerik, T. Peters, K. Stingl, H. Sachs, A. Stett, P. Szurman, B. Wilhelm, R. Wilke, Subretinal electronic chips allow blind patients to read letters and combine them to words. Proc. Roy. Soc. B: Biol. Sci. **278** (1711), 1489–1497 (2011)
287. K. Stingl, K.U. Bartz-Schmidt, D. Besch, A. Braun, A. Bruckmann, F. Gekeler, U. Greppmaier, S. Hipp, G. Hortdorfer, C. Kernstock, A. Koitschev, A. Kusnyerik, H. Sachs, A. Schatz, K.T. Stingl, T. Peters, B. Wilhelm, E. Zrenner, Artificial vision with wirelessly powered subretinal electronic implant alpha-IMS. Proc. Roy. Soc. B **280**(1757), 20130077 (2013)
288. Retina Implant AG, Subretinal implant technology. http://www.retina-implant.de/en/patients/technology/default.aspx (2016)
289. Pixium Vision, Iris® bionic vision restoration system. http://www.pixium-vision.com/en/technology-1/iris-vision-restoration-system (2017)
290. M.S. Humayun, J.D. Dorn, L. da Cruz, G. Dagnelie, J.A. Sahel, P.E. Stanga, A.V. Cideciyan, J.L. Duncan, D. Eliott, E. Filley, A.C. Ho, A. Santos, A.B. Safran, A. Arditi, L.V. Del Priore, R.J. Greenberg, Interim results from the international trial of second sight's visual prosthesis. Ophthalmology **119**(4), 779–788 (2012)
291. S. Klauke, M. Goertz, S. Rein, D. Hoehl, U. Thomas, R. Eckhorn, F. Bremmer, T. Wachtler, Stimulation with a wireless intraocular epiretinal implant elicits visual percepts in blind humans. Invest. Ophthalmol. Vis. Sci. **52**(1), 449–455 (2011)
292. A.E. Hadjinicolaou, R.T. Leung, D.J. Garrett, K. Ganesan, K. Fox, D.A.X. Nayagam, M.N. Shivdasani, H. Meffin, M.R. Ibbotson, S. Prawer, B.J. O'Brien, Electrical stimulation of retinal ganglion cells with diamond and the development of an all diamond retinal prosthesis. Biomaterials **33**(24), 5812–5820 (2012)
293. H. Lorach, G. Goetz, R. Smith, X. Lei, Y. Mandel, T. Kamins, K. Mathieson, P. Huie, J. Harris, A. Sher, D. Palanker, Photovoltaic restoration of sight with high visual acuity. Nature Med. **21**(5), 476–482 (2015)
294. K. Mathieson, J. Loudin, G. Goetz, P. Huie, L.L. Wang, T.I. Kamins, L. Galambos, R. Smith, J.S. Harris, A. Sher, D. Palanker, Photovoltaic retinal prosthesis with high pixel density. Nat. Photonics **6**(6), 391–397 (2012)
295. Pixium Vision, Prima bionic vision restoration system. http://www.pixium-vision.com/en/technology-1/prima-vision-restoration-system (2017)
296. M.N. Shivdasani, C.D. Luu, R. Cicione, J.B. Fallon, P.J. Allen, J. Leuenberger, G. J. Suaning, N.H. Lovell, R.K. Shepherd, C.E. Williams, Evaluation of stimulus parameters and electrode geometry for an effective suprachoroidal retinal prosthesis. J. Neural Eng. **7**(3) (2010)

297. R. Cicione, M.N. Shivdasani, J.B. Fallon, C.D. Luu, P.J. Allen, G.D. Rathbone, R.K. Shepherd, C.E. Williams, Visual cortex responses to suprachoroidal electrical stimulation of the retina: effects of electrode return configuration. J. Neural Eng. **9**(3) (2012)
298. T. Fujikado, M. Kamei, H. Sakaguchi, H. Kanda, T. Morimoto, Y. Ikuno, K. Nishida, H. Kishima, T. Maruo, K. Konoma, M. Ozawa, K. Nishida, Testing of semichronically implanted retinal prosthesis by suprachoroidal-transretinal stimulation in patients with retinitis pigmentosa. Invest. Ophthalmol. Vis. Sci. **52**(7), 4726–4733 (2011)
299. L.N. Ayton, P.J. Blamey, R.H. Guymer, C.D. Luu, D.A. Nayagam, N.C. Sinclair, M.N. Shivdasani, J. Yeoh, M.F. McCombe, R.J. Briggs, N.L. Opie, J. Villalobos, P.N. Dimitrov, M. Varsamidis, M.A. Petoe, C.D. McCarthy, J.G. Walker, N. Barnes, A.N. Burkitt, C.E. Williams, R.K. Shepherd, P.J. Allen, C. Bionic Vision Australia Research, First-in-human trial of a novel suprachoroidal retinal prosthesis. PLoS One **9**(12), e115239 (2014)
300. C. Veraart, F. Duret, M. Brelen, J. Delbeke, Vision rehabilitation with the optic nerve visual prosthesis, in *Proceedings of the 26th Annual International Conference of the IEEE Engineering in Medicine and Biology Society*, vols. 1–7, 26 (2004), pp. 4163–4164
301. M.E. Brelen, V. Vince, B. Gerard, C. Veraart, J. Delbeke, Measurement of evoked potentials after electrical stimulation of the human optic nerve. Invest. Ophthalmol. Vis. Sci. **51**(10), 5351–5355 (2010)
302. J.J. Sun, Y.L. Lu, P.J. Cao, X.L. Li, C.S. Cai, X.Y. Chai, Q.S. Ren, L.M. Li, Spatiotemporal properties of multipeaked electrically evoked potentials elicited by penetrative optic nerve stimulation in rabbits. Invest. Ophthalmol. Vis. Sci. **52**(1), 146–154 (2011)
303. R.A. Normann, B.A. Greger, P. House, S.F. Romero, F. Pelayo, E. Fernandez, Toward the development of a cortically based visual neuroprosthesis. J. Neural Eng. **6**(3) (2009)
304. E.M. Schmidt, M.J. Bak, F.T. Hambrecht, C.V. Kufta, D.K. O'Rourke, P. Vallabhanath, Feasibility of a visual prosthesis for the blind based on intracortical microstimulation of the visual cortex. Brain **119**(Pt 2), 507–522 (1996)
305. P.H. Schiller, W.M. Slocum, M.C. Kwak, G.L. Kendall, E.J. Tehovnik, New methods devised specify the size and color of the spots monkeys see when striate cortex (area v1) is electrically stimulated. Proc. Natl. Acad. Sci. U.S.A. **108**(43), 17809–17814 (2011)
306. K. Deisseroth, Optogenetics. Nature Meth. **8**(1), 26–29 (2011)
307. L. Fenno, O. Yizhar, K. Deisseroth, The development and application of optogenetics, in *Annual Review of Neuroscience*, vol. 34, ed. by S.E. Hyman et al. (2011), pp. 389–412
308. V. Gradinaru, M. Mogri, K.R. Thompson, J.M. Henderson, K. Deisseroth, Optical deconstruction of Parkinsonian neural circuitry. Science **324**(5925), 354–359 (2009)
309. G. Nagel, T. Szellas, W. Huhn, S. Kateriya, N. Adeishvili, P. Berthold, D. Ollig, P. Hegemann, E. Bamberg, Channelrhodopsin-2, a directly light-gated cation-selective membrane channel. Proc. Natl. Acad. Sci. U.S.A. **100**(24), 13940–13945 (2003)
310. B. Schobert, J.K. Lanyi, Halorhodopsin is a light-driven chloride pump. J. Biol. Chem. **257** (17), 306–313 (1982)
311. B.Y. Chow, X. Han, A.S. Dobry, X.F. Qian, A.S. Chuong, M.J. Li, M.A. Henninger, G.M. Belfort, Y.X. Lin, P.E. Monahan, E.S. Boyden, High-performance genetically targetable optical neural silencing by light-driven proton pumps. Nature **463**(7277), 98–102 (2010)
312. E.S. Boyden, F. Zhang, E. Bamberg, G. Nagel, K. Deisseroth, Millisecond-timescale, genetically targeted optical control of neural activity. Nature Neurosci. **8**(9), 1263–1268 (2005)
313. B. Fan, W. Li, Miniaturized optogenetic neural implants: a review. Lab Chip **15**(19), 3838–3855 (2015)
314. J.M. Barrett, R. Berlinguer-Palmini, P. Degenaar, Optogenetic approaches to retinal prosthesis. Vis. Neurosci. **31**(4–5), 345–354 (2014)
315. B.R. Arenkiel, J. Peca, I.G. Davison, C. Feliciano, K. Deisseroth, G.J. Augustine, M.D. Ehlers, G.P. Feng, In vivo light-induced activation of neural circuitry in transgenic mice expressing channelrhodopsin-2. Neuron **54**(2), 205–218 (2007)

316. S.L. Zhao, C. Cunha, F. Zhang, Q. Liu, B. Gloss, K. Deisseroth, G.J. Augustine, G.P. Feng, Improved expression of halorhodopsin for light-induced silencing of neuronal activity. Brain Cell Biol. **36**(1–4), 141–154 (2008)
317. F. Zhang, V. Gradinaru, A.R. Adamantidis, R. Durand, R.D. Airan, L. de Lecea, K. Deisseroth, Optogenetic interrogation of neural circuits: technology for probing mammalian brain structures. Nat. Protoc. **5**(3), 439–456 (2010)
318. K.M. Tye, J.J. Mirzabekov, M.R. Warden, E.A. Ferenczi, H.-C. Tsai, J. Finkelstein, S.-Y. Kim, A. Adhikari, K.R. Thompson, A.S. Andalman, L.A. Gunaydin, I.B. Witten, K. Deisseroth, Dopamine neurons modulate neural encoding and expression of depression-related behaviour. Nature **493**(7433), 537 (2013)
319. K.M. Tye, R. Prakash, S.-Y. Kim, L.E. Fenno, L. Grosenick, H. Zarabi, K.R. Thompson, V. Gradinaru, C. Ramakrishnan, K. Deisseroth, Amygdala circuitry mediating reversible and bidirectional control of anxiety. Nature **471**(7338), 358–362 (2011)
320. D. Chaudhury, J.J. Walsh, A.K. Friedman, B. Juarez, S.M. Ku, J.W. Koo, D. Ferguson, H.-C. Tsai, L. Pomeranz, D.J. Christoffel, A.R. Nectow, M. Ekstrand, A. Domingos, M.S. Mazei-Robison, E. Mouzon, M.K. Lobo, R.L. Neve, J.M. Friedman, S.J. Russo, K. Deisseroth, E.J. Nestler, M.-H. Han, Rapid regulation of depression-related behaviours by control of midbrain dopamine neurons. Nature **493**(7433), 532 (2013)
321. A.M. Aravanis, L.P. Wang, F. Zhang, L.A. Meltzer, M.Z. Mogri, M.B. Schneider, K. Deisseroth, An optical neural interface: in vivo control of rodent motor cortex with integrated fiberoptic and optogenetic technology. J. Neural Eng. **4**(3), S143–S156 (2007)
322. Y. LeChasseur, S. Dufour, G. Lavertu, C. Bories, M. Deschenes, R. Vallee, Y. De Koninck, A microprobe for parallel optical and electrical recordings from single neurons in vivo. Nature Meth. **8**(4), 319–325 (2011)
323. J. Wang, F. Wagner, D.A. Borton, J.Y. Zhang, I. Ozden, R.D. Burwell, A.V. Nurmikko, R. van Wagenen, I. Diester, K. Deisseroth, Integrated device for combined optical neuromodulation and electrical recording for chronic in vivo applications. J. Neural Eng. **9**(1) (2012)
324. N. Grossman, V. Poher, M.S. Grubb, G.T. Kennedy, K. Nikolic, B. McGovern, R.B. Palmini, Z. Gong, E.M. Drakakis, M.A.A. Neil, M.D. Dawson, J. Burrone, P. Degenaar, Multi-site optical excitation using chr2 and micro-led array. J. Neural Eng. **7**(1) (2010)
325. K.Y. Kwon, B. Sirowatka, A. Weber, W. Li, Opto-mu ecog array: a hybrid neural interface with transparent mu ecog electrode array and integrated leds for optogenetics. IEEE Trans. Biomed. Circuits Syst. **7**(5), 593–600 (2013)
326. M. Schwaerzle, P. Elmlinger, O. Paul, P. Ruther, Miniaturized 3 × 3 optical fiber array for optogenetics with integrated 460 nm light sources and flexible electrical interconnection, in *2015 28th IEEE International Conference on Micro Electro Mechanical Systems* (*MEMS*) (2015)
327. R.D. Airan, K.R. Thompson, L.E. Fenno, H. Bernstein, K. Deisseroth, Temporally precise in vivo control of intracellular signalling. Nature **458**(7241), 1025–1029 (2009)
328. J.A. Cardin, M. Carlen, K. Meletis, U. Knoblich, F. Zhang, K. Deisseroth, L.H. Tsai, C.I. Moore, Targeted optogenetic stimulation and recording of neurons in vivo using cell-type-specific expression of channelrhodopsin-2. Nat. Protoc. **5**(2), 247–254 (2010)
329. P. Anikeeva, A.S. Andalman, I. Witten, M. Warden, I. Goshen, L. Grosenick, L.A. Gunaydin, L.M. Frank, K. Deisseroth, Optetrode: a multichannel readout for optogenetic control in freely moving mice. Nature Neurosci. **15**(1), 163–170 (2012)
330. E. Stark, T. Koos, G. Buzsaki, Diode probes for spatiotemporal optical control of multiple neurons in freely moving animals. J. Neurophysiol. **108**(1), 349–363 (2012)
331. T.V.F. Abaya, M. Diwekar, S. Blair, P. Tathireddy, L. Rieth, G.A. Clark, F. Solzbacher, Characterization of a 3D optrode array for infrared neural stimulation. Biomed. Opt. Express **3**(9), 2200–2219 (2012)
332. Y. Iwai, S. Honda, H. Ozeki, M. Hashimoto, H. Hirase, A simple head-mountable led device for chronic stimulation of optogenetic molecules in freely moving mice. Neurosci. Res. **70**(1), 124–127 (2011)

333. L. Campagnola, H. Wang, M.J. Zyka, Fiber-coupled light-emitting diode for localized photo stimulation of neurons expressing channelrhodopsin-2. J. Neurosci. Meth. **169**(1), 27–33 (2008)
334. T. Ishizuka, M. Kakuda, R. Araki, H. Yawo, Kinetic evaluation of photosensitivity in genetically engineered neurons expressing green algae light-gated channels. Neurosci. Res. **54**(2), 85–94 (2006)
335. H. Cao, L. Gu, S.K. Mohanty, J.C. Chiao, An integrated μLED optrode for optogenetic stimulation and electrical recording. IEEE Trans. Biomed. Eng. **60**(1), 225–229 (2013)
336. N. McAlinden, D. Massoubre, E. Richardson, E. Gu, S. Sakata, M.D. Dawson, K. Mathieson, Thermal and optical characterization of micro-LED probes for in vivo optogenetic neural stimulation. Opt. Lett. **38**(6), 992–994 (2013)
337. K.Y. Kwon, H.M. Lee, M. Ghovanloo, A. Weber, W. Li, Design, fabrication, and packaging of an integrated, wirelessly-powered optrode array for optogenetics application. Front. Syst. Neurosci. **9**, 69 (2015)
338. H.M. Lee, K.Y. Kwon, W. Li, M. Ghovanloo, A power-efficient switched-capacitor stimulating system for electrical/optical deep brain stimulation. IEEE J. Solid-State Circ. **50** (1), 360–374 (2015)
339. M.A. Rossi, V. Go, T. Murphy, Q. Fu, J. Morizio, H.H. Yin, A wirelessly controlled implantable LED system for deep brain optogenetic stimulation. Front. Integr. Neurosci. **9**, 8 (2015)
340. M. Hashimoto, A. Hata, T. Miyata, H. Hirase, Programmable wireless light-emitting diode stimulator for chronic stimulation of optogenetic molecules in freely moving mice. Neurophotonics **1**(1), 011002 (2014)
341. S.T. Lee, P.A. Williams, C.E. Braine, D.T. Lin, S.W. John, P.P. Irazoqui, A miniature, fiber-coupled, wireless, deep-brain optogenetic stimulator. IEEE Trans. Neural Syst. Rehabil. Eng. **23**(4), 655–664 (2015)
342. C.T. Wentz, J.G. Bernstein, P. Monahan, A. Guerra, A. Rodriguez, E.S. Boyden, A wirelessly powered and controlled device for optical neural control of freely-behaving animals. *J. Neural Eng.* **8**(4) (2011)
343. T.-I. Kim, J.G. McCall, Y.H. Jung, X. Huang, E.R. Siuda, Y. Li, J. Song, Y.M. Song, H.A. Pao, R.-H. Kim, C. Lu, S.D. Lee, I.-S. Song, G. Shin, R. Al-Hasani, S. Kim, M.P. Tan, Y. Huang, F.G. Omenetto, J.A. Rogers, M.R. Bruchas, Injectable, cellular-scale optoelectronics with applications for wireless optogenetics. Science **340**(6129), 211–216 (2013)
344. S.I. Park, D.S. Brenner, G. Shin, C.D. Morgan, B.A. Copits, H.U. Chung, M.Y. Pullen, K.N. Noh, S. Davidson, S.J. Oh, J. Yoon, K.-I. Jang, V.K. Samineni, M. Norman, J.G. Grajales-Reyes, S.K. Vogt, S.S. Sundaram, K.M. Wilson, J.S. Ha, R. Xu, T. Pan, T.-I. Kim, Y. Huang, M.C. Montana, J.P. Golden, M.R. Bruchas, R.W. Gereau Iv, J.A. Rogers, Soft, stretchable, fully implantable miniaturized optoelectronic systems for wireless optogenetics. Nat. Biotech. (Advance online publication, 2015)
345. A.D. Bi, J.J. Cui, Y.P. Ma, E. Olshevskaya, M.L. Pu, A.M. Dizhoor, Z.H. Pan, Ectopic expression of a microbial-type rhodopsin restores visual responses in mice with photoreceptor degeneration. Neuron **50**(1), 23–33 (2006)
346. H. Tomita, E. Sugano, H. Isago, T. Hiroi, Z. Wang, E. Ohta, M. Tamai, Channelrhodopsin-2 gene transduced into retinal ganglion cells restores functional vision in genetically blind rats. Exper. Eye Res. **90**(3), 429–436 (2010)
347. H. Tomita, E. Sugano, H. Yawo, T. Ishizuka, H. Isago, S. Narikawa, S. Kugler, M. Tamai, Restoration of visual response in aged dystrophic RCS rats using AAV-mediated channelopsin-2 gene transfer. Invest. Ophthalmol. Vis. Sci. **48**(8), 3821–3826 (2007)
348. P.S. Lagali, D. Balya, G.B. Awatramani, T.A. Munch, D.S. Kim, V. Busskamp, C.L. Cepko, B. Roska, Light-activated channels targeted to on bipolar cells restore visual function in retinal degeneration. Nature Neurosci. **11**(6), 667–675 (2008)
349. B. Lin, A. Koizumi, N. Tanaka, S. Panda, R.H. Masland, Restoration of visual function in retinal degeneration mice by ectopic expression of melanopsin. Proc. Natl. Acad. Sci. U.S.A. **105**(41), 16009–16014 (2008)

350. I. Reutsky-Gefen, L. Golan, N. Farah, A. Schejter, L. Tsur, I. Brosh, S. Shoham, Holographic optogenetic stimulation of patterned neuronal activity for vision restoration. Nat. Commun. **4** (2013)
351. B. McGovern, R.B. Palmini, N. Grossman, E.M. Drakakis, V. Poher, M.A.A. Neil, P. Degenaar, A new individually addressable micro-LED array for photogenetic neural stimulation. IEEE Trans. Biomed. Circ. Syst. **4**(6), 469–476 (2010)
352. L. Chaudet, M. Neil, P. Degenaar, K. Mehran, R. Berlinguer-Palmini, B. Corbet, P. Maaskant, D. Rogerson, P. Lanigan, E. Bamberg, B. Roska, Development of optics with micro-LED arrays for improved opto-electronic neural stimulation. Optogenetics: Opt. Meth. Cell. Control **8586** (2013)
353. J.T. DiPiro, R.G. Martindale, A. Bakst, P.F. Vacani, P. Watson, M.T. Miller, Infection in surgical patients: effects on mortality, hospitalization, and postdischarge care. Am. J. Health-System Pharmacy **55**(8), 777–781 (1998)
354. C.D. Owens, K. Stoessel, Surgical site infections: epidemiology, microbiology and prevention. J. Hosp. Infect. **70**(Suppl 2), 3–10 (2008)